NOTICE

The quality of this microform is heavily dependent upon the quality of the original thesis submitted for microfilming. Every effort has been made to ensure the highest quality of reproduction possible.

If pages are missing, contact the university which granted the degree.

Some pages may have indistinct print especially if the original pages were typed with a poor typewriter ribbon or if the university sent us an inferior photocopy.

Reproduction in full or in part of this microform is governed by the Canadian Copyright Act, R.S.C. 1970, c. C-30, and subsequent amendments.

AVIS

La qualité de cette microforme dépend grandement de la qualité de la thèse soumise au microfilmage. Nous avons tout fait pour assurer une qualité supérieure de reproduction.

S'il manque des pages, veuillez communiquer avec l'université qui a conféré le grade.

La qualité d'impression de certaines pages peut laisser à désirer, surtout si les pages originales ont été dactylographiées à l'aide d'un ruban usé ou si l'université nous a fait parvenir une photocopie de qualité inférieure.

La reproduction, même partielle, de cette microforme est soumise à la Loi canadienne sur le droit d'auteur, SRC 1970, c. C-30, et ses amendements subséquents.

SKIN-EFFECT CONSIDERATIONS ON TRANSIENT RESPONSE OF A TRANSMISSION LINE EXCITED BY AN ELECTROMAGNETIC PULSE

by

Edward S.M. Mok, B.A.Sc.

A thesis submitted to the
School of Graduate Studies and Research
in partial fulfillment of the requirements for the degree of

Master in Applied Science

Ottawa-Carleton Institute for Electrical Engineering

Department of Electrical Engineering
Faculty of Engineering
University of Ottawa

January, 1991

ISBN 0-315-68052-0

UNIVERSITÉ D'OTTAWA
UNIVERSITY OF OTTAWA

Abstract

The electromagnetic pulse can have a very serious damaging effect to modern digital and analog equipment. Many analytical models to solve the susceptibility problems have been developed, but emphasis was mainly on lossless transmission lines. In this thesis, the transient skin-effect resistance is taken into account to characterize a single transmission line above a lossy ground exposed to a time-varying electromagnetic field. As a result of incorporating the skin-effect phenomena and the equivalent sources due to the external fields into the classical transmission line theory, an integral-differential equation is derived. By means of a mixed time-domain finite differences (TD-FD) scheme, the induced voltage and the current at any point on the line is predicted and discussed.

Acknowledgement

The author wishes to express his deepest gratitude to his supervisor Dr. G. I. Costache for his encouragement and guidance throughout this work. The author would also like to express his appreciation to the professional EMC team members including S. Xavier, D. R. Goulette, R. Crawhall, and P. K. Lau of Bell-Northern Researh for sharing their experience and invaluable information for the research. The author is also indebted to his colleague, Mr. D. Ladd, for his unforgettable help in the process of computer simulations, and to his friend, Mr. Boris Chiu, for his suggestions for the graphics presentation in this thesis. Finally, a heartful thank is extended to my dear parents and the family members for their patience and understanding.

The University of Ottawa requires the signatures of all persons using or photocopying the document. Please sign below, and give address and date.

Contents

List of Figures

List of Tables

List of Symbols

The following is a list of the *key* symbols used in this thesis:

$r(t)$	transient skin-effect resistance
$r_{d.c.}$	d.c. resistance
ρ	normalized transient skin-effect resistance
$Z(s)$	longitudinal impedance of a lossy line
l_{ext}	external inductance of a lossy line
l_{eq}	equivalent inductance of a lossy line
c_{st}	line capacitance
c_{eq}	equivalent capacitance of a lossy line
g_o	conductance of a lossy line
μ	permeability
ϵ	permittivity
σ	conductivity
τ_c	the intrinsic time constant of a cylindrical conductor
τ_g	the intrinsic time constant of a lossy ground
E	electric field
H	magnetic field
B	magnetic induction
Φ	magnetic flux
EMP	electromagnetic pulse
ESD	electrostatic discharge
θ	angle of incidence
ϕ	azimuth angle
v	induced voltage

w	induced current proportional to the induced voltage
t_n	the normalized time
Δt_n	discretization time step
$\Delta\xi$	discretization space step
k	integer of discretization space step
l	integer of discretization time step
v_{ph}	velocity of propagation
TDFD	time-domain finite-difference
x, y, z	the axes in Cartesian coordinate system

"Although the achievements of science may, indeed, throw us back into barbarism, the abandonment of our search for knowledge and material betterment would only make vegetables of us."

- Vannevar Bush

Chapter 1

Introduction

1.1 The motivations

Nowadays communication systems must be able to operate in their intended operational environment without suffering from any electromagnetic disturbance. In particular, electromagnetic interference on conductors due to external fields must be avoided since it can cause performance degradation of many telecommunications equipment and switching circuits. The adverse effects on high-speed circuits which are extremely sensitive to voltage and current surges should also be minimized. Measurements of the induced voltages due to fast transients can only be done with expensive devices such as EMI simulators, and surge transient generators. However, mathematical models can be developed to predict the induced voltages for better understanding of the impact of the external time-varying electromagnetic fields on transmission lines.

1.2 The objectives

The fundamental objective of the research presented in this thesis is to introduce a new algorithm that can be used to study the impact of an external time-varying field on a transmission line above a lossy ground.

The problem is to develop a numerical model which can predict the induced voltage onto a lossy transmission line, and which can investigate the propagation of the induced voltage from the beginning of a line to its end. In addition, the algorithm must be able to generate the numerical solutions in time-domain.

The numerical algorithm must further be extended to multi-conductors so that it can

be applied, in general, as a computer-aided design (CAD) tool to predict the influence of an electromagnetic pulse (EMP), an electrostatic discharge (ESD), or lightning on transmission lines. Using the developed algorithm, system designers can have better analysis and understanding of equipment susceptibility which becomes very important in EMI/C engineering.

1.3 The theoretical approach

To predict the induced voltage onto the line due to an EMP excitation or other fast transients such as ESD or lightning, transmission line theory in combination with Maxwell's equations are used. For small time values, the transient skin-effect in a transmission line is no longer negligible, and it must be added to the classical transmission line theory. This transient skin-effect can be taken into account by defining a transient skin-effect resistance developed by using Laplace transform [1,2]. As a result of incorporating the transient skin-effect resistance and the equivalent sources due to the external fields into the classical transmission line theory, an integral-differential equation is derived. By using the modified equations, induced voltages onto a transmission line are then predicted.

1.4 A perception of the modified telegraphist's equations

The study of the transient response of electric lines subjected to external fields were done in the past by using the classical transmission line equations which ignored the transient skin-effect in conductors. For small time values, the current distribution inside a conductor line is not uniform. When a line is excited by a pulse with rise time in the order of nano- or pico- seconds, the current tends to shift to the surface of the conductor [51]. As a result, an uneven current distribution takes place inside the conductor (see Figure 1.1), and the flux linkage and therefore the internal inductance will vary with time. The longitudinal line impedance, which is a function of the line resistance and inductance, will follow the change of the internal inductance, and exhibits a transient characteristic. This transient phenomenon can be characterized by a parameter called the transient resistance that takes into account the skin-effect in a transmission line [1],[2],[8],[45].

Figure 1.1: Current Distribution Inside A Conductor

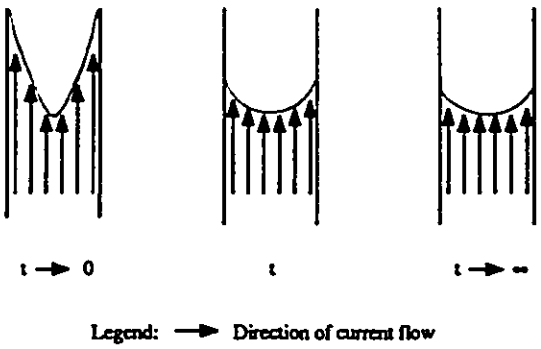

For a line externally-excited by a time-varying electromagnetic field, the penetration phenomena of the field inside the conductor and the lossy ground must also be taken into account. Various models that assist in the understanding of the impact of external electromagnetic fields on transmission lines have been developed by solving field equations [5,6,11,12], [14-20], [26,27], [31-34], [37,38], [42-44], [46,47]. In essence, the effect of an external wave on a line can be regarded as an absorption of electromagnetic energy by the line. From Faraday's electromagnetic induction law, the incident fields onto the line can be represented by forcing functions or distributed voltage and current sources which takes into account the time rate of change of the magnetic flux linkage and the transverse electric field impinging onto the conductor line [12].

As a matter of fact, the classical telegraphist's equations must be modified accordingly. On the one hand, d.c. resistance concept must be substituted by the use of a transient parameter $r(t)$ which takes into account the skin-effect inside a conductor line. On the other hand, equivalent voltage and current sources due to the external electromagnetic fields must be added to the telegraphist's equations. As a consequence, the classical transmission line theory is modified so as to include the transient skin-effect and the equivalent sources on the conductor line.

The modified transmission line equations will consist of the Volterra type integral-differential equation which is usually difficult to solve analytically. In Laplace domain,

the integral is represented by the complicated zeroth order modified Bessel functions. A relatively easier method to solve the integral-differential equation is the time-domain finite-difference (TD-FD) technique which was pioneered by Yee[1966]. This numerical technique is, in fact, promising in adapting to the capabilities of the new generation of computers. Also, it requires only the recent data in the discretization space-time mesh. Moreover, the time-domain approach is superior to the frequency domain method. The main reason is that a single input pulse $x(t)$ is sufficient to get a single output pulse $y(t)$ which covers a wide frequency spectrum. The complete frequency domain solution, however, requires a number of single frequency excitations and a wide spectrum must be used to avoid Gibb's phenomenon which may take place in the inverse Fourier transform. Because of this, the time-domain finite-difference method is chosen for this research.

Chapter 2

The longitudinal transient parameter of a transmission line

This chapter introduces the transient skin-effect resistance $r(t)$ of a transmission line above lossy ground. The derivations for this transient parameter is based on Laplace transform and modified Bessel functions.

2.1 The transient skin-effect resistance

The skin-effect in a transmission line above lossy ground can be taken into account by the longitudinal impedance in the line equation which is written in Laplace domain as:

$$-\frac{dV(x,p)}{dx} = Z(p) \cdot I(p) \quad . \tag{2.1}$$

In this equation, p is the Laplace variable, $Z(p)$ is a function of the skin-effect inside the conductor line and the ground return. By defining a parameter called the skin-effect resistance, $R(p)$, the longitudinal impedance can be expressed as:

$$Z(p) = p \cdot l_{ext} + R(p) \tag{2.2}$$

where l_{ext} is the external inductance per unit length governed by the formula:

$$l_{ext} = \frac{\mu_o}{2\pi} \cdot ln\left(\frac{2h}{a}\right) \quad . \tag{2.3}$$

In the above equation, h is the height and a is the radius of the conductor line above lossy ground as depicted in Figure 2.1. The solution to the longitudinal impedance $Z(p)$

Figure 2.1: Transmission Line Above Lossy Ground

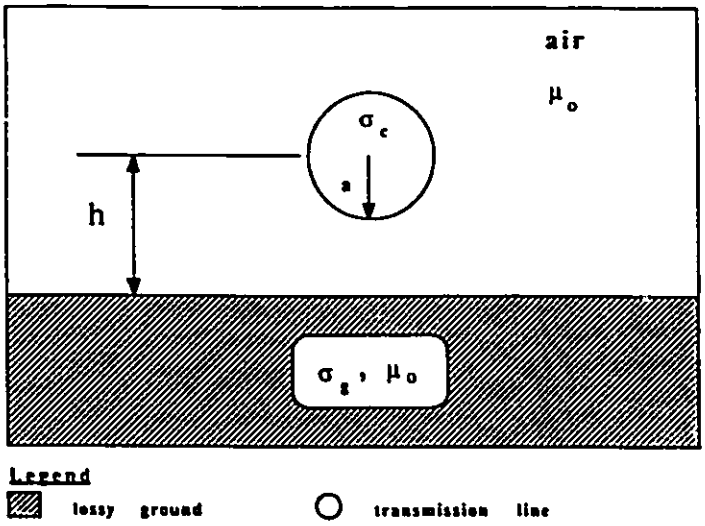

of a cylindrical conductor and its ground image as shown in Figure 2.2 can be determined by solving field equations [1,2]. The derived expression of this line impedance written in Laplace domain is given by [1]:

$$\begin{aligned} Z(p) = \; & p \cdot \frac{\mu_o}{2\pi} ln\left(\frac{2h}{a}\right) \\ & - p \cdot \frac{\mu_o}{2\pi} \cdot \frac{J_1\left(\sqrt{-p\tau_c}\right)}{\left(\sqrt{-p\tau_c}\right) \cdot J_o\left(\sqrt{p\tau_c}\right)} \\ & + p \cdot \frac{\mu_o}{\pi} \cdot \int_0^\infty \frac{e^{-2hx} dx}{x + \sqrt{x^2 + p \cdot \tau_g}} \end{aligned} \tag{2.4}$$

where $\tau_c = \mu_o \sigma_c a^2$ is a time constant characterizing the transient skin-effect inside the conductor line of conductivity σ_c, and $\tau_g = \mu_o \sigma_g h^2$ is a time constant characterizing the

Figure 2.2: Transmission Line Under The Electromagnetic Environment

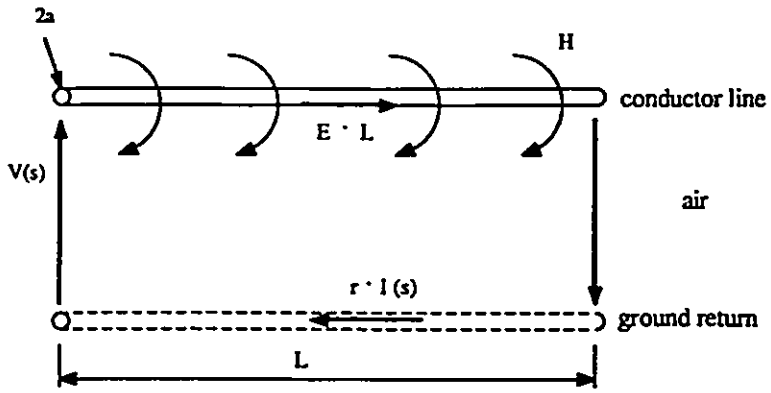

transient skin-effect inside the lossy ground of conductivity σ_g. In this equation, the first term is the external inductance per unit length, the second term takes into account the internal transient resistance, and the third term is proportional to the ground transient resistance.

The time-domain parameter $r(t)$ representing the transient skin-effect resistance can be determined through the inverse Laplace transform of the longitudinal impedance [1].

$$r(t) = L^{-1}\left[\frac{Z(p)}{p} - l_{ext}\right] . \tag{2.5}$$

The transient resistance corresponding to the line conductor, $r_c(t)$, was obtained by using Heaviside's generalized inversion formula [2]:

$$r_c(t) = \frac{1}{\sigma_c \pi a^2} \cdot \left[1 + \sum_{k=1}^{\infty} e^{-\left(x_k^2 \cdot \frac{t}{\tau_c}\right)}\right] \tag{2.6}$$

where the terms x_k are the roots of the Bessel functions of the first kind, and can be represented as:

$$x_1 \approx 3.83\ , x_2 \approx 7.01\ , \ldots\ , x_k\ , \ldots\ , k\pi + \frac{\pi}{4} \quad . \tag{2.7}$$

The transient resistance corresponding to the ground return, $r_g(t)$, has been solved and presented in [1]:

$$r_g(t) = \frac{\mu_o}{\pi \tau_g} \cdot \left[\frac{1}{2\sqrt{\pi}} \cdot \sqrt{\frac{\tau_g}{t}} + \frac{1}{4} \cdot e^{\frac{\tau_g}{t}} \cdot erfc\left(\sqrt{\frac{\tau_g}{t}}\right) - \frac{1}{4} \right] \quad . \tag{2.8}$$

The overall transient skin-effect resistance corresponding to a transmission line above lossy ground is given by the sum of the transient resistance of the conductor line and that of the ground return:

$$r(t) = r_c(t) + r_g(t) \quad . \tag{2.9}$$

To simplify the calculations, asymptotic expressions for this transient parameter have been used and are summarized in the following:

$$r(t) \approx r_{d.c.} \cdot \frac{\tau_c}{\tau_g} \left\{ \frac{1}{2\sqrt{\pi}} \sqrt{\frac{\tau_g}{t}} \left(1 + \sqrt{\frac{\tau_g}{\tau_c}} - \frac{1}{4} + \frac{1}{4\sqrt{\pi}} \sqrt{\frac{t}{\tau_g}} \right) \right\} \tag{2.10}$$

for $t \leq 0.1\ \tau_g$,

$$\begin{aligned} r(t) \approx \ r_{d.c.} \ & \frac{\tau_c}{\tau_g} \left\{ \frac{1}{4} \cdot e^{\frac{\tau_g}{t}} \cdot erfc\left(\frac{\tau_g}{t}\right) - \frac{1}{4}\left(1 - \frac{\tau_g}{\tau_c}\right) \right. \\ + \ & \left. \frac{1}{2\sqrt{\pi}} \sqrt{\frac{\tau_g}{t}} \left(1 + \sqrt{\frac{\tau_g}{\tau_c}} \right) + \frac{3}{8\sqrt{\pi}} \left(\frac{\tau_g^{\frac{3}{2}}}{\tau_c} \right) \sqrt{\frac{t}{\tau_g}} \right\} \end{aligned} \tag{2.11}$$

for $0.1\ \tau_g \leq t \leq 10\ \tau_g$,

$$r(t) \approx r_{d.c.} \left\{ 1 + e^{-14.7\left(\frac{t}{\tau_c}\right)} \cdot \frac{1}{4} \cdot \frac{\tau_c}{t} - \frac{1}{3\sqrt{\pi}} \cdot \frac{\tau_g}{\sqrt{t\tau_c}} + \frac{1}{8} \cdot \frac{\tau_g^3}{\tau_c t^2} \right\} \tag{2.12}$$

for $t \geq 10\ \tau_g$. From the above expressions, one can observe that the transient skin-effect resistance will tend to infinity for $t = 0$ and to the d.c. resistance for $t = \infty$. To see this transient skin-effect phenonmenon in a transmission line above lossy ground is investigated as a function of time for various ground conductivities. The calculated values of the normalized transient resistance for the configuration represented in Figure 2.3 are plotted in Figure 2.4. One can remark very high values of this transient parameter for

Figure 2.3: Dimension of A Cylindrical Conductor above Lossy Ground

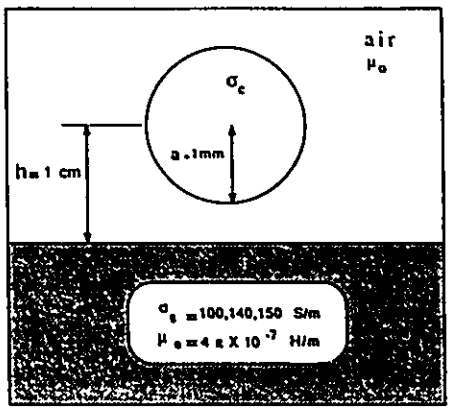

time in the order of nanoseconds.

2.2 The calculations of the skin-effect resistance near zero time

The transient skin-effect resistance of a transmission line above lossy ground, which tends to infinity in the neighbourhood of zero time, can be approximated by using the following asymptotic expression based on the equations for the skin-effect inside the conductor line and the ground return [3]:

Figure 2.4: The Transient Skin-Effect Resistance

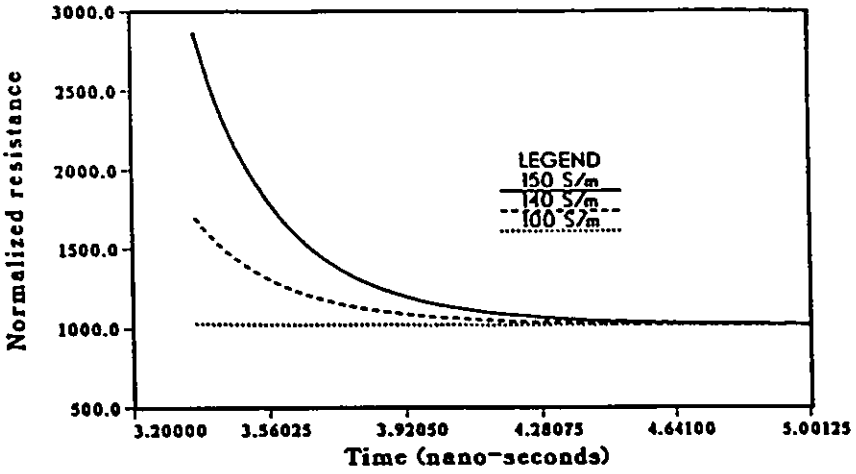

$$\begin{aligned} \rho(t_n) &= \frac{R(t)}{R(\infty)} \\ &\approx \frac{a_1}{\sqrt{\pi t_n}} + a_2 + \frac{2a_3}{\sqrt{\pi}}\sqrt{t_n} + a_4 t_n + \frac{4}{3}a_5 t_n \sqrt{\frac{t_n}{\pi}} + \dots , \end{aligned} \tag{2.13}$$

where the variable $t_n = \frac{t}{\tau_g}$ is the normalized time, and the coefficients have been derived and are listed as follows:

$$\begin{aligned} a_1 &= \frac{K}{2} + \frac{1}{2\sqrt{l}} , \\ a_2 &= -\left(\frac{K}{4} - \frac{1}{4}\right) , \\ a_3 &= \frac{K}{8} + \frac{3\sqrt{l}}{10} , \\ a_4 &= \frac{3l}{16} , \\ a_5 &= -\frac{3K}{32} + \frac{63}{256}\sqrt{l} , \\ &\dots , \\ K &= \frac{1}{\pi h^2 \sigma_g r_o} , \quad \textit{and} \\ l &= \frac{t}{\tau_c} \cdot \frac{1}{t_n} . \end{aligned}$$

The above asymptotic expression for the transient skin-effect resistance of a transmission line above lossy ground consists of many decreasing terms and thus convergent for $\frac{t}{\tau_g} \ll 1$.

Chapter 3

Impact of external time-varying EM fields on transmission lines

In this chapter, the impact of an external time-varying electromagnetic field represented by equivalent sources on a lossy transmission line is discussed. First, the applied field is formulated by taking into considerations the incident wave and the ground reflection. Then, the calculated field is transformed by using Maxwell's equations into equivalent voltage and current sources distributed on the transmission line. By taking into account these excitation sources and the transient skin-effect in a transmission line, a new transmission line equation is introduced.

3.1 The external transient electromagnetic field

Let us consider a transmission line of length L above a lossy ground illuminated by a time-varying electromagnetic field such as those generated by electromagnetic pulse (EMP), electrostatic discharge (ESD), or lightning. Figure 3.1 shows the geometry of the external fields coupled to a conductor line.

The time-varying electromagnetic field, which excites the transmission line, can be resolved into the transverse components of the electric field and the component of the magnetic flux normal to the plane perpendicular to the ground and passing through the conductor line. The component of the electric field normal to this vertical plane, and the component of the magnetic field parallel to that plane will have no induction effect on the transmission line [4]. To solve for the voltage induced onto a transmission line subjected to a transient electromagnetic field, therefore, requires the knowledge of the projections E_x and E_y of the applied electric field onto the vertical plane, and the normal flux, H_z,

Figure 3.1: The Orientation of a Transmission Line above Imperfect Ground

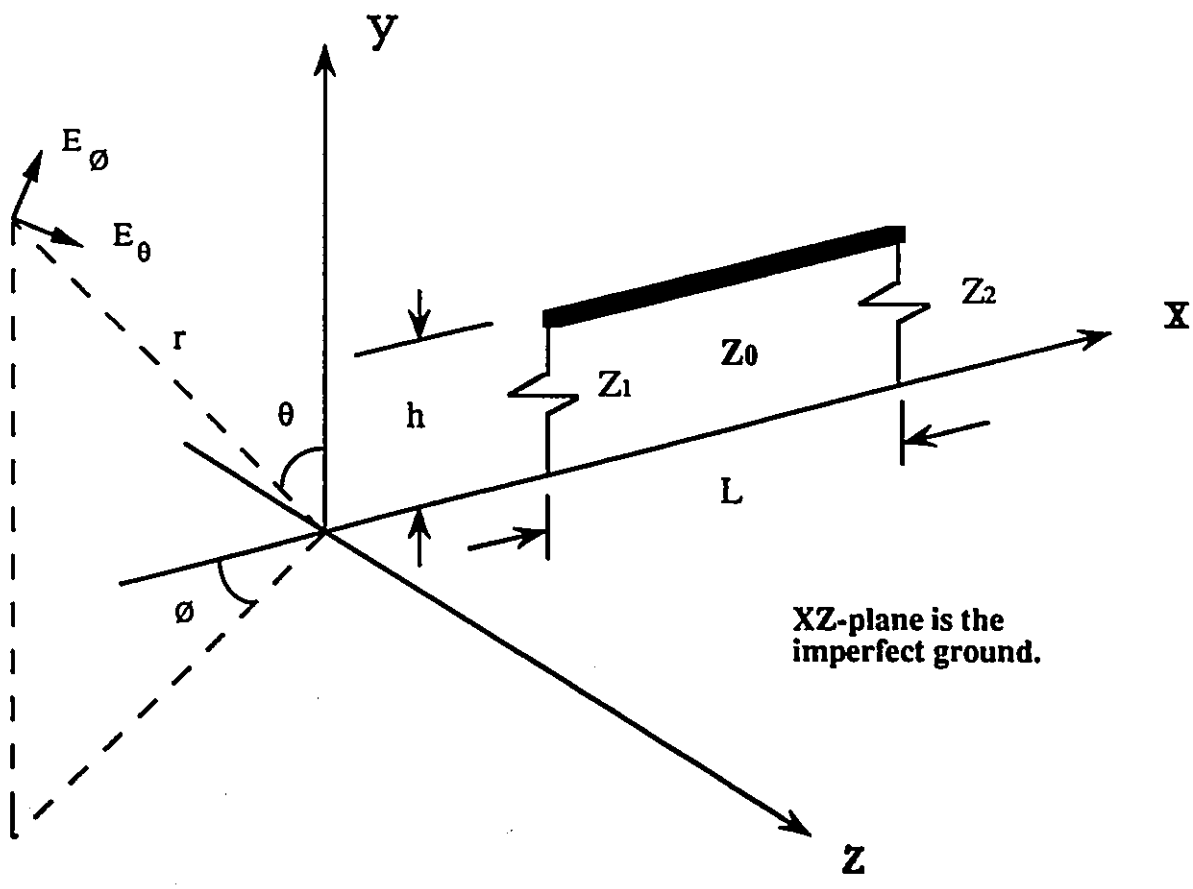

Figure 3.2: Oblique Incidence of the Electric Field

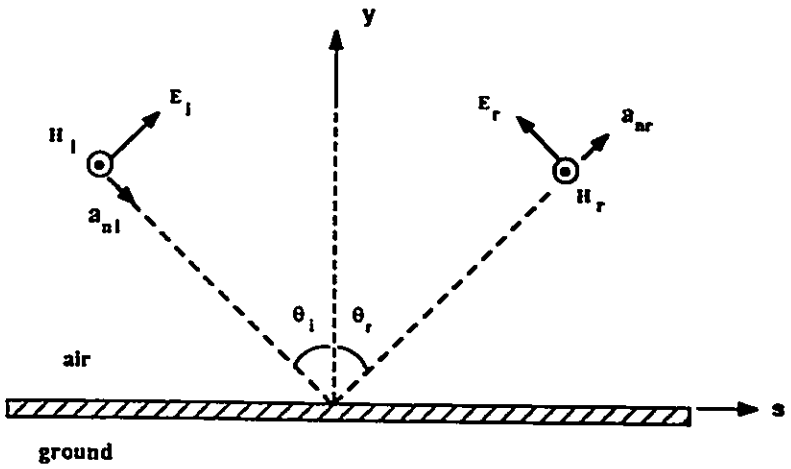

can be subsequently calculated from the E-field via Maxwell's equations.

To compute the applied time-varying electric field, parallel and perpendicular polarizations are considered. For parallel polarization, the electric field is parallel to the plane of incidence, and for perpendicular polarization, the electric field is perpendicular to the plane of incidence. In all cases, a perfect ground plane is considered so as to simplify the derivations for the expression of the incident field. For a lossy ground, the penetration of the electromagnetic field into the ground has already been taken into account by the transient skin-effect resistance defined in chapter 2. Under this circumstance, the total electric field impinging onto the transmission line will be the superposition of the its incident wave and the ground reflection:

$$\vec{E}_{total} = \vec{E}_i + \vec{E}_r \tag{3.1}$$

where $\vec{E}_i$ and $\vec{E}_r$ denote the incident and the reflected fields respectively. In Figure 3.2, an oblique incidence of a parallely-polarized electric field is outlined. The incident and the reflected fields with reference to this diagram can be written in terms of the directions $\vec{a}_s$ and $\vec{a}_y$ and the propagation constants $\vec{k}_i$ and $\vec{k}_r$:

$$\vec{E}_i = (\vec{a}_x E_x + \vec{a}_y E_y) \cdot e^{-j\vec{k}_i \cdot \vec{r}} \quad , \tag{3.2}$$

$$\vec{E}_r = (-\vec{a}_x E_x + \vec{a}_y E_y) \cdot e^{-j\vec{k}_r \cdot \vec{r}} \quad . \tag{3.3}$$

The dot product of the propagation constant $\vec{k}$ and the radius vector $\vec{r}$ in the two above equations can be evaluated as:

$$\begin{aligned} \vec{k}_i \cdot \vec{r} &= (\vec{a}_x k_x - \vec{a}_y k_y) \cdot (\vec{a}_x x + \vec{a}_y y) \ , \quad \text{where } s \leq 0 \, . \\ &= k_x x - k_y y \\ &= (\beta \sin\phi \cos\theta)\, x - (\beta \cos\phi)\, y \end{aligned} \tag{3.4}$$

$$\begin{aligned} \vec{k}_r \cdot \vec{r} &= (\vec{a}_x k_x + \vec{a}_y k_y) \cdot (\vec{a}_x x + \vec{a}_y y) \ , \quad \text{where } s \geq 0 \, . \\ &= k_x x + k_y y \\ &= (\beta \sin\phi \cos\theta)\, x + (\beta \cos\phi)\, y \end{aligned} \tag{3.5}$$

where θ is the angle of incidence, ϕ is the azimuth angle, and β is the phase constant. It follows from equations (3.1) to (3.5) that the total applied electric field can be derived as:

$$\begin{aligned} \vec{E}_{total} = \Big\{ & \vec{a}_x E_o \cos\theta \cos\phi \cdot \left[e^{-j\beta(x \sin\phi \cos\theta - y \cos\phi)} - e^{-j\beta(x \sin\phi \cos\theta + y \cos\phi)} \right] \\ & + \vec{a}_y E_o \sin\theta \cdot \left[e^{-j\beta(x \sin\phi \cos\theta - y \cos\phi)} + e^{-j\beta(x \sin\phi \cos\theta + y \cos\phi)} \right] \Big\} \cdot e^{-j\beta r} \quad , \end{aligned} \tag{3.6}$$

where the term $e^{-j\beta r}$ has taken into account the propagation of the incident wave from the source to the beginning of the line. The corresponding time-domain electric field can be derived by taking the inverse Laplace transform of the above equation, and is given by:

$$\vec{E}_{total} = \vec{a}_x \, e_- (x \, , y \, , t) \cdot \cos\theta \cos\phi \ + \vec{a}_y \, e_+ (x \, , y \, , t) \cdot \sin\theta \tag{3.7}$$

where the functions $e_{\pm}(x, y, t)$ are detailed in the form:

$$e_{\pm}(x, y, t) = f\left[t - \left(\frac{r + x\sin\phi\cos\theta - y\cos\phi}{c_o}\right)\right] \pm f\left[t - \left(\frac{r + x\sin\phi\cos\theta + y\cos\phi}{c_o}\right)\right] \quad . \tag{3.8}$$

In the above formula, c_o is the speed of light and r is the radial distance from the excitation source to the beginning of a transmission line. In matrix representation, the electric field components for parallel polarization are re-written as [12]:

$$\begin{bmatrix} E_x^e(x, y, t) \\ E_y^e(x, y, t) \end{bmatrix} = \begin{bmatrix} \cos\phi \cdot \cos\theta \cdot e_-(x, y, t) \\ \sin\theta \cdot e_+(x, y, t) \end{bmatrix} \tag{3.9}$$

and those for perpendicular polarization are put as:

$$\begin{bmatrix} E_x^e(x, y, t) \\ E_y^e(x, y, t) \end{bmatrix} = \begin{bmatrix} \sin\phi \cdot e_-(x, y, t) \\ 0 \end{bmatrix} \quad . \tag{3.10}$$

In equation (3.8), $f(t)$ is a function of the incident electric field which is taken in this research to be an electromagnetic pulse (EMP) of the double exponential form:

$$f(t) \approx E_o[exp(-\alpha t) - exp(-\beta t)] \tag{3.11}$$

where the rise time and the duration of the pulse depend on the coefficients α and β.

3.2 Equivalent sources to represent the external fields

The external time-varying electromagnetic field satisfies the local form of Maxwell's equations:

$$\nabla \times \vec{E} = -\frac{d\vec{B}}{dt} \quad , \tag{3.12}$$

$$\nabla \times \vec{B} = -\epsilon_o \mu_o \frac{d\vec{E}}{dt} \tag{3.13}$$

and can be determined by taking the surface integral of the two above equations such as:

$$\int_S \nabla \times \vec{E} \cdot d\vec{A} = -\frac{d}{dt} \int_S \vec{B} \cdot d\vec{A} \quad . \tag{3.14}$$

By using Stokes theorem, the surface integral of the curl of the electric field can be interpreted as the line integral of the electric field. It follows from equation (3.14) that this line integral of the electric field is proportional to the time rate of change of the magnetic flux crossing the plane perpendicular to the ground and passing through the transmission line:

$$\oint_\Gamma \vec{E} \cdot d\vec{l} = -\frac{d}{dt} \int_S \vec{B} \cdot d\vec{A} \quad . \tag{3.15}$$

By resolving the electric field and the magnetic field into their components described in the last section, equation (3.15) can be expressed in the explicit form:

$$\begin{aligned} &\int_0^h \left[E_y(x+\Delta x\,, y) - E_y(x\,, y)\right] dy \\ &- \left[E_x(x\,, h) - E_x(x\,, 0)\right] \cdot \Delta x \end{aligned} \tag{3.16}$$

$$= \quad -\frac{d}{dt} \int_x^{x+\Delta x} \int_0^h B_z(x\,, y)\; dy\, dx \quad .$$

By dividing equation (3.16) by Δx on both sides, and taking the limit $\Delta x \to 0$, one can

arrive at the following expression:

$$-\frac{d}{dx}\int_0^h E_y(x\,,y)\,dy = \frac{d}{dt}\int_0^h B_z(x\,,y)\,dy - [E_x(x\,,h) - E_x(x\,,0)] \quad . \tag{3.17}$$

where the line integral of the electric field on the left hand side is the voltage, v_e, induced onto the transmission line due to the y-component of the electric field, the line integral on the right hand side is the normal magnetic flux, Φ_z, and the last two terms represent the x-component of the electric field parallel to the transmission line. The equivalent expression of equation (3.17) is:

$$-\frac{dv_e}{dx} = \frac{d\Phi_z}{dt} - [E_x(x\,,h\,,t) - E_x(x\,,0\,,t)] \tag{3.18}$$

which indicates that the external time-varying electromagnetic field can be represented by an equivalent voltage source [4]. In equation (3.18), the electric field component, $E_x(x\,,0\,,t)$, tangential to the perfect ground plane is zero.

The total voltage $v(x,t)$ in the presence of the external field is the sum of the induced voltage $v_e(x,t)$ and the voltage on the line $u(x,t)$ in the absence of the external fields:

$$v(x\,,t) = u(x\,,t) + v_e(x\,,t) \quad . \tag{3.19}$$

By substitution of $v(x\,,t)$ in the classical transmission line equation, one can relate the induced voltage to the applied electromagnetic field as follows:

$$-\frac{du}{dx} = l_{ext}\frac{di}{dt} \quad , \tag{3.20}$$

$$-\frac{d(u+v_e)}{dx} = -\frac{du}{dx} - \frac{dv_e}{dx} \quad ,$$

$$-\frac{dv}{dx} = l_{ext}\frac{di}{dt} + \frac{d\Phi_z}{dt} - [E_x(x\,,h) - E_x(x\,,0)] \quad .$$

Similarly, the induced current on the transmission line can be related to the induced voltage as follows:

$$-\frac{di}{dx} = c_{st}\frac{du}{dt} \quad , \tag{3.21}$$

$$-\frac{di}{dx} = c_{st}\frac{d(v-v_e)}{dt} \quad ,$$

$$-\frac{di}{dx} = c_{st}\frac{dv}{dt} - c_{st}\frac{dv_e}{dt} \quad .$$

3.3 The classical and modified transmission line equations

In the absence of the external fields, the modified telegrapher's equations taking into account the transient skin-effect are [8]:

$$-\frac{\partial u(x\,,t)}{\partial x} = l_{ext}\frac{\partial i(x\,,t)}{\partial t} + \frac{\partial}{\partial t}\int_0^t r(t-t')\,i(x\,,t')\,dt' \quad , \tag{3.22}$$

$$-\frac{\partial i(x\,,t)}{\partial x} = c_{st}\frac{\partial u(x\,,t)}{\partial t} + g_o u(x\,,t) \tag{3.23}$$

where l_{ext} is the external line inductance, c_{st} is the line capacitance, and g_o is the line conductance. The function $r(t)$ in the modified line equation (3.22) is the transient skin-

effect resistance declared in chapter 2, and is given by the sum of the skin-effect resistance of the cylindrical conductor, $r_c(t)$ in equation (2.6), and the skin-effect resistance of the lossy ground, $r_g(t)$ in equation (2.8). Compared to the classical theory, the modified transmission line equations (3.22) and (3.23) take into account the transient skin-effect by means of a convolution integral whose kernel is proportional to the transient resistance.

In the presence of the incident electromagnetic fields, an equivalent voltage source and an equivalent current source derived in section 3.2 are added to the line equations (3.22) and (3.23). As a result, the new transmission line equations are:

$$\begin{aligned} -\frac{\partial v(x,t)}{\partial x} &= l_{ext}\ \frac{\partial i(x,t)}{\partial t} + \frac{\partial}{\partial t}\int_0^t r(t-t')\cdot i(x,t')\,dt' \\ &+\ \frac{\partial \Phi_z}{\partial t} - [E_x(x,h) - E_x(x,0)]\quad , \end{aligned} \tag{3.24}$$

$$\begin{aligned} -\frac{\partial i(x,t)}{\partial x} &= c_{st}\ \frac{\partial v(x,t)}{\partial t} + g_o v(x,t) \\ &-\ \left(c_{st}\frac{\partial}{\partial t} + g_o\right)\cdot \int_0^h E_y(x,y,t)\,dy\ . \end{aligned} \tag{3.25}$$

by means of which the induced voltage and its propagation on a lossy transmission line is investigated and studied throughout the research.

3.4 The determination of the magnetic flux

In the new transmission line equations, the unknown quantities are $v(x,t)$ and $i(x,t)$ that can be solved by applying numerical techniques, whereas the known quantities are the transient skin-effect resistance marked out in chapter 2 and the external electric field formulated in sections 3.1 and 3.2. At the same time, the time derivative of the normal component of the magnetic field can be expressed in terms of the electric field by using Faraday's law of induction. Since Φ_z is the area integral of the magnetic flux density B_z, the incident flux can be related to the incident electric field by equating the curl of the electric field proportional to the time derivative of the magnetic induction:

$$\nabla \times \vec{E} = -\frac{\partial \vec{B}}{\partial t} \quad . \tag{3.26}$$

The left hand side of equation (3.26) has been simplified and written as:

$$\vec{a_z}\left(\frac{\partial E_y}{\partial x} - \frac{\partial E_x}{\partial y}\right) \tag{3.27}$$

while the right hand side is re-written in the form:

$$\left(-\mu_o \frac{\partial H_z}{\partial t}\right)\vec{a}_z \quad . \tag{3.28}$$

These two expressions (3.27) and (3.28) will combine to form the equation:

$$-\mu_o \frac{\partial H_z}{\partial t} = \frac{\partial E_y}{\partial x} - \frac{\partial E_x}{\partial y} \tag{3.29}$$

and the corresponding integral of this equation will appear as:

$$-\mu_o \int_0^h \frac{\partial}{\partial t} H_z(x, y, t)\, dy = \int_0^h \left(\frac{\partial}{\partial x} E_y - \frac{\partial}{\partial y} E_x\right) dy \quad . \tag{3.30}$$

In this equation, the line integral of the left hand side is, in fact, the time derivative of total magnetic flux normal to the plane perpendicular to the ground and passing through the transmission line above ground. It follows that

$$-\frac{\partial \Phi_z}{\partial t} = \int_0^h \left(\frac{\partial}{\partial x} E_y - \frac{\partial}{\partial y} E_x \right) dy \quad . \tag{3.31}$$

Hence, the normal component of the magnetic flux can be calculated given the values of E_x and E_y.

Chapter 4

The time-domain finite-difference approach

The modified transmission line equations discussed in chapter 3 consist of an integral-differential equation governing the induced voltage onto the lossy conductor line due to the time-varying electromagnetic field. In order to solve the integral-differential equation for the induced voltage and its propagation on the line, the time-domain finite-difference method is recommended.

4.1 The finite-difference algorithm

In the finite-difference algorithm, space and time discretizations are used. The discretization space step will be represented by k, and the time step by l. In Figure 4.1, the space discretization of a conductor line is shown. On the transmission line, two sets of nodes are imposed; one set represents the nodal voltages $v_{k,l}$, while the other set stands for the nodal currents $w_{k-1/2,l}$, and the positions of these nodal voltages and currents alternate along the length of the line.

To calculate the voltage $v_{k,l+1}$, equation (4.47) is used. Figure 4.2 shows an example to compute the voltage $v_{1,1}$. It is calculated from the voltage $v_{1,0}$, the current $w_{3/2,0}$, and the current $w_{1/2,0}$. Next, the current $w_{k-1/2,l+1}$ is calculated by using equation (4.48). Figure 4.3 displays an example to evaluate the current $w_{1/2,1}$. It is obtained from the current $w_{1/2,0}$, the voltage $v_{1,1}$, and the voltage $v_{0,1}$. Once the current $w_{1/2,1}$ is known, the value of the current $w_{3/2,0}$ is updated as shown in Figure 4.4. In general, the equation used to update the current at the most recent previous time step and at the next space step is $w_{k+1/2,l} = w_{k-1/2,l+1}$. The above procedure demonstrated in the three figures will

Figure 4.1: Space Discretizations of a Transmission Line

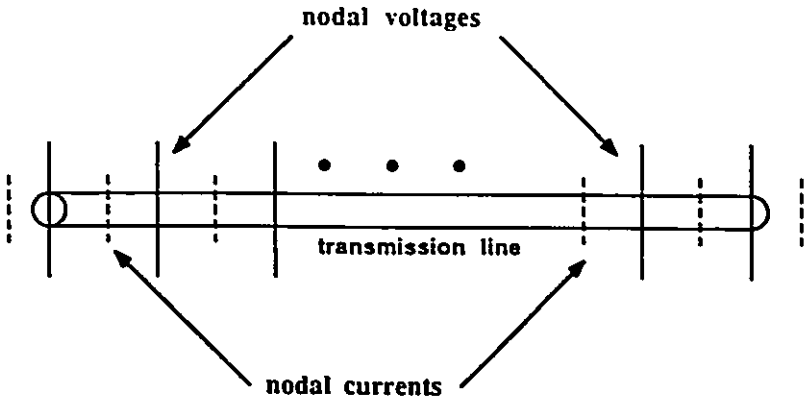

Figure 4.2: Calculation of Induced Voltage $v_{1,1}$

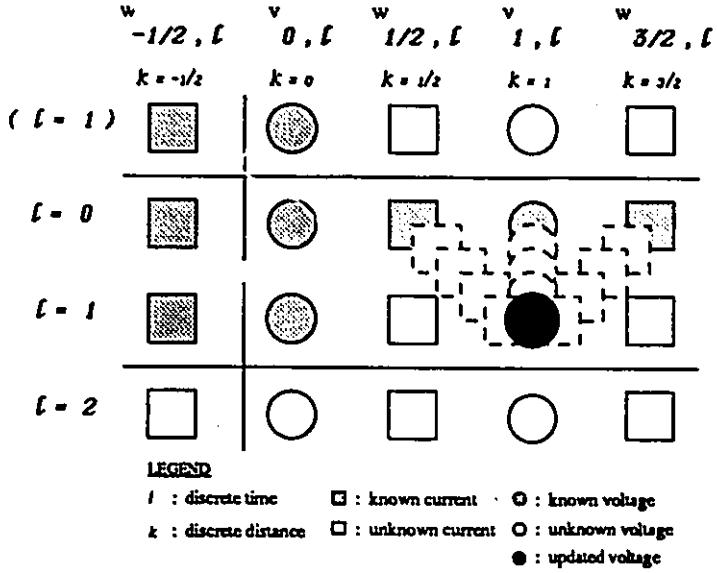

Figure 4.3: Calculation of Induced Current $w_{1/2,1}$

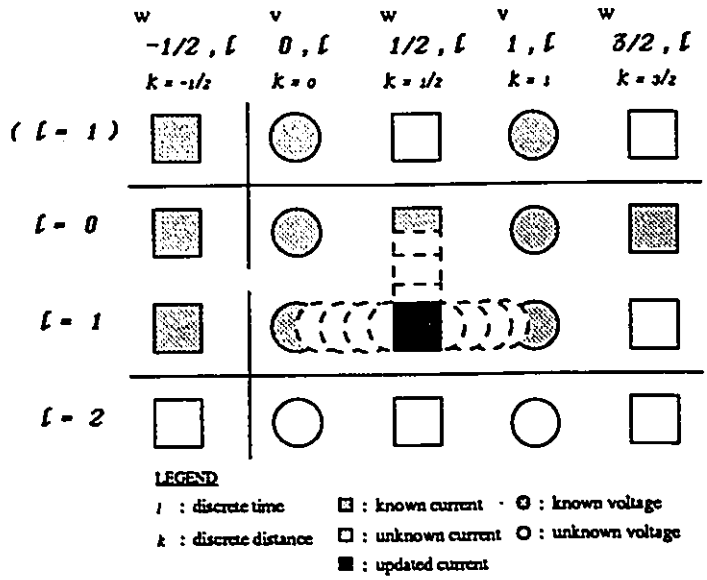

Figure 4.4: Calculation of Induced Current $w_{3/2,0}$

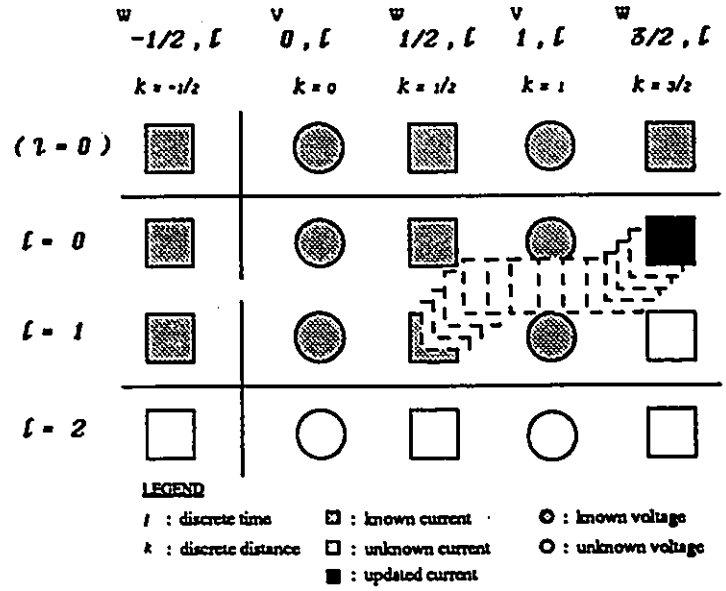

Figure 4.5: The Finite Difference Algorithm

```
For timestep=0, maxtimestep,1
   For  spacestep=0, maxspacestep,1
      If ( 0 < spacestep < max ) then
        V[ spacestep, timestep+1 ] : =  g1 * V[ spacestep, timestep ] - g2 * { I[ spacestep+1, timestep ]
                                        - I[ spacestep, timestep ] } + field ;
        I[ spacestep, timestep+1 ] : = g3 * I[ spacestep, timestep ] - g4 * { V[spacestep, timestep+1]
                                       - V[ spacestep-1, timestep+1 ] }  + g5 * skin-effect  - g6 * field ;
        I[ spacestep+1, timestep ] : = I [spacestep, timestep+1 ] ;
      else if  ( spacestep = 0 ) then
         calculate  V[ 0, timestep ]  from boundary conditions;
      else
         calculate  V[ maxspacestep, timestep ]  from boundary conditions;
      endif
   endfor
endfor
```

be repeated to obtain the voltage at the next space step and at the same time step. The finite-difference algorithm is easily programmed and the corresponding pseudo-codes are listed in Figure 4.5.

The finite-difference algorithm makes use of a recursive procedure. Given the initial conditions, the voltage $v_{k=1,l=1}$ is calculated. Next, the current $w_{k=-1/2,l=1}$ is evaluated by using the voltage $v_{1,1}$, the incident flux, and the initial conditions. The calculated voltage $v_{1,1}$, and current $w_{-1/2,1}$, then, form part of the history from which the voltage $v_{k=2,l=1}$ is computed. This iterative process continues until the space step k reaches the maximum and all of the nodal voltages on the transmission line have been found. The process will resume again at the next time step $l = 2$ for the space steps $k = 0, 1, 2, ...M$. The voltage on the transmission line will finally converge at the maximum time step $l = N$.

4.2 The discretization of telegrapher's equations

The numerical technique for the discretization of telegrapher's equations will be explained in the following sections.

4.2.1 Normalized variables and finite-difference formulas

For simplicity, the following parameters are used for the modified telegrapher's equations:

$$t_n = \frac{t}{\tau_g} \quad , \tag{4.1}$$

$$\xi = \frac{x}{v_{ph}\tau_g} \quad , \tag{4.2}$$

$$\rho(t) = \frac{r(t)}{r_o} \quad , \tag{4.3}$$

$$w = Z_o \cdot i \quad , \tag{4.4}$$

where r_o is the d.c. resistance, Z_o is the characteristic impedance of the line, i is the current , and v_{ph} is the phase velocity given by the following formula:

$$v_{ph} = \frac{1}{\sqrt{l_{ext}c_{st}}} \quad . \tag{4.5}$$

In terms of the normalized parameters defined in equations (4.1) to (4.4), the modified telegrapher's equations become:

$$-\frac{\partial v(\xi\,,t_n)}{\partial \xi} = \frac{w(\xi,t_n)}{\partial t_n} + \nu_r \frac{\partial}{\partial t_n}\int_0^{t_n} \rho(t_n - t_n')\, w(\xi\,,t_n')\, dt_n' + v_{ph}\tau_g \left\{ \frac{\partial \Phi_z(\xi\,,t_n)}{\tau_g \partial t_n} - E_x(\xi\,,\xi'\,,t_n) + E_x(\xi\,,0\,,t_n) \right\} \quad , \tag{4.6}$$

$$-\frac{\partial w(\xi\,,t_n)}{\partial \xi} = \frac{\partial v(\xi\,,t_n)}{\partial t_n} + \nu_g v(\xi\,,t_n) - \left\{ \frac{\partial}{\partial t_n} + \nu_g \right\} \cdot \int_0^h E_y(\xi\,,\xi'\,,t_n)\, d\xi' \,, \tag{4.7}$$

where the coefficients ν_r, ν_g and ξ' are defined as:

$$\nu_r = \frac{r_o v_o \tau_g}{Z_o} \quad , \tag{4.8}$$

$$\nu_g = g_o v_o \tau_g Z_o \quad , \tag{4.9}$$

$$\xi' = \frac{h}{v_o \tau_g} \quad . \tag{4.10}$$

Furthermore, the normalized distance, ξ, and the normalized time, t_n, are expressed in terms of the space step k and the time step l:

$$\xi = k \cdot \Delta\xi \, , 0 \leq k \leq \left(\frac{\xi_{max}}{\Delta\xi}\right) \quad , \tag{4.11}$$

$$t_n = l \cdot \Delta t_n \, , 0 \leq l \leq \left(\frac{t_{n,max}}{\Delta t_n}\right) \quad . \tag{4.12}$$

The partial derivatives of the voltage and current with respect to time or with respect to the distance of propagation in the line equations (4.6) and (4.7) can be substituted by the forward finite-difference formulas in terms of the space step k and the time step l:

$$\frac{\partial v(\xi, t_n)}{\partial \xi} \approx \frac{1}{\Delta\xi}\left(v_{k,l+1} - v_{k-1,l+1}\right) \quad , \tag{4.13}$$

$$\frac{\partial w(\xi, t_n)}{\partial \xi} \approx \frac{1}{\Delta\xi}\left(w_{k+\frac{1}{2},l} - w_{k-\frac{1}{2},l}\right) \quad , \tag{4.14}$$

$$\frac{\partial v(\xi, t_n)}{\partial t_n} \approx \frac{1}{\Delta t_n}\left(v_{k,l+1} - v_{k,l}\right) \quad , \tag{4.15}$$

$$\frac{\partial w(\xi, t_n)}{\partial t_n} \approx \frac{1}{\Delta t_n}\left(w_{k-\frac{1}{2},l+1} - w_{k-\frac{1}{2},l}\right) \quad . \tag{4.16}$$

Simultaneously, the voltage, the current and the incident electric field are approximated by the mean finite-difference formulas:

$$v(\xi, t_n) \approx \frac{1}{2}(v_{k,l+1} + v_{k,l}) \quad , \tag{4.17}$$

$$w(\xi, t_n) \approx \frac{1}{2}\left(w_{k-\frac{1}{2},l+1} + w_{k-\frac{1}{2},l}\right) \quad , \tag{4.18}$$

$$E_y(\xi, t_n) \approx \frac{1}{2}\left(E^y_{k,l+1} + E^y_{k,l}\right) \quad , \tag{4.19}$$

$$E_x(\xi, t_n) \approx \frac{1}{2}\left(E^x_{k,l+1} + E^x_{k,l}\right) \quad . \tag{4.20}$$

4.2.2 The discretization of the integral differential term

By using Simpson's rule, the integral-differential term which takes into account the transient skin-effect in a transmission line can be expressed as a series [7]. From Leibniz theorem, the integral-differential term is written as:

$$\frac{\partial}{\partial t_n}\int_0^{t_n} \rho(t'_n)\, w(\xi, t'_n)\, dt'_n = \rho(0)\, w(\xi, t_n) + \int_0^{t_n} \frac{\partial}{\partial t_n}[\rho(t_n - t'_n)] \cdot w(\xi, t'_n)\, dt'_n \quad , \tag{4.21}$$

where $\rho(t_n) < \infty$ for $0 \leq t_n \leq \infty$. The integral in the above equation can be expanded by using trapezium formula:

$$\begin{aligned} \frac{\partial}{\partial t_n}\int_0^{t_n} \rho(t_n - t'_n)\, w(\xi, t'_n)\, dt'_n \approx\ & \rho_o \cdot w_{k,l} + \left\{\frac{1}{2}\rho' \cdot w_{k,l} + \rho'_1 \cdot w_{k,l-1}\right. \\ & + \cdots + \rho'_m \cdot w_{k,m} + \cdots \\ & + \left.\rho'_{l-1} \cdot w_{k,1} + \frac{1}{2}\rho'_l \cdot w_{k,0}\right\} \cdot \Delta t_n \end{aligned} \tag{4.22}$$

where ρ'_m is the time derivative of the normalized transient skin-effect resistance which can be interpreted in terms of the forward finite-difference formula:

$$\rho'_m = \frac{1}{\Delta t_n}(\rho_{m+1} - \rho_m) \quad . \tag{4.23}$$

If the first term in equation (4.22) is also replaced by the mean finite-difference formula:

$$\rho_o \cdot w_{k,l} \approx \frac{1}{2}\left(\rho_o \cdot w_{k,l+1} + \rho_1 \cdot w_{k,l}\right) \quad , \tag{4.24}$$

then the integral-differential term will appear as:

$$\begin{aligned} \frac{\partial}{\partial t_n}\int_0^{t_n} \rho\left(t_n - t'_n\right) \cdot w\left(\xi\ , t'_n\right) dt'_n \quad = \quad & \frac{1}{2}\rho_o \cdot w_{k,l+1} + \frac{1}{2}\rho_1 \cdot w_{k,l} \\ & + \frac{1}{2}\left(\rho_1 - \rho_0\right) w_{k,l} + \left(\rho_2 - \rho_1\right) \cdot w_{k,l-1} + \cdots \\ & + \left(\rho_{l-m+1} - \rho_{l-m}\right) \cdot w_{k,m} + \cdots \\ & + \left(\rho_l - \rho_{l-1}\right) \cdot w_{k,1} + \frac{1}{2}\left(\rho_{l+1} - \rho_l\right) \cdot w_{k,0} \quad , \end{aligned} \tag{4.25}$$

and after simplification, the numerical integration formula to be used in the finite-difference algorithm is given by:

$$\begin{aligned} \frac{\partial}{\partial t_n}\int_0^{t_n} \rho\left(t_n - t'_n\right) \cdot w\left(\xi\ , t'_n\right) dt_n \quad \approx \quad & \frac{1}{2}\rho_o \cdot w_{k,l+1} - \frac{1}{2}\left(\rho_o - 2\rho_1\right) \cdot w_{k,l} \\ & + \sum_{m=0}^{l-1} \left(\rho_{l-m+1} - \rho_{l-m}\right) \cdot w_{k,m} \quad . \end{aligned} \tag{4.26}$$

4.2.3 The incident electric field formulation

In this section, the function of the incident electric field is referred to that described in chapter 3. The mean finite-difference formula for the x-component of the incident electric field is given by:

$$E_x\left(\xi\ , \xi'\ , t_n\right) \approx \left(E^x_{k,l+1} + E^x_{k,l}\right) \tag{4.27}$$

where the discretization variables $E^x_{k,l+1}$ and $E^x_{k,l}$ for parallel polarization of the electric field will be:

$$E^x_{k,l+1} = \cos\phi\cos\theta \cdot e_-\left(k\Delta\xi\,, k'\Delta\xi'\,, (l+1)\,\Delta t_n\right) \quad , \tag{4.28}$$

$$E^x_{k,l} = \cos\phi\cos\theta \cdot e_-\left(k\Delta\xi\,, k'\Delta\xi'\,, l\Delta t_n\right) \quad , \tag{4.29}$$

and for perpendicular polarization, they will be:

$$E^x_{k,l+1} = \sin\phi \cdot e_-\left(k\Delta\xi\,, k'\Delta\xi'\,, (l+1)\,\Delta t_n\right) \quad , \tag{4.30}$$

$$E^x_{k,l} = \sin\phi \cdot e_-\left(k\Delta\xi\,, k'\Delta\xi'\,, l\Delta t_n\right) \quad . \tag{4.31}$$

In the above equation, the functions $e_-(\xi\,, \xi'\,, t_n)$ defined in equation (3.8) will also be written in terms of the space step k and the time step l as:

$$e_-(\xi\,, \xi'\,, t_n) = f\left\{t_n\tau_g - \left(\frac{r + \xi v_{ph}\tau_g \sin\phi\cos\theta - \xi'\cos\phi}{v_{ph}}\right)\right\} - f\left\{t_n\tau_g - \left(\frac{r + \xi v_{ph}\tau_g \sin\phi\cos\theta + \xi'\cos\phi}{v_{ph}}\right)\right\} \quad . \tag{4.32}$$

Moreover, from the function of the incident electric field defined in chapter 3, the induced electromagnetic force , $v_e(\xi\,, t_n)$, which is the line integral of $E_y(\xi\,, \xi'\,, t_n)$, is obtained as:

$$v_e(\xi\,, t_n) = \begin{cases} \int_0^h \sin\theta \cdot e_+(\xi\,, \xi'\,, t_n)\, d\xi' \,, \text{for parallel polarization} \quad , \\ 0 \,, \text{for perpendicular polarization} \quad , \end{cases} \tag{4.33}$$

where $e_+(\xi\ ,\xi'\ ,t_n)$ has been defined in equation (3.8). The numerical integration of the above equation can be represented by the sum:

$$v_e(\xi\ ,t_n) \approx \sum_{k'=0}^{k'=l'} \sin\theta \cdot e_+(k\Delta\xi\ ,k'\Delta\xi'\ ,t_n) \cdot v_{ph}\tau_g\Delta\xi' \quad , \tag{4.34}$$

where the maximum space step l' for the summation is:

$$l' = h - v_{ph}\tau_g\Delta\xi' \quad . \tag{4.35}$$

Next, the induced emf $v_e(\xi\ ,t_n)$ is re-written by using the mean finite-difference formula:

$$v_e(\xi\ ,t_n) \approx \frac{1}{2}\left(v^e_{k,l+1} + v^e_{k,l}\right) \quad , \tag{4.36}$$

and the time derivative of $v_e(\xi\ ,t_n)$ is replaced by the forward finite-difference formula:

$$\frac{\partial v_e(\xi\ ,t_n)}{\partial t_n} \approx \frac{1}{\Delta t_n}\left(v^e_{k,l+1} - v^e_{k,l}\right) \quad , \tag{4.37}$$

where from equation (4.34), the variables $v^e_{k,l+1}$ and $v^e_{k,l}$ are put as:

$$v^e_{k,l+1} \approx \sum_{k'=0}^{k'=l'} \sin\theta \cdot e_+(k\Delta\xi\ ,k'\Delta\xi'\ ,(l+1)\,\Delta t_n) \cdot \Delta\xi' v_{ph}\tau_g \quad , \tag{4.38}$$

$$v^e_{k,l} \approx \sum_{k'=0}^{k'=l'} \sin\theta \cdot e_+(k\Delta\xi\ ,k'\Delta\xi'\ ,l\Delta t_n) \cdot \Delta\xi' v_{ph}\tau_g \quad . \tag{4.39}$$

The final expressions for the induced emf $v_e(\xi, t_n)$, and its time derivative to be used in the finite-difference algorithm are re-instated as follows:

$$v_e(\xi, t_n) \approx \frac{\nu_o \tau_g \Delta\xi'}{2} \sum_{k'=0}^{k'=l'} \sin\theta \cdot [e_+(k\Delta\xi, k'\Delta\xi', (l+1)\Delta t_n) + e_+(k\Delta\xi, k'\Delta\xi', l\Delta t_n)] \quad , \tag{4.40}$$

$$\frac{\partial v_e(\xi, t_n)}{\partial t_n} \approx \frac{\nu_o \tau_g \Delta\xi'}{\Delta t_n} \sum_{k'=0}^{k'=l'} \sin\theta \cdot [e_+(k\Delta\xi, k'\Delta\xi', (l+1)\Delta t_n) - e_+(k\Delta\xi, k'\Delta\xi', l\Delta t_n)] \quad . \tag{4.41}$$

4.2.4 The discretization formula of the time derivative of the normal flux

The time derivative of the magnetic flux normal to the plane perpendicular to the ground and passing through the transmission line can be expressed in terms of the resolved components of the incident electric field as shown in chapter 3. So, the discretization of the time derivative of the normal flux will be carried out by using the discretization formulas of the electric field.

For parallel polarization, the derivative of $E_y(x, y, t)$ with respect to the propagation distance x is:

$$\begin{aligned} \frac{\partial E_y(x, y, t)}{\partial x} = \sin\theta \Big\{ & ex1(x, y, t) \cdot \frac{\alpha}{v_{ph}} \sin\phi\cos\theta \\ & - ex2(x, y, t) \cdot \frac{\beta}{v_{ph}} \sin\phi\cos\theta \\ & + ex3(x, y, t) \cdot \frac{\alpha}{v_{ph}} \sin\phi\cos\theta \\ & - ex4(x, y, t) \cdot \frac{\beta}{v_{ph}} \sin\phi\cos\theta \Big\} \quad , \end{aligned} \tag{4.42}$$

where the coefficients α and β are the coefficients in the double exponential form of the incident electric field, and where

$$
\begin{aligned}
ex1\,(x\,,y\,,t) &= exp\left\{-\alpha\left(t-\frac{r+x\sin\phi\cos\theta-y\cos\phi}{v_{ph}}\right)\right\} \quad , \\
ex2\,(x\,,y\,,t) &= exp\left\{-\beta\left(t-\frac{r+x\sin\phi\cos\theta-y\cos\phi}{v_{ph}}\right)\right\} \quad , \\
ex3\,(x\,,y\,,t) &= exp\left\{-\alpha\left(t-\frac{r+x\sin\phi\cos\theta+y\cos\phi}{v_{ph}}\right)\right\} \quad , \\
ex4\,(x\,,y\,,t) &= exp\left\{-\beta\left(t-\frac{r+x\sin\phi\cos\theta+y\cos\phi}{v_{ph}}\right)\right\} \quad .
\end{aligned}
$$

In a similar manner, the derivative of $E_x\,(x\,,y\,,t)$ with respect to the vertical distance y is expressed as:

$$
\begin{aligned}
\frac{\partial E_x\,(x\,,y\,,t)}{\partial y} = \quad & \cos\phi\cos\theta\left\{ex1\,(x\,,y\,,t)\cdot\left(-\frac{\alpha}{v_{ph}}\cos\phi\right)\right. \\
& -ex2\,(x\,,y\,,t)\cdot\left(-\frac{\beta}{v_{ph}}\right) \\
& -ex3\,(x\,,y\,,t)\cdot\frac{\alpha}{v_{ph}}\cos\phi \\
& \left.+\,ex4\,(x\,,y\,,t)\cdot\frac{\beta}{v_{ph}}\cos\phi\right\} \quad .
\end{aligned} \tag{4.43}
$$

By putting the two above equations (4.42) and (4.43) in equation (3.31), the corresponding discretization formula of the normal flux is derived as:

$$
\begin{aligned}
-\frac{\partial\Phi_z}{\tau_g\partial t_n} \approx \quad & v_{ph}\tau_g\sum_{\xi'=0}^{h-\Delta\xi'}\left\{\sin\theta\left[ex1\,(\xi\,,\xi'\,,t_n)\cdot\frac{\alpha}{v_{ph}}\sin\phi\cos\theta\right.\right. \\
& -ex2\,(\xi\,,\xi'\,,t_n)\cdot\frac{\beta}{v_{ph}}\sin\phi\cos\theta \\
& +ex3\,(\xi\,,\xi'\,,t_n)\cdot\frac{\alpha}{v_{ph}}\sin\phi\cos\theta \\
& \left.-\,ex4\,(\xi\,,\xi'\,,t_n)\cdot\frac{\beta}{v_{ph}}\sin\phi\cos\theta\right] \\
& -\cos\phi\cos\theta\left[ex1\,(\xi\,,\xi'\,,t_n)\cdot\left(-\frac{\alpha}{v_{ph}}\cos\phi\right)\right. \\
& -ex2\,(\xi\,,\xi'\,,t_n)\cdot\left(-\frac{\beta}{v_{ph}}\right)-ex3\,(\xi\,,\xi'\,,t_n)\cdot\frac{\alpha}{v_{ph}}\cos\phi \\
& \left.\left.+\,ex4\,(\xi\,,\xi'\,,t_n)\cdot\frac{\beta}{v_{ph}}\cos\phi\right]\right\} \quad .
\end{aligned} \tag{4.44}
$$

For perpendicular polarization, $E_x(x\,,y\,,t)$ is the only component of the electric field incident on the transmission line. In addition, the time derivative of the normal flux in equation (3.31) is now only dependent on the value of $E_x(x\,,y\,,t)$. With reference to equation (3.10), the derviative $\frac{\partial E_x(x\,,y\,,t)}{\partial y}$ is given by:

$$\begin{aligned}\frac{\partial E_x(x\,,y\,,t)}{\partial y} \;=\;& \sin\phi\left\{ex1\,(x\,,y\,,t)\cdot\left(-\frac{\alpha}{v_{ph}}\cos\phi\right)\right. \\ & -ex2\,(x\,,y\,,t)\cdot\left(-\frac{\beta}{v_{ph}}\right) \\ & -ex3\,(x\,,y\,,t)\cdot\frac{\alpha}{v_{ph}}\cos\phi \\ & \left.+\,ex4\,(x\,,y\,,t)\cdot\frac{\beta}{v_{ph}}\cos\phi\right\}\quad,\end{aligned} \tag{4.45}$$

and the corresponding discretization formula for the time derivative of the normal flux is, therefore,:

$$\begin{aligned}-\frac{\partial\Phi_z}{\tau_g\partial l_n} \;\approx\;& v_{ph}\tau_g\sum_{\xi'=0}^{h-\Delta\xi'}\sin\phi\left\{ex1\,(\xi\,,\xi'\,,t_n)\cdot\left(-\frac{\alpha}{v_{ph}}\cos\phi\right)\right. \\ & -ex2\,(\xi\,,\xi'\,,t_n)\cdot\left(-\frac{\beta}{v_{ph}}\right) \\ & -ex3\,(\xi\,,\xi'\,,t_n)\cdot\frac{\alpha}{v_{ph}}\cos\phi \\ & \left.+\,ex4\,(\xi\,,\xi'\,,t_n)\cdot\frac{\beta}{v_{ph}}\cos\phi\right\}\quad.\end{aligned} \tag{4.46}$$

Finally, by substitution of the above discretization formulas in the modified line equations presented in chapter 3, the discretized telegrapher's equations turns out to be:

$$\begin{aligned}v_{k,l+1} \;=\;& \left(\frac{1-\nu_g\frac{\Delta t_n}{2}}{1+\nu_g\frac{\Delta t_n}{2}}\right)v_{k,l}-\left(\frac{\frac{\Delta t_n}{\Delta\xi}}{1+\nu_g\frac{\Delta t_n}{2}}\right)\cdot\left(w_{k+\frac{1}{2},l}-w_{k-\frac{1}{2},l}\right)\;+ \\ & \left(\frac{1}{1+\nu_g\frac{\Delta t_n}{2}}\right)\cdot\left(\Delta t_n\cdot\tau_g\cdot\frac{\Delta v_e(\xi\,,t_n)}{\Delta t_n\cdot\tau_g}+\nu_g\cdot\Delta t_n\cdot v_e(\xi\,,t_n)\right)\quad,\end{aligned} \tag{4.47}$$

$$
\begin{aligned}
w_{k-\frac{1}{2},l+1} \quad = \quad & \left(\frac{1+\frac{1}{2}\nu_r\Delta t_n\left(\rho_o-2\rho_1\right)}{1+\frac{1}{2}\nu_r\rho_o\Delta t_n}\right) w_{k-\frac{1}{2},l} \quad - \\
& \left(\frac{\Delta t_n}{1+\frac{1}{2}\nu_r\rho_o\Delta t_n}\right)\cdot\left(v_{k,l+1}-v_{k-1,l+1}\right) \quad + \\
& \left(\frac{\nu_r\Delta t_n}{1+\frac{1}{2}\nu_r\rho_o\Delta t_n}\right)\cdot\left(\sum_{m=0}^{l-1}\rho_{l-m+1}-\rho_{l-m}\right) w_{k-\frac{1}{2},m} \quad - \\
& \left(\frac{v_o\tau_g\Delta t_n}{1+\frac{1}{2}\nu_r\rho_o\Delta t_n}\right)\cdot\left(\frac{\Delta\Phi_z}{\tau_g\Delta t_n}+E_x\left(\xi\ ,h\ ,t_n\right)-E_x\left(\xi\ ,0\ ,t_n\right)\right) \quad .
\end{aligned}
\tag{4.48}
$$

where ρ_o is the normalized skin-effect resistance at the zero time step, $l = 0$, and ρ_1 is the normalized skin-effect resistance at the first time step, $l = 1$.

Chapter 5

The boundary conditions

The discretization telegrapher's equations discussed in the last chapter can be solved together with the boundary conditions representing the loads at the two ends of a transmission line. In this chapter, the finite-difference equation for a linear load connected to the beginning or the end of a transmission line is presented.

5.1 Boundary conditions at the receiving end

The boundary condition at the receiving end of a transmission line and the corresponding finite-difference formula presented in the following sections is primarily for a (1) purely resistive, (2) purely capacitive or (3) purely inductive load. For any other combination of linear loads, the boundary condition can be described by the composition of these discretization formulas.

5.1.1 Purely resistive load

For a transmission line terminated in a purely resistive load at the receiving end, the boundary condition is given by:

$$v = R_2 \cdot i \quad , \tag{5.1}$$

where $R_2 = Z_2$ is the load referred to Figure 3.1. If the maximum space step is m, where $m = \frac{\xi_{max}}{\Delta\xi}$, then the finite-difference formula corresponding to the boundary condition will be:

$$v_{m,l+1} = \frac{R_2}{Z_o} \cdot w_{m+\frac{1}{2},l} \quad . \tag{5.2}$$

By substitution of the above equation in the discretized telegrapher's equation (4.47), the voltage at the load can be derived and is given by:

$$\begin{aligned} v_{m,l+1} \quad = \quad & \left\{ \frac{1 + \frac{1}{2}\nu_g \Delta t_n}{\left(1 + \frac{1}{2}\nu_g \Delta t_n + \frac{\Delta t_n}{\Delta \xi} \cdot \frac{Z_o}{R_2}\right)} \right\} \cdot \\ & \left\{ \left(\frac{1 - \frac{1}{2}\nu_g \Delta t_n}{1 + \frac{1}{2}\nu_g \Delta t_n} v_{m,l} \right) + \left(\frac{\frac{\Delta t_n}{\Delta \xi}}{1 + \frac{1}{2}\nu_g \Delta t_n} \right) w_{m-\frac{1}{2},l} \right\} \quad + \\ & \left(\frac{1}{1 + \frac{1}{2}\nu_g \Delta t_n} \right) \left\{ \frac{1}{\Delta t_n} \left(v^e_{k,l+1} - v^e_{k,l} \right) + \nu_g v_e \left(\xi \, , t_n \right) \right\} \quad . \end{aligned} \tag{5.3}$$

5.1.2 Purely capacitive load

For a transmission line terminated in a purely capacitive load at the receiving end, the boundary condition is represented by:

$$i = C_2 \frac{dv}{dt} \quad , \tag{5.4}$$

where $sC_2 = \frac{1}{Z_2}$ is the capacitive reactance written in Laplace domain. The replacement of the time-derivative of the voltage in the above equation by the forward finite-difference formula yields the following expression for this boundary condition:

$$w_{m+\frac{1}{2},l} = \frac{Z_o C_2}{\tau_g \Delta t_n} \cdot \left(v_{m,l+1} - v_{m,l} \right) \quad . \tag{5.5}$$

By putting the above expression in the discretized telegrapher's equation (4.47), the voltage at the load can be determined and is written as:

$$v_{m,l+1} = \left(\frac{k_1\tau_g\Delta t_n + k_2 Z_o C_2}{\tau_g\Delta t_n + k_2 Z_o C_2}\right) v_{m,l} + \left(\frac{k_2\tau_g\Delta t_n}{\tau_g\Delta t_n + k_2 Z_o C_2}\right) w_{k-\frac{1}{2},l} + \left(\frac{\tau_g\Delta t_n}{\tau_g\Delta t_n + k_2 Z_o C_2}\right)\left\{v^e_{k,l+1} - k_1 v^e_{k,l}\right\} \quad , \tag{5.6}$$

where the coefficients k_1 and k_2 are defined as:

$$k_1 = \frac{1 - \frac{1}{2}g_o v_{ph}\tau_g Z_o \Delta t_n}{1 + \frac{1}{2}g_o v_{ph}\tau_g Z_o \Delta t_n} \quad , \tag{5.7}$$

$$k_2 = \frac{\frac{\Delta t_n}{\Delta \xi}}{1 + \frac{1}{2}g_o v_{ph}\tau_g Z_o \Delta t_n} \quad . \tag{5.8}$$

5.1.3 Purely inductive load

For a transmission line terminated in a purely inductive load at the receiving end, the boundary condition is taken as:

$$v = L_2\frac{di}{dt} \quad , \tag{5.9}$$

where $sL_2 = Z_2$ is the inductive reactance written in Laplace domain. The finite-difference formula equivalent to this boundary condition has been derived [8] and is transcribed by:

$$w_{m+\frac{1}{2},l} = \frac{Z_o\tau_g\Delta t_n}{L_2} v_{m,l+1} + \frac{Z_o\tau_g\Delta t_n}{L_2}\sum_{n=3}^{n=l} v_{m,n} \quad . \tag{5.10}$$

By substitution of the above expression in the discretized telegrapher's equation (4.47), the voltage at the load can be obtained and stated as:

$$
\begin{aligned}
v_{m,l+1} \;=\; & \left(\frac{L_2}{L_2 + k_2 Z_o \tau_g \Delta t_n}\right)\left\{k_1 \cdot v_{m,l} - k_2 \cdot w_{k=0-\frac{1}{2},l}\right\} \\
& + \frac{k_2 Z_o \tau_g \Delta t_n}{L + k_2 Z_o \tau_g \Delta t_n} \cdot \sum_{n=3}^{n=l} v_{m,n} \\
& - \left(\frac{k_2 Z_o \tau_g \Delta t_n}{L_2 + k_2 Z_o \tau_g \Delta t_n}\right)\left\{v^c_{k,l+1} - v^c_{k,l}\right\} \quad .
\end{aligned} \tag{5.11}
$$

where the coefficients k_1 and k_2 have been defined in equations (5.7) and (5.8).

5.2 Boundary conditions at the transmitting end

The boundary conditions for the transmitting end are analogous to those for the receiving end of a transmission line. The relationship between the voltage and the current, and the corresponding finite-difference formula are summarized in the following. For purely resistive load of value R_1,

$$
v \;=\; -R_1 \cdot i \quad , \tag{5.12}
$$

$$
v_{k=0,l+1} \;=\; -\frac{R_1}{Z_o} \cdot w_{k=0-\frac{1}{2},l} \quad . \tag{5.13}
$$

For purely capacitive load of value C_1,

$$
i \;=\; -C_1 \frac{dv}{dt} \quad , \tag{5.14}
$$

$$
w_{k=0-\frac{1}{2},l} \;=\; -\frac{Z_o C_2}{\tau_g \Delta t_n}\left(v_{k=0,l+1} - v_{k=0,l}\right) \quad . \tag{5.15}
$$

For purely inductive load of value L_1,

$$
v \;= -L_1 \frac{di}{dt} \quad , \tag{5.16}
$$

$$w_{k=0-\frac{1}{2},l} = -\left[\frac{Z_o \tau_g \Delta t_n}{L_2}\left(v_{k=0,l+1} + \sum_{n=3}^{n=l} v_{k=0,n}\right)\right] \quad . \tag{5.17}$$

By substitution of the above equations in the discretized telegrapher's equation (4.47), the following expressions for the voltage at the load can be derived. For purely resistive load,

$$v_{1,l+1} = \frac{R_1}{R_1 + k_2 Z_o}\left[k_1 v_{1,l} - k_2 w_{2,l} + k_3\left(E^y_{k,l}|_1 - E^y_{k,l}|_2\right)\right] + k_4 E^y_{k,l}|_3 \quad , \tag{5.18}$$

where k_1 and k_2 are from equations (5.7) and (5.8), k_3 and k_4 are functions of k_2:

$$k_3 = \frac{1}{1+k_2} \quad , \tag{5.19}$$

$$k_4 = \frac{2k_2}{1+k_2} \quad , \tag{5.20}$$

and the parameters $E^y_{k,l}|_1$, $E^y_{k,l}|_2$, $E^y_{k,l}|_3$ are respectively functions of the line integral of the y-component of the incident electric field, $v_e\left(k\Delta\xi\,, l\Delta t_n\right)$, as stated in the modified telegrapher's equation (4.47):

$$E^y_{k,l}|_1 = \frac{\Delta v_e\left((k+1)\,\xi\,, l\Delta t_n\right)}{\Delta t_n} \quad , \tag{5.21}$$

$$E^y_{k,l}|_2 = \frac{\Delta v_e\left(k\,\xi\,, l\Delta t_n\right)}{\Delta t_n} \quad , \tag{5.22}$$

$$E^y_{k,l}|_3 = \frac{1}{2}\left(v_e\left(k\,\xi\,, (l+1)\,\Delta t_n\right) - v_e\left(k\,\xi\,, l\Delta t_n\right)\right) \quad . \tag{5.23}$$

For purely capacitive load,

$$v_{1,l+1} = \left(\frac{1}{\tau_g \Delta t_n + k_2 Z_o C_1}\right) \cdot \left[(k_1 \tau_g \Delta t_n + k_2 Z_o C_1)\, v_{1,l} - (k_2 \tau_g \Delta t_n)\, w_{2,l} + \tau_g \Delta t_n \left(E^y_{k,l}|_1 - k_1 E^y_{k,l}|_2\right)\right] \quad . \tag{5.24}$$

For purely inductive load,

$$v_{1,l+1} = \left(\frac{1}{L_1 + k_2 Z_o \tau_g \Delta t_n}\right) \cdot \left[L_1 \left(k_1 v_{1,l} - k_2 w_{2,l} + E^i_{k,l}|_1 - k_1 E^y_{k,l}|_2\right) - k_2 Z_o \tau_g \Delta t_n \sum_{n=3}^{n=l} v_{1,n}\right] \quad . \tag{5.25}$$

5.3 Combinations of linear loads

The above finite-difference equations for the voltages at the ends of a transmission line can be selected and then combined to form expressions to represent the boundary conditions of a transmission line terminated in a combination of the resistive, capacitive or inductive load.

In the case of a transmission line terminated in a series combination of a resistance, R, and an inductor, L, the boundary condition at the receiving end of the line is given by:

$$v = R \cdot i + L\frac{di}{dt} \quad , \tag{5.26}$$

and the corresponding finite-difference formula is written as:

$$v_{m,l+1} = \frac{R}{Z_o} w_{m+1/2,l} + \frac{L}{Z_o \tau_g \Delta t_n}\left(w_{m+1/2,l} - w_{m+1/2,l-1}\right) \quad . \tag{5.27}$$

The above expression can be made independent of the current $w_{m+1/2,l}$ by putting it in the discretized telegrapher's equation (4.47). The resulting equation for the voltage at the load has been derived (Appendix B), and can be briefed as follows:

$$v_{m,N+1} = \frac{k_5}{k_5 + k_2 k_6} \left[k_1 v_{m,N} - k_2 k_6 \sum_{n=2}^{NN} \frac{k_5^{n-2}}{k_5^N} v_{m,N} + k_2 w_{m-1/2,N} \right] \quad , \tag{5.28}$$

where $2 \leq NN \leq N$, and the coefficients k_5 and k_6 represent:

$$\begin{aligned} k_5 &= \frac{R\tau_g \Delta t_n + L}{L} \quad , \\ k_6 &= \frac{Z_o \tau_g \Delta t_n}{L + R\tau_g \Delta t_n} \quad . \end{aligned} \tag{5.29}$$

Another combination of linear loads is that a transmission line is terminated in a resistance, R, in parallel with a capacitor, C. In this case, the total current in the load, i_{total}, is the sum of the current in the resistor, i_r, and that in the capacitor, i_c, and is denoted by:

$$i_{total} = i_r + i_c \quad , \tag{5.30}$$

and the corresponding finite-difference formula can be obtained by adding the current in the resistor defined by equation (5.2) and that in the capacitor stated in equation (5.5):

$$w_{m+\frac{1}{2},l} = Z_o \left(\frac{1}{R} + \frac{C}{\tau_g \Delta t_n} \right) v_{m,l+1} - \frac{Z_o C}{\tau_g \Delta t_n} v_{m,l} \quad . \tag{5.31}$$

By substitution of the above expression in the discretized telegrapher's equation (4.47), the voltage at the load can be determined (Appendix B), and written as:

$$v_{m,l+1} = k_7 \cdot \left[\left(k_1 + k_2 \frac{Z_o C}{\tau_g \Delta t_n} \right) v_{m,l} + k_2 w_{m-\frac{1}{2},l} + E^y_{k,l}|_1 - k_1 E^y_{k,l}|_2 \right] \tag{5.32}$$

where k_7 is the coefficient calculated from:

$$k_7 = \frac{R\tau_g \Delta t_n}{R\tau_g \Delta t_n + k_2 (\tau_g \Delta t_n + RC)} \quad . \tag{5.33}$$

For other combinations of linear loads, similar procedures can be utilized to get the finite-difference equation for the load voltage at the beginning of a transmission line.

Chapter 6

Some constraints of the time-domain finite-difference algorithm

The solution by the time-domain finite-difference algorithm presented in chapter 4 is feasible in solving EMI/C related problems on equipment susceptibility. In the implementation of the numerical algorithm, however, certain conditions have to be satisfied in order to get satisfactory results. To combat with these constraints, a stability criterion has been established [8], and the limitations on the space and time discretizations for the algorithm will be discussed.

6.1 The stability criterion

The discretized telegrapher's equations (4.47) and (4.48) may generate divergent solution for the induced voltage on the transmission line if the coefficient $\frac{\Delta t_n}{\Delta \xi}$ is greater than unity. This phenomenon was proved in [8]. It was pointed out that the voltage or current governed by the modified discretization transmission line equations could be expressed in the phasor form:

$$w_{k+1/2,l} = w_{k,l} \cdot e^{jm\frac{\Delta\xi}{2}} , \tag{6.1}$$

$$w_{k-1/2,l} = w_{k,l} \cdot e^{-jm\frac{\Delta\xi}{2}} , \tag{6.2}$$

where m is an integer. By substitution of these spectral spatial representations in the transmission line equations, the discretization voltage can be written as:

$$v_{k,l+1} = k_1 v_{k,l} - k_2 \left(e^{jm\frac{\Delta\xi}{2}} - e^{-jm\frac{\Delta\xi}{2}} \right) w_{k,l} + e_1 \quad , \tag{6.3}$$

$$v_{k,l+1} = k_1 v_{k,l} - j2\sin\left(m\frac{\Delta\xi}{2} \right) k_2 w_{k,l} + e_1 \quad , \tag{6.4}$$

where e_1 stands for the equivalent voltage and current sources due to the external time-varying electromagnetic field. Also, the current can be expressed in terms of the spectral spatial phasor $e^{jm\xi}$:

$$w_{k,l+1} = k_3 w_{k,l} - k_4 e^{jm\frac{\Delta\xi}{2}} \left(1 - e^{-jm\Delta\xi} \right) v_{k,l+1} + k_5 \sum_{m=0}^{l-1} \left(\rho_{l-m+1} - \rho_{l-m} \right) w_{k,m} \quad , \tag{6.5}$$

where $v_{k,l+1}$ is defined in equation (6.4). By combining (6.4) with (6.5) , the following equation for the current can be derived:

$$\begin{aligned} w_{k,l+1} = & - j2\sin\left(m\frac{\Delta\xi}{2} \right) k_1 k_4 v_{k,l} + \left[k_3 - 4\sin^2\left(m\frac{\Delta\xi}{2} \right) k_2 k_3 \right] w_{k,l} \\ & + k_5 \sum_{m=0}^{l-1} \left(\rho_{l-m+1} - \rho_{l-m} \right) w_{k,m} + e_2 \quad , \end{aligned} \tag{6.6}$$

where e_2 is also a representation of the equivalent sources due to the external fields. The pair of equations (6.4) and (6.6) can be transcribed in matrix form as:

$$\begin{aligned} \begin{bmatrix} v_{k,l+1} \\ w_{k,l+1} \end{bmatrix} = & \begin{bmatrix} k_1 & -j2k_2\sin\left(m\frac{\Delta\xi}{2} \right) \\ -j2k_1\sin\left(m\frac{\Delta\xi}{2} \right) & k_3\left(1 - 4k_2\sin^2\left(m\frac{\Delta\xi}{2} \right) \right) \end{bmatrix} \begin{bmatrix} v_{k,l} \\ w_{k,l} \end{bmatrix} \\ & + \begin{bmatrix} e_1 \\ e_2 + k_5 \sum_{m=0}^{l-1} \left(\rho_{l-m+1} - \rho_{l-m} \right) w_{k,m} \end{bmatrix} . \end{aligned} \tag{6.7}$$

In the above equation, the determinant of the "amplification matrix" must be zero in order that the numerical solutions are stable [8]:

$$\begin{vmatrix} k_1 & -j2k_2 \sin\left(m\frac{\Delta\xi}{2}\right) \\ -j2k_1 \sin\left(m\frac{\Delta\xi}{2}\right) & k_3\left(1-4k_2\sin^2\left(m\frac{\Delta\xi}{2}\right)\right) \end{vmatrix} = 0 \quad . \tag{6.8}$$

From the above determinant, a characteristic equation can be obtained and is given by:

$$x^2 - 2ax + b = 0 \quad , \tag{6.9}$$

where the coefficients a and b are:

$$a = \frac{1+\frac{1}{2}(\rho_o-\rho_1)\nu_r\Delta t_n - \frac{1}{4}\nu_g\Delta t_n - 2\left[\left(\frac{\Delta t_n}{\Delta\xi}\right)\left(\sin m\frac{\Delta\xi}{2}\right)\right]^2}{\left(1+\frac{1}{2}\nu_g\Delta t_n\right)\cdot\left(1+\frac{1}{2}\rho_o\nu_r\Delta t_n\right)} \quad , \tag{6.10}$$

$$b = \frac{\left(1-\frac{1}{2}\nu_g\Delta t_n\right)\left[1+\frac{1}{2}(\rho_o-\rho_1)\nu_r\Delta t_n\right]}{\left(1+\frac{1}{2}\nu_g\Delta t_n\right)\cdot\left(1+\frac{1}{2}\rho_o\nu_r\Delta t_n\right)} \quad . \tag{6.11}$$

In order to have stable numerical solutions by the finite-difference algorithm, the solution x in the above characteristic equation must satisfy the condition $|x| \leq 1$, or the product of the roots x_1 and x_2 must not be greater than unity [8] such that

$$|b| = |x_1 \cdot x_2| \leq 1 \quad . \tag{6.12}$$

Since also for any real solution x,

$$|x_{1,2}|_{max} = |a| + \sqrt{a^2 - b} \leq 1 \quad . \tag{6.13}$$

By combining (6.12) and (6.13), the necessary and sufficient condition for stable numerical solutions can be obtained and is given by:

$$|a| \leq \frac{b+1}{2} \leq 1 \quad . \tag{6.14}$$

By using (6.10) and (6.11) in the above inequality, the necessary and sufficient condition for convergent numerical solutions is derived and represented by:

$$\frac{\Delta t_n}{\Delta \xi} \leq 1 \quad . \tag{6.15}$$

In general, the normalized time step is chosen to be the same as the normalized space step for efficient numerical computations.

6.2 The space and time discretizations

The normalized variables in the modified discretization telegraphers' equations consist of the space and time steps:

$$\Delta t_n = \frac{\Delta t}{\tau_g} \quad , \tag{6.16}$$

$$\Delta \xi = \frac{\Delta x}{v_{ph} \tau_g} \quad . \tag{6.17}$$

Let N be the total number of time steps and M be the total number of space steps. Then, the two above equations can be expressed in terms of the maximum time and the maximum transmission line length that can be used in the finite-difference algorithm:

$$\Delta t_n = \frac{t_{max}}{\tau_g \cdot N} \quad , \tag{6.18}$$

$$\Delta \xi = \frac{L}{v_{ph} \cdot \tau_g \cdot M} \quad , \tag{6.19}$$

where L is the length of the transmission line. Since the ratio $\frac{\Delta t_n}{\Delta \xi}$ has been chosen to be unity to satify the stability criterion, the maximum available time for the numerical solutions can be found by equating (6.18) and (6.19):

$$\frac{t_{max}}{N\tau_g} = \frac{L}{Mv_{ph}\tau_g} \quad ,$$

$$\frac{t_{max}}{N} = \frac{L}{Mv_{ph}} \quad ,$$

$$t_{max} = \frac{N\,L}{M\,v_{ph}} \quad . \tag{6.20}$$

Thus, the maximum available time for the numerical solutions depends on the $\frac{N}{M}$ multiples of the time taken by the induced voltage to travel from the beginning to the end of a transmission line.

The choice of the space step, $\Delta\xi$, will be limited by a number of factors. First, in equation (6.19), $\Delta\xi$ is dependent on τ_g which is the intrinsic penetration time of the external time-varying electromagnetic field into the lossy ground. Second, $\Delta\xi$ is also limited by the maximum available time for the numerical solutions since the space step $\Delta\xi$ is chosen to be the same as the time step Δt_n to satisfy the necessary and sufficient stability criterion. Third, $\Delta\varsigma$ must suitably be chosen in order that for each small increment in the distance of propagation x, the incident electromagnetic field does not vary to a great extent. Otherwise, fluctuations of the numerical solutions will take place over a certain time span. Finally, the maximum line length to be used in the algorithm must not be greater than twice the normalization constant, $v_{ph}\tau_g$. This criterion for the numerical algorithm has been proved in [3].

Chapter 7

Applications of the modified transmission line equations

In this chapter, the induced voltages on a bent conductor and on a system of multi-conductors predicted by using the modified transmission line equations and the corresponding finite-difference algorithm are discussed. In addition, the equivalent representations of a bent line and the multi-conductors are used.

7.1 Bent conductors

A bent conductor can be represented by a cascaded transmission line. Each section of the cascaded transmission line is oriented at a different azimuth angle to the plane of incidence of the external electromagnetic field. In case of a flat conductor, the discontinuity of the bent transmission line can be represented by a 'T' [9], [10], [21-25]. Figure 7.1 shows the equivalent circuit which consists of the leakage inductance ΔL, the stray capacitance C_p , and a small change in the effective electrical length Δx. For simplicity, the values of the leakage inductance ΔL and the stray capacitance C_p were taken from [9] and [10] respectively and used to calculate the induced voltages onto the transmission line.

To predict the induced voltages on a bent conductor, the following equations governing the forward induced voltage and the transmitted induced voltage at the discontinuity are used:

$$v_3 = v_1 - \frac{\Delta L}{2} \cdot \frac{di_1}{dt} \quad , \tag{7.1}$$

$$i_2 = i_1 - C_p \cdot \frac{dv_3}{dt} \quad . \tag{7.2}$$

Figure 7.1: The equivalent circuit of the discontinuity

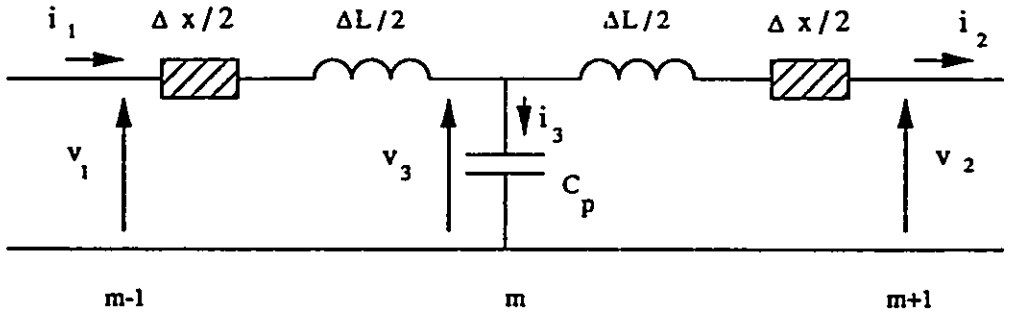

The corresponding discretization formulas to be included in the finite-difference algorithm are derived and given by:

$$v_{m,l} = v_{m-1,l} - \frac{\Delta L}{2Z_o\tau_g\Delta t_n}\cdot(w_{m-1,l+1} - w_{m-1,l}) \quad , \tag{7.3}$$

$$w_{m+1,l} = w_{m-1,l} - \frac{C_p}{\tau_g\Delta t_n}\cdot(v_{m,l+1} - v_{m,l}) \quad . \tag{7.4}$$

By substitution of the two above expressions in the modified discretization transmission line equations, one can finally obtain a simplified voltage equation characterizing the discontinuity of a bent conductor:

$$\begin{aligned} v_{m,l+1} = {} & \left(\frac{1}{1+C_p/(\tau_g\Delta t_n)}\right)\cdot\left\{\left(\frac{1-\nu_g\Delta t_n/2}{1+\nu_g\Delta t_n/2}\right)\cdot v_{m,l} - \left(\frac{\Delta t_n\Delta\xi}{1+\nu_g\Delta t_n/2}\right)\right. \\ & \left.\cdot\left[\frac{C_p}{\nu_g\Delta t_n}\left(v_{k-1,l} - \frac{\Delta L}{2Z_o\tau_g\Delta t_n}\left(w_{k-1/2,l+1} - w_{k-1/2,l}\right)\right)\right]\right\} \\ & + \frac{1}{1+\nu_g\Delta t_n/2}\cdot[1+\nu_g\Delta E_y(\xi\,,t_n)] \quad . \end{aligned} \tag{7.5}$$

7.2 Multi-conductors

The transmssion line equations governing the voltage and the current in each of the parallel conductors are in the form:

$$-\frac{\partial [v]}{\partial x} = [R][i] + [L]\frac{\partial [i]}{\partial t} \quad , \tag{7.6}$$

$$-\frac{\partial [i]}{\partial x} = [G][v] + [C]\frac{\partial [v]}{\partial t} \quad , \tag{7.7}$$

where $[R]$, $[L]$, $[G]$, and $[C]$ are respectively the matrices of resistance, inductance, conductance and capacitance characterizing the parallelly-coupled transmission lines. In equation (7.6), the transient skin-effect resistance has not been taken into account for multi-conductors situated above perfect ground plane. In addition, v is the voltage and i is the current represented by the matrices:

$$[v] = [v_1\ v_2\ v_3\ \cdots\ v_n]^T \quad , \tag{7.8}$$

(7.9)

$$[i] = [i_1\ i_2\ i_3\ \cdots\ i_n]^T \quad . \tag{7.10}$$

The matrices of inductance and capacitance in the above transmission line equations can be simplified if the mutual coupling is mainly contributed by two immediate neighbours. In this case, the matrices of capacitance and inductance can be written as:

$$[C] = \begin{bmatrix} c_{1,1} & c_{1,2} & 0 & \cdots & 0 & 0 \\ c_{2,1} & c_{2,2} & c_{2,3} & \cdots & 0 & 0 \\ 0 & c_{3,2} & c_{3,3} & \cdots & 0 & 0 \\ \cdots & \cdots & \cdots & \cdots & \cdots & \cdots \\ 0 & 0 & 0 & \cdots & c_{n-1,n-1} & c_{n-1,n} \\ 0 & 0 & 0 & \cdots & c_{n,n-1} & c_{n,n} \end{bmatrix} \quad , \tag{7.11}$$

$$[L] = \begin{bmatrix} l_{1,1} & l_{1,2} & 0 & \cdots & 0 & 0 \\ l_{2,1} & l_{2,2} & l_{2,3} & \cdots & 0 & 0 \\ 0 & l_{3,2} & l_{3,3} & \cdots & 0 & 0 \\ \cdots & \cdots & \cdots & \cdots & \cdots & \cdots \\ 0 & 0 & 0 & \cdots & l_{n-1,n-1} & l_{n-1,n} \\ 0 & 0 & 0 & \cdots & l_{n,n-1} & l_{n,n} \end{bmatrix} . \tag{7.12}$$

By using a linear transformation technique [15], the above matrices can be diagonalized. The matrix involved in the linear transformation of the matrices of inductance and capacitance is presented in [15]:

$$[A] = [a_{i,j}] = \left[\frac{\phi_{i-1}(\mu_j)}{\delta_j}\right] , \tag{7.13}$$

where the functions $\phi_i(\mu)$ are defined as:

$$\begin{aligned} \phi_i(\mu) &= \mu \cdot \phi_{i-1}(\mu) - \phi_{i-2}(\mu) \ , i \geq 2 \\ \phi_o(\mu) &= 1 \ , \quad \phi_1(\mu) = \mu \ , \end{aligned} \tag{7.14}$$

δ_j is the normalization factor given by:

$$\delta_j^2 = \sum_{k=1}^{n} [\phi_{k-1}(\mu_j)]^2 \ , \tag{7.15}$$

and the variable μ_p is determined by the formula:

$$\mu_p = -2\cos\left(\frac{p\pi}{n+1}\right) \ , p = 1, 2, 3, \cdots, n. \tag{7.16}$$

Once the transformation matrix $[A]$ and its transpose matrix are calculated, the matrices of capacitance and inductance can be diagonalized and determined by:

$$[L_{diag}] = [A]^T [L] [A] \quad , \tag{7.17}$$

$$[C_{diag}] = [A]^T [C] [A] \quad . \tag{7.18}$$

By using the diagonalized matrices of inductance and capacitance, a set of n independent transmission line equations can be derived and represented by:

$$-\frac{\partial v_n}{\partial x} = r_n i_n + l_{eq}\frac{\partial i_n}{\partial t} + e_1 \quad , \tag{7.19}$$

$$-\frac{\partial i_n}{\partial x} = g_n v_n + c_{eq}\frac{\partial v_n}{\partial t} + e_2 \quad . \tag{7.20}$$

where e_1, e_2 are the equivalent voltage and current sources due to the incident electromagnetic field, l_{eq} is the equivalent inductance and c_{eq} is the equivalent capacitance of each conductor. The expressions for l_{eq} and c_{eq} are respectively given by:

$$\begin{aligned} l_{eq} = \; & a_{1,n}\,(a_{1,n}\,, l_{n,n} + a_{2,n}\, l_{1,2}) + a_{N,n}\,(a_{N-1,n} l_{N-1,n} + a_{N,n}\, l_{N,N}) \\ & + \sum_{i=2}^{N-1} a_{i,n}\,(a_{i-1,n}\, l_{i-1,i} + a_{i,n}\, l_{i,i} + a_{i+1,n}\, l_{i+1,i}) \quad , \end{aligned} \tag{7.21}$$

$$\begin{aligned} c_{eq} = \; & a_{1,n}\,(a_{1,n}\,, c_{n,n} + a_{2,n}\, c_{1,2}) + a_{N,n}\,(a_{N-1,n}\, c_{N-1,1} + a_{N,n}\, c_{N,N}) \\ & + \sum_{i=2}^{N-1} a_{i,n}\,(a_{i-1,n}\, c_{i-1,i} + a_{i,n}\, c_{i,i} + a_{i+1,n}\, c_{i+1,i}) \quad , \end{aligned} \tag{7.22}$$

the coefficient $a_{i,j}$ is the eigenvalue of the transformation matrix $[A]$ in equation (7.12), and the variable 'n' denotes the n^{th} conductor while the letter 'N' is the total number of conductors.

Chapter 8

The numerical solutions

To find out if the skin-effect in a transmission line is important, the lossless line model, the d.c. resistance concept, and the transient resistance approach are used to calculate the induced voltage for comparison. In Figure 8.1, a transmission line of one metre long is illuminated by a parallelly-polarized electromagnetic pulse (EMP) with the normalized peak amplitude of 1 V/m. The transmission line is also terminated at the two ends in its characteristic impedance of 317.73 ohms. The numerical results for the three above considerations are shown in Figure 8.2. One can see that the predicted induced voltage onto the lossy line is over-estimated if the lossless line model or the d.c. resistance concept is used.

The difference in the predicted induced voltages obtained by using the above three approaches would be considerable when the peak of the EMP goes up to 50 kV/m. For the worst case, the induced voltage is predicted by using the transient skin-effect resistance approach, and by using the d.c. resistance concept. The results are compared and represented respectively in Figure 8.3 for the induced voltage at the beginning of the line, and in Figure 8.4 for the induced voltage at the end of the line. The numerical results show that the difference in the predicted induced voltages can be as large as 100 volts, and thus skin-effect considerations on the transient response of a transmission line exicted by a time-varying electromagnetic field is essential.

8.1 Validation of the numerical algorithm

To verify the time-domain finite-difference algorithm discussed in this thesis, the predictions of induced voltages are compared with the measurements presented in [5] for a

Figure 8.1: Transient Skin-effect in a Lossless or Lossy Line

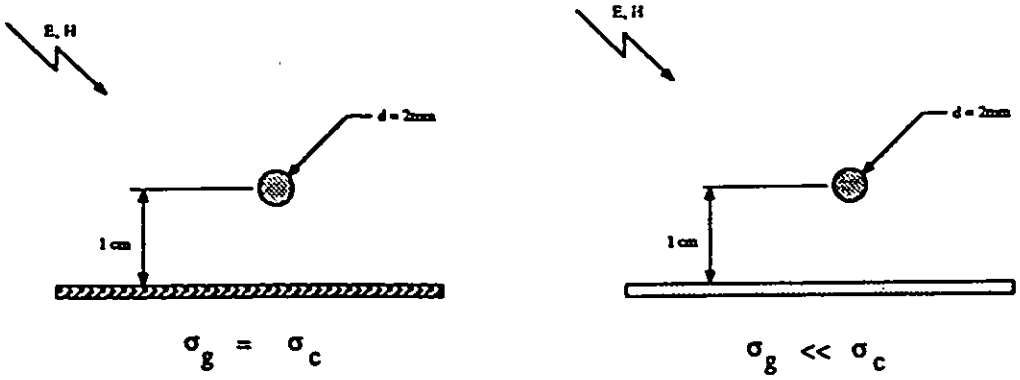

Figure 8.2: The Difference in the Predicted Induced Voltages

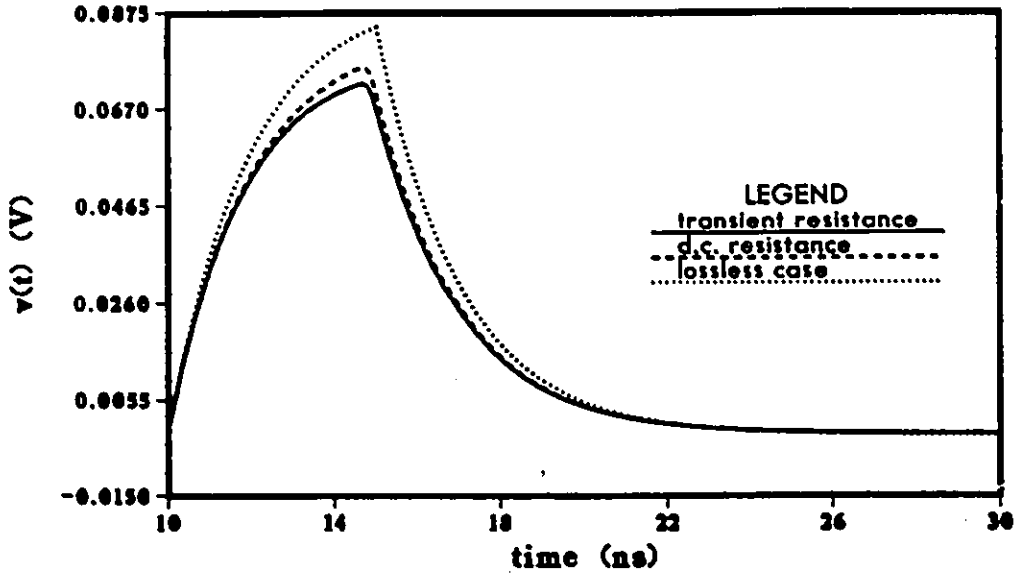

Figure 8.3: Induced Voltage at the Sending End

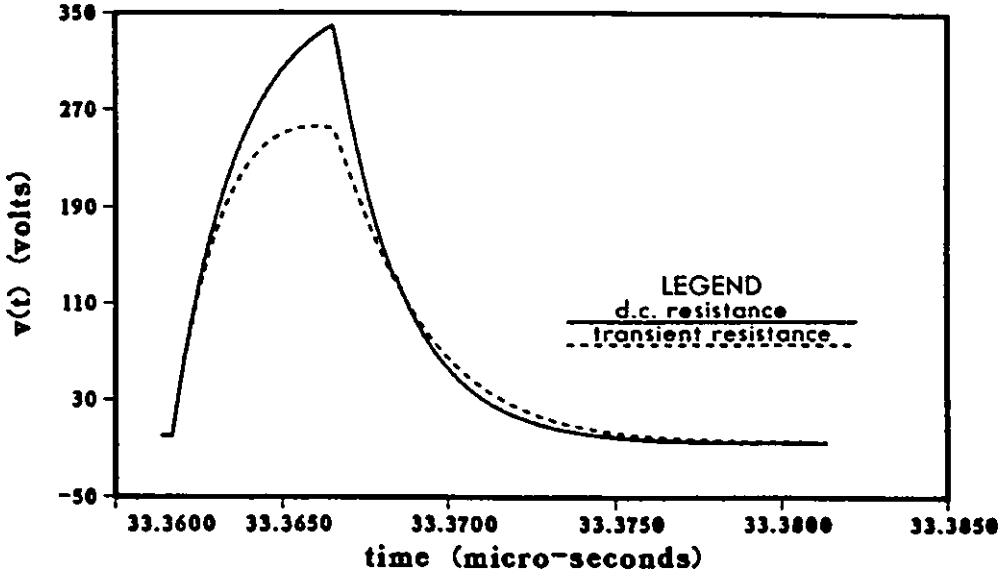

Figure 8.4: Induced Voltage at the Receiving End

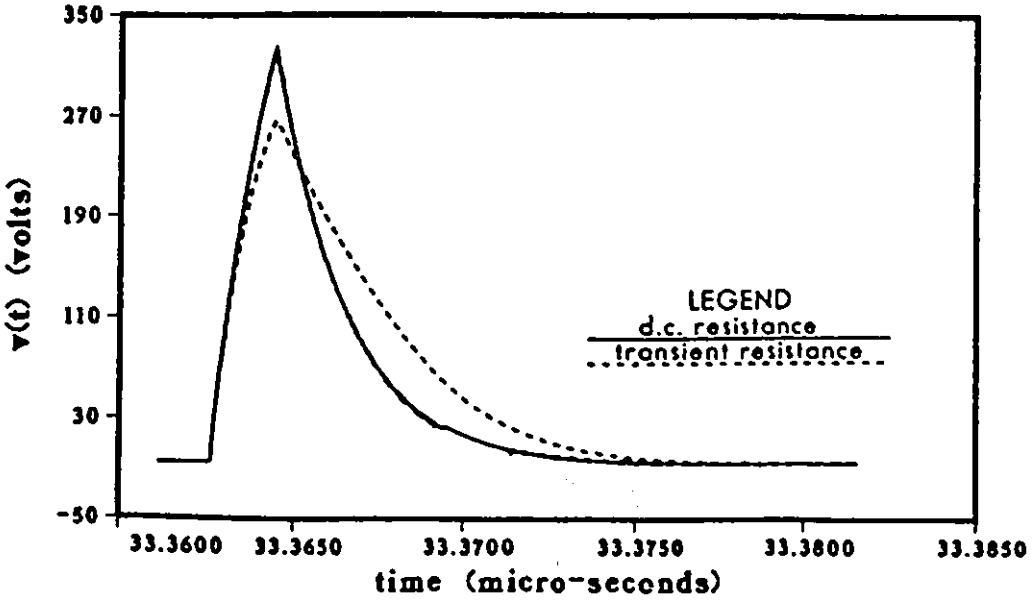

Figure 8.5: Transmission line excited by non-uniform fields

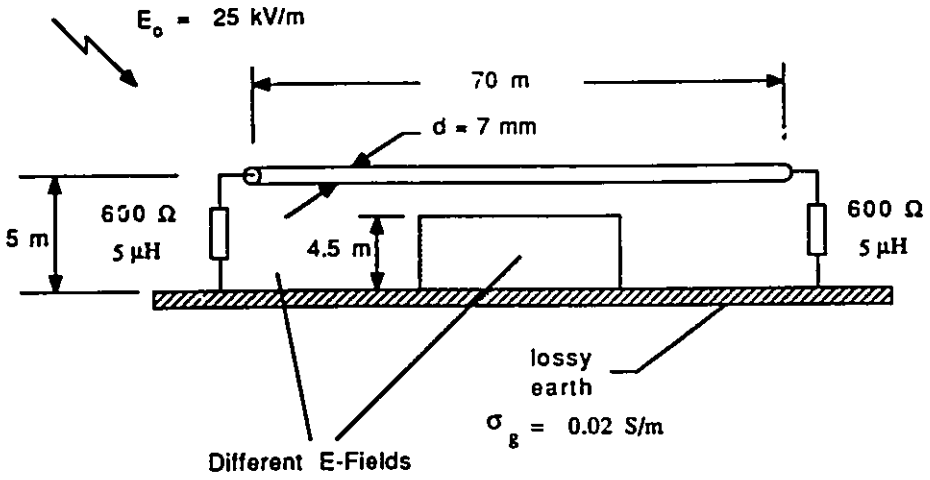

transmission line with geometrical dimensions given in Figure 8.5. In this figure, a lossy transmission line is excited by an EMP with peak value of 25 kV/m. If a locomotive is situated under the transmission line, the incident electric field will be locally disturbed. As a result, the total electric field impinging on the transmission line will be non-uniform. In the calculations of the induced current due to the incident field, the finite-difference algorithm was used and the electric field data were taken from [5]. The numerical results were plotted in Figure 8.6 for two situations, one taking into account the transient skin-effect inside the conductor line, and one assuming a simplified d.c. resistance concept. When the skin-effect is taken into account, the numerical result is relatively closer to the measurements, whereas when the d.c. resistance concept is used, the predicted peak value of the induced current deviates from the measurements. The above comparison between the numerical results and the measurements not only verifies the time-domain finite-difference algorithm introduced in this thesis, but also infers the potential application of the algorithm to the case of non-uniform or near field excitation of a lossy transmission line.

Figure 8.6: Magnitude of the Induced Current at the Receiving End

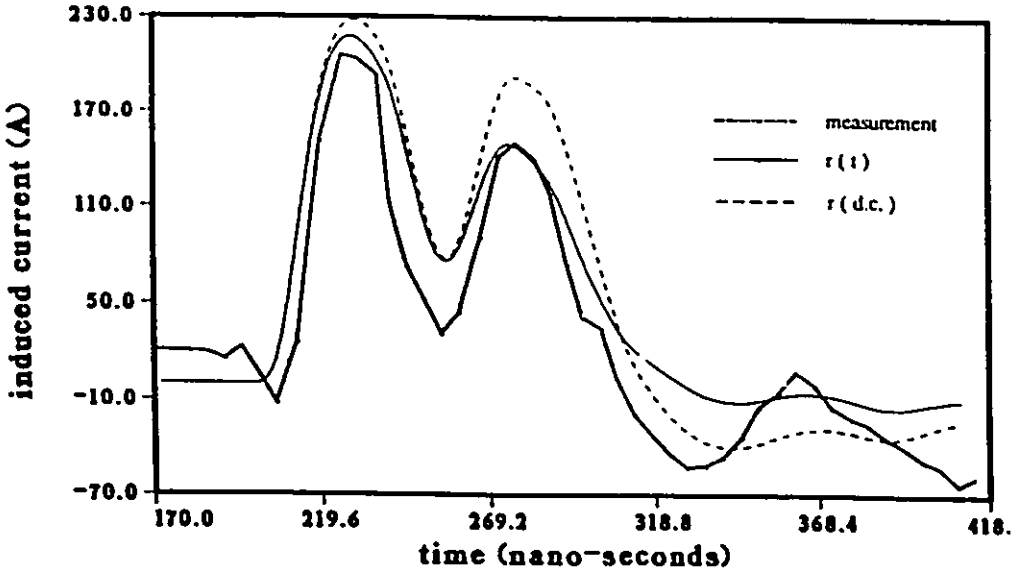

8.2 Predictions of induced voltages on a bent conductor

The finite-difference algorithm is tested if it can be used to predict the induced voltage on a bent cylindrical conductor. The test is divided into two parts: one is to see the effect of the ground conductivity on the induced voltage, and the other one is to compare the numerical results with those presented in [13].

In the first part of the test, a single 90-degree bent lossy transmission line is considered and is represented in Figure 8.7. The change in the effective electrical length at the sharp corner has, however, not been taken into account in the thesis, and future research will be done. The bent conductor is excited by an EMP with peak amplitude of 50 kV/m at an angle of incidence of 45-degree and at an azimuth angle of 45-degree. By using the transient resistance concept in the time-domain finite-difference algorithm, the induced voltage due to the external time-varying electromagnetic field is predicted for various ground conductivities. The results are then compared and depicted in Figure 8.8. The results show the difference between the calculated induced voltage for lossy ground and that for perfect ground. If the ground is a good conductor, the induced voltage predicted by using the transient resistance approach is close to that predicted by using the d.c. resistance concept. If the ground is lossy, the predicted induced voltage obtained by using the transient

Figure 8.7: A bent round conductor excited by an electromagnetic pulse

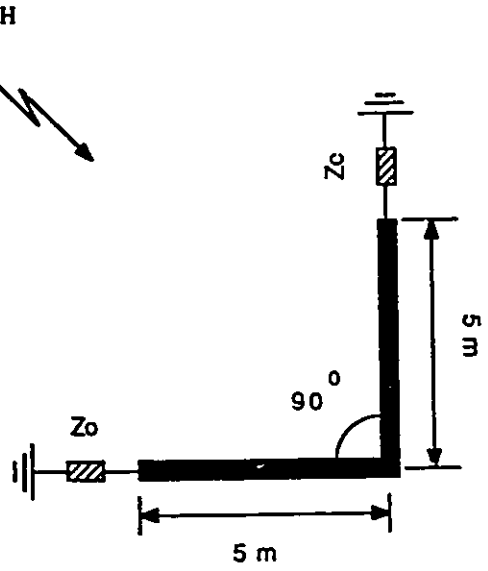

Figure 8.8: The induced voltage at the receiver

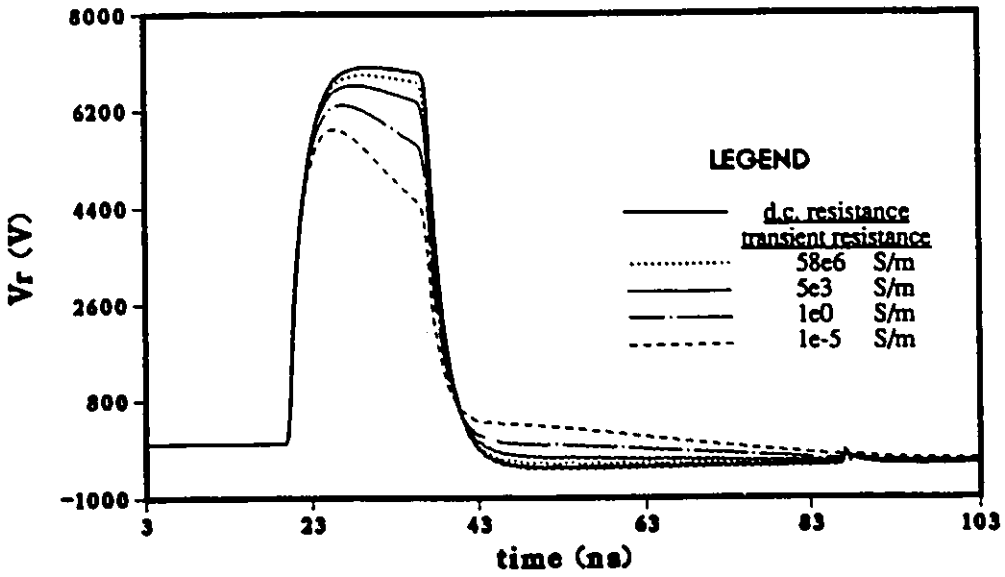

Figure 8.9: A bent thin transmission line exited by an EMP

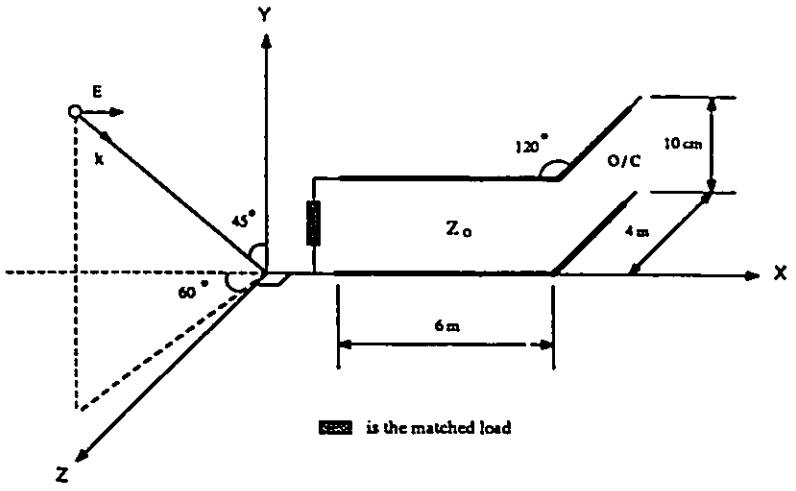

resistance approach is much less than that obtained by using the d.c. resistance concept. In other words, the transient skin-effect in a transmission line above lossy ground has a serious effect on the predicted induced voltage, while the the skin-effect in the conductor line above perfect ground has less effect on the induced voltage. This is because the time constant of a perfect ground is so small that the transient skin-effect will fade away at the rising edge of the electromagnetic pulse which acts as the excitation source.

In the second part of the test, the predictions of the induced voltage are compared to those presented in [13]. In Figure 8.9, a 10-m long, bent thin cylindrical conductor is situated 10-cm above perfect ground. The line is matched at the transmitting end while it is open-cirucited at the receiving end. A 50-kV/m electromagnetic pulse ,whose electric field component is perpendicularly-polarized, is impinging onto the transmission line at an angle of incidence of 45-degree. By using the transient resistance and the d.c. resistance concepts in the finite-difference algorithm, the induced voltages on the transmission line are predicted and represented in Figure 8.10. Essentially, the predictions of the induced voltages are similar to those calculated in [13]. In Figure 8.10, pulse A is the induced voltage at the beginning of the line when the incident field reaches the line. Pulse B is the induced voltage when pulse A first hits the bending corner of the line. When pulse B travels to the open-ciruited end of the line, its amplitude is doubled and is represented by pulse C. Pulse C then returns from the receiving end to the bending corner again and

Figure 8.10: The predicted induced voltages on the line

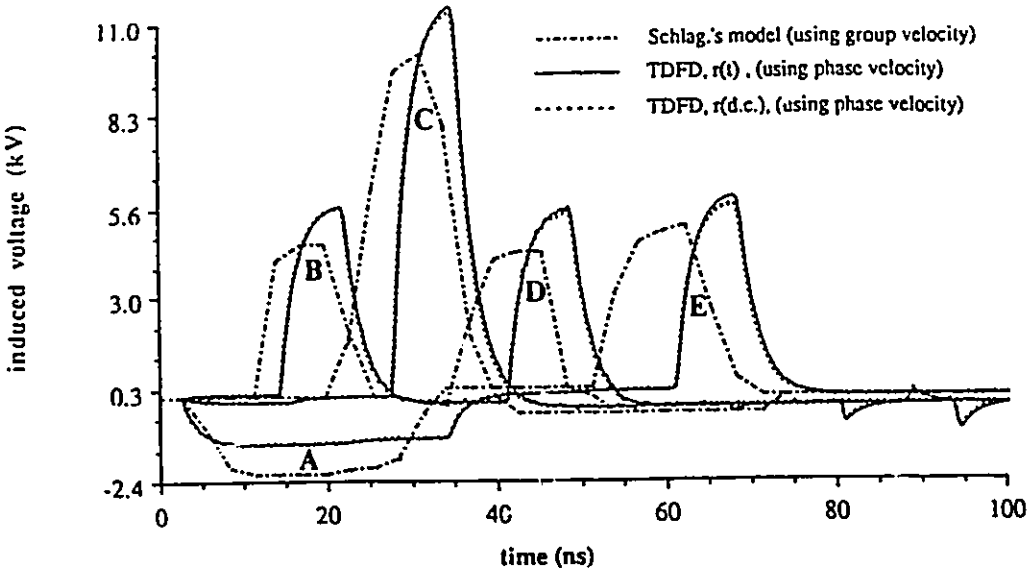

results in pulse D. One can observe from the results that the predictions of the induced voltages on the transmission line are in good agreement with those presented in [13].

8.3 Predictions of induced voltage on multiple conductors

The finite-difference algorithm is further tested for the predictions of the induced voltages on multi-conductors. In this test, two configurations of the multiple round conductors are considered: one is the two parallel matched transmission lines above perfect ground, and the other one is the three parallel open-circuited transmission lines above the same ground.

In Figure 8.11, there are two 10-m long parallel transmission lines excited by a 10-kV/m electromagnetic pulse. The two conductor lines are spaced at 0.5-cm apart and each of them is situated at 10-cm above perfect ground. In the calculations of the induced voltage onto each line, the values of the inductances and capacitances for this geometry were taken from [18]. The corresponding equivalent inductance and the equivalent capacitance for each line are determined by using the approach discussed in chapter 7, and are represented in table 8.1. By using the time-domain finite-difference algorithm, the induced voltage onto line 1 at the receiving end is predicted for two cases: one taking into account the transient skin-effect in the transmission line, and the other one using the d.c. resistance

Figure 8.11: Two parallel transmission line excited by an EMP

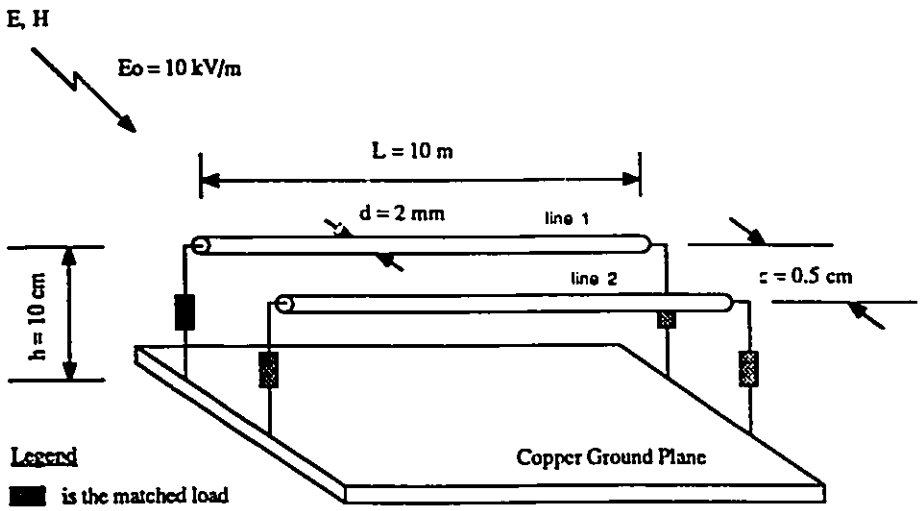

Table 8.1: The equivalent inductance and capacitance for two lines

Self and Mutual Inductances : (μH/m)	Self and Mutual Capacitances : (pF/m)
L11 = 1.0596	C11 = 20.3548
L12 = 0.7378	C12 = -14.1731
L21 = 0.7378	C21 = -14.1731
L22 = 1.0596	C22 = 20.3548
Equivalent Inductance : (μH/m)	**Equivalent Capacitance : (pF/m)**
L1 = 0.3218	C1 = 34.5300
L2 = 1.7970	C2 = 6.1820

Figure 8.12: The predicted induced voltage on line 1

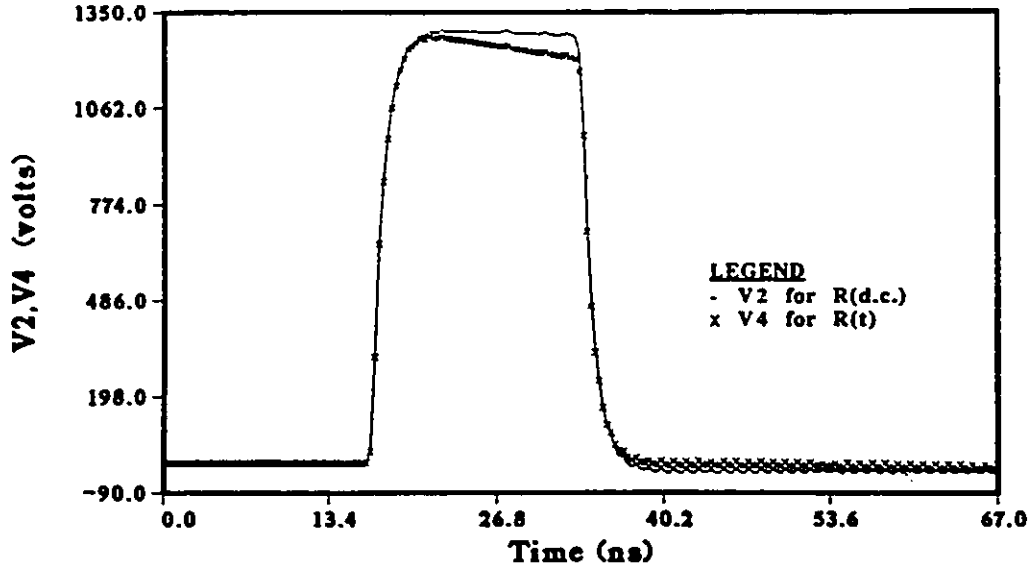

concept. In Figure 8.12, the predicted induced voltage at the receiving end is represented. When comparing the results obtained by using the transient resistance approach to that obtained by using the d.c. resistance concept, one can remark that the difference between the predicted induced voltages is not significant. This is simply due to the very good conducting ground plane, and is also in agreement with the results obtained for the bent conductor.

In order to verify the solutions obtained by the finite-difference algorithm applied to a system of multi-conductors, the induced voltages are calculated and compared to those presented in [13] for the geometry shown in Fig 8.13. The thin cylindrical conductors are 5-m long, and equally-spaced at a distance of 2 cm. The lines are also terminated in matched load at the sending end but open-circuited at the receiving end. For this configuration, the mutual inductance is determined by using the formula given by [53]:

$$L_m = 0.0025 \cdot log_e \left(\frac{2h}{D}\right) \qquad [\mu H/in] \quad , \tag{8.1}$$

where D is the spacing of the parallel conductors. The corresponding mutual capacitance can be calculated by using the formula:

Figure 8.13: Three parallel transmission line excited by an EMP

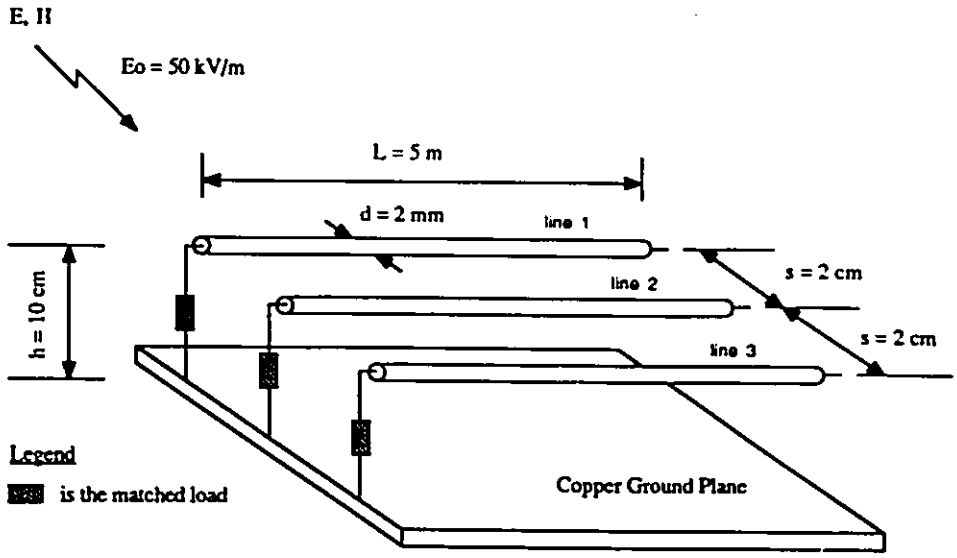

$$[C] = \frac{1}{v_o} \cdot [L]^{-1} \quad , \tag{8.2}$$

where $[C]$, $[L]$ are respectively the matrices of capacitance and inductance, and v_o is the velocity of propagation. The computed values for the inductances and capacitances are listed in table 8.2. By using the above values in the finite-difference algorithm, the induced voltages at the two ends of each line due to an EMP excitation are predicted. The results are computed for a 50-kV/m perpendiculary-polarized electric field with an angle of incidence of 5-degree, and are then represented in Figure 8.14. It is found that the predicted induced voltages onto the multi-conductors are similar to those presented in [13]. Also, the results reveal that the induced voltages on the three lines have the same shapes, and are slightly different from each other due to the coupling among them. In Figure 8.14, the induced voltages are distinguished by the letters A, B and C. Pulse A is the induced voltage caused by the incident fields at the beginning of the transmission line; pulse B is the induced voltage when pulse A travels from the sending end to the open-ciruited end; and pulse C is the induced voltage when pulse B returns from the receiving end to the transmitting end. Again, one can remark that the predictions of the induced voltages are comparable to those presented in [13].

Table 8.2: The equivalent inductance and capacitance for three lines

Self and Mutual Inductances : (μH/m)	Self and Mutual Capacitances : (pF/m)
L11 = 1.0596 L12 = 0.4542 L13 = 0.3207	C11 = 11.8368 C12 = - 4.3347 C13 = 1.7245
L21 = 0.4542 L22 = 1.0596 L23 = 0.4542	C21 = - 4.3347 C22 = 13.1729 C23 = - 4.3347
L31 = 0.3207 L32 = 0.4542 L33 = 1.0596	C31 = 1.7245 C32 = - 4.3347 C33 = 11.8368
Equivalent Inductances : (μH/m)	**Equivalent Capacitances : (pF/m)**
L1 = 0.4173	C1 = 0.1864
L2 = 0.1060	C2 = 0.1184
L3 = 0.1702	C3 = 0.6375

Figure 8.14: The induced voltages on the three parallel lines

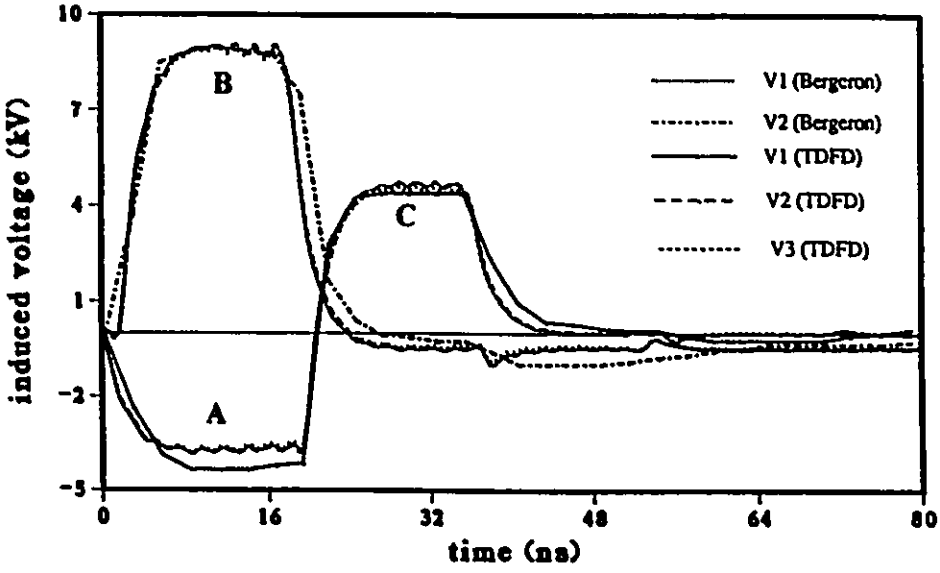

Figure 8.15: The multiple 90-degree bent flat conductor

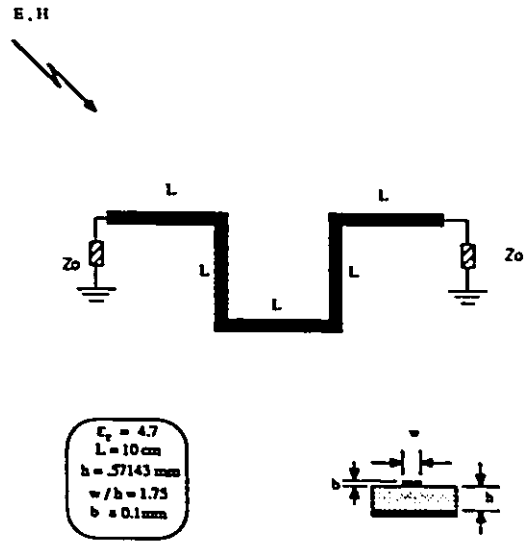

8.4 The propagation of induced voltage on a flat conductor

The application of the time-domain finite-difference algorithm introduced in this thesis can be extended to the case in which a flat conductor above perfect ground is considered. A highly-conducting ground plane is intentionally chosen for this research so that the difference between the predicted induced voltage obtained by using the transient resistance approach and that obtained by using the d.c. resistance concept is not significant.

8.4.1 The induced voltage on a bent flat conductor

To show that the finite-difference algorithm can be applied to solve for the induced voltage on a flat conductor above perfect ground, a 4-right-angled bent conductor is chosen and its dimensions are represented in Figure 8.15. In this problem, the discontinuity due to the bending of the flat conductor has been taken into account and can be represented by a T-circuit discussed in the last chapter. For simplicity, the values of the leakage inductance and the stray capacitance were taken from [9] as 0.09587 nH and 0.0950 pF respectively. In the calculations of the induced voltages on the flat conductor, the applied electric field is assumed to be an electrostatic discharge (ESD) pulse with peak value of 4 kV/m. The results are given in Figure 8.16. The results show that the amplitude of the induced

Figure 8.16: The predicted induced voltage at the receiver

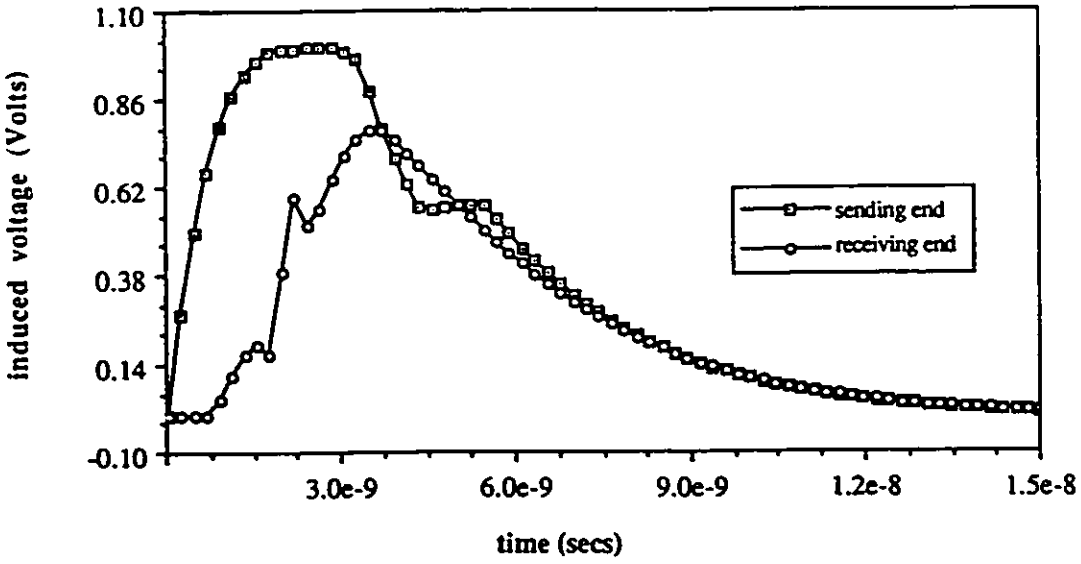

voltage that travels from the beginning to the end of the line is reduced due to the lossy characteristic of the flat conductor. In addition, the dips at the rising edge of the received signal is probably due to the reflections from the discontinuity of the transmission line.

8.4.2 Induced voltage on the multiple flat conductors

The finite-differences algorithm is further applied to a system of multiple flat conductors above perfect ground. The geometry is picked up from [19] and is shown in Figure 8.17. All the flat conductors are matched, and are excited by a 10-kV/m ESD pulse. The values of the inductances and capacitances were taken from [19], and the equivalent inductance and capacitance of each flat conductor are shown in table 8.3. By using the time-domain finite-differences, the induced voltage on each line is predicted and is shown in Figure 8.18. From the results, one can again remark that the induced voltages on the three lines are slightly different due to the coupling among them. Also, the fluctuations at the falling edge of each of the predicted induced voltages are considered as the ringing effect on a flat conductor.

Figure 8.17: Three Parallel Flat Conductors Excited by an Electromagnetic Pulse

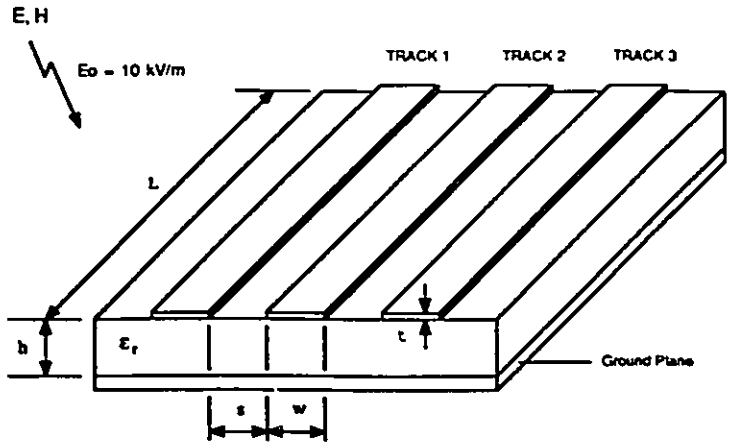

Epoxy glass of dielectric constant 4.65
w = 60 mil, w/h =1, s = 10 mil, t = 1.4 mil, L = 30.48 cm
Each track is terminated in matched load at both ends.

Table 8.3: The equivalent, self, and mutual inductances and capacitances

Self and Mutual Inductances : (nH/m)	Self and Mutual Capacitances : (pF/m)
L11 = 3.8970 L12 = 1.6238 L13 = 0.8252	C11 = 1.0413 C12 = -0.3432 C13 = -0.0140
L21 = 1.6238 L22 = 3.7129 L23 = 1.6238	C21 = -0.3432 C22 = 1.1987 C23 = -0.3432
L31 = 0.8252 L32 = 1.6238 L33 = 3.8790	C31 = -0.0140 C32 = -0.3432 C33 = 1.0413
Equivalent Inductances : (nH/m)	**Equivalent Capacitances : (pF/m)**
L1 = 0.1504	C1 = 0.1605
L2 = 0.3888	C2 = 0.1041
L3 = 0.6097	C3 = 0.6346

Figure 8.18: Induced voltages on tracks 1, 2, and 3 at the receiver

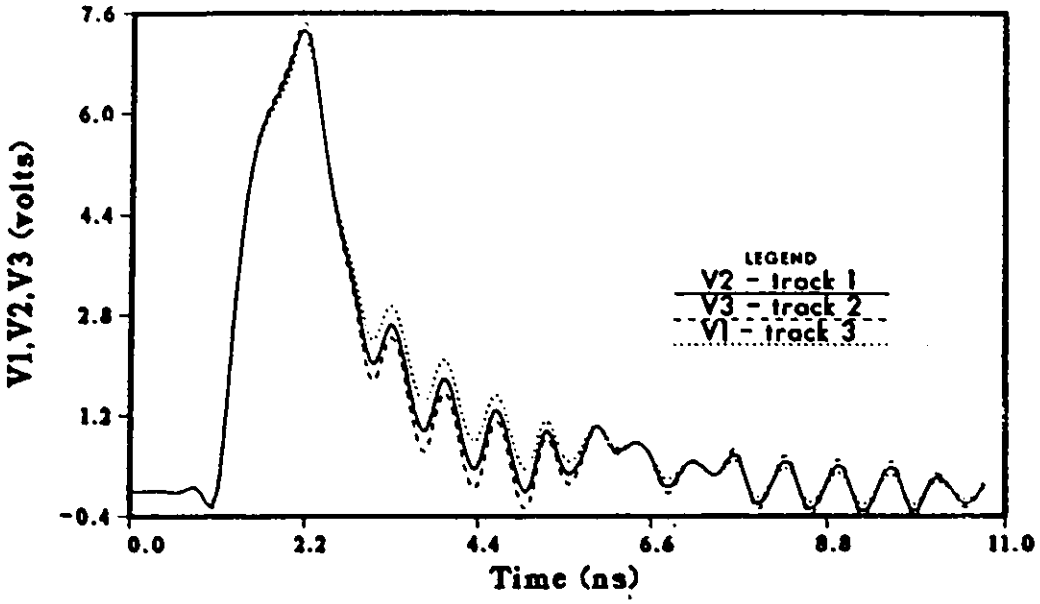

Chapter 9

Conclusions

In this thesis, the transient skin-effect of a transmission line situated above a lossy ground subjected to a time-varying electromagnetic field was shown to have significant effects on the predictions of the induced voltages onto the line. In order to have a better understanding of the impact of the external time-varying fields on a transmission line above a lossy ground, the transient skin-effect should be taken into account.

The transient skin-effect in a lossy transmission line was characterized by a time-domain parameter which was called the transient skin-effect resistance. The corresponding formula for this parameter taking into account the skin-effect in both the conductor line and the lossy ground was presented. Moreover, the external time-varying electromagnetic field which excited the lossy transmission line was represented by equivalent voltage and current sources. The formulations of these equivalent distributed sources were derived from Maxwell's equations.

By taking into account the transient skin-effect in a lossy transmission line, and the equivalent sources due to the external electromagnetic fields, the modified transmission line equations were introduced. These expressions consisted of an integral-differential equation whose kernel was proportional to the transient skin-effect resistance were solved by using the time-domain finite-difference approach.

The finite-difference formulas for the modified transmission line equations and for the boundary conditions were generated for this research. By using these derived expressions, a finite-difference algorithm which could be easily programmed was established. The algorithm was set to produce directly the time-domain solutions of the modified transmission line equations. The numerical algorithm could also predict the induced voltages and currents on a lossy transmission line as well as the propagation of the induced voltages and

currents on the line.

Furthermore, the finite-difference algorithm was applied to solve for the induced voltages on a bent conductor and on a system of multi-conductors. The corresponding finite-difference equations characterizing the bent line and the parallelly-coupled transmission lines had been derived and included in the programs prepared for this research. In fact, the comparisons of the numerical results to the calculations presented in different references had verified the developed finite-difference algorithm. Again, the predicted induced voltages compared to other recently published measurements for non-uniform field excitation of a lossy line had confirmed the reliability of the algorithm.

In this thesis, much mathematics had been done to obtain the equations for the transient skin-effect resistance, the equivalent sources due to the external fields, the boundary conditions and those for the multi-conductors and the bent conductors. Although there had been a lot of pre-processing, the time-domain finite-difference algorithm was absolutely easy to implement. Finally, the presented time-domain finite-difference algorithm could be developed as a computer-aided design tool so as to have a better understanding of the susceptibility of equipment related to EMI/C engineering.

Appendix A

Discretizations of the modified transmission line equations

The modified telegraphers' equations which take into account the transient skin-effect of a lossy transmission line and the equivalent sources due to a time-varying electromagnetic field are given by:

$$-\frac{\partial v(x,t)}{\partial x} = l_{eq}\ \frac{\partial i(x,t)}{\partial t} + \frac{\partial}{\partial t}\int_0^t r(t-t')\cdot i(x,t')\,dt' + \frac{\partial \Phi_z}{\partial t} - [E_x(x,h) - E_x(x,0)]\quad , \tag{A.1}$$

$$-\frac{\partial i(x,t)}{\partial x} = c_{eq}\ \frac{\partial v(x,t)}{\partial t} + g_o v(x,t) - \left(c_{st}\frac{\partial}{\partial t} + g_o\right)\cdot\int_0^h E_y(x,y,t)\,dy\quad , \tag{A.2}$$

where l_{eq} and c_{eq} are the equivalent inductance and capacitance for a lossy line. For one conductor line, l_{eq} becomes the external line inductance l_{ext}, and c_{st} becomes the line capacitance c_{st}. The telegraphers' equations are then normalized and written as:

$$-\frac{\partial v(\xi,t_n)}{v_{ph}\tau_g\partial\xi} = l_{eq}\frac{w(\xi,t_n)}{Z_o\tau_g\partial t_n} + \frac{\tau_{d.c.}}{Z_o}\frac{\partial}{\partial t_n}\int_0^{t_n}\rho(t_n-t_n')\,w(\xi,t_n')\,dt_n' + \frac{\partial\Phi_z(\xi,)}{\tau_g\partial t_n} - E_x\left(\xi,\frac{L}{v_{ph}\tau_g},t_n\right) + E_x(\xi,0,t_n) \quad , \tag{A.3}$$

$$-\frac{1}{Z_o}\frac{\partial w(\xi,t_n)}{v_{ph}\tau_g\partial\xi} = c_{eq}\frac{\partial v(\xi,t_n)}{\partial t_n} + g_o v(\xi,t_n) - \left\{\frac{\partial}{\partial t_n}+g_o\right\}\cdot c_{eq}\int_0^h E_y(\xi,\xi',t_n)\,d\xi' \quad , \tag{A.4}$$

where v_{ph} is the velocity of propagation given by:

$$v_{ph} = \frac{1}{\sqrt{l_{eq}c_{eq}}} \quad , \tag{A.5}$$

and Z_o is the characteristic impedance of the transmission line. The above equations can be re-written as:

$$-\frac{\partial v(\xi,t_n)}{\partial\xi} = l_{eq}\frac{v_{ph}}{Z_o}\frac{w(\xi,t_n)}{\partial t_n} + \frac{\tau_{d.c.}v_{ph}\tau_g}{Z_o}\frac{\partial}{\partial t_n}\int_0^{t_n}\rho(t_n-t_n')\,w(\xi,t_n')\,dt_n' + v_{ph}\tau_g\left\{\frac{\partial\Phi_z(\xi,t_n)}{\tau_g\partial t_n} - E_x\left(\xi,\frac{L}{v_{ph}\tau_g},t_n\right) + E_x(\xi,0,t_n)\right\} \quad , \tag{A.6}$$

$$-\frac{\partial w(\xi,t_n)}{v_{ph}\tau_g\partial\xi} = Z_o v_{ph}c_{eq}\frac{\partial v(\xi,t_n)}{\partial t_n} + \tau_g Z_o v_{ph}\left\{g_o v(\xi,t_n) - c_{eq}\frac{\partial}{\partial t_n} + g_o\int_0^h E_y(\xi,\xi',t_n)\,d\xi'\right\} \quad . \tag{A.7}$$

These expressions can be simplified by defining the following variables:

$$p = l_{eq}\frac{v_{ph}}{Z_o} \quad , \tag{A.8}$$

$$q = Z_o v_{ph} c_{eq} \quad , \tag{A.9}$$

$$\nu_r = \frac{r_{d.c.} v_{ph} \tau_g}{Z_o} \quad , \tag{A.10}$$

$$\nu_g = g_o Z_o v_{ph} \tau_g \quad . \tag{A.11}$$

The resulting telegrapher's equations are put in the form:

$$-\frac{\partial v(\xi\,,t_n)}{\partial \xi} = p \cdot \frac{w(\xi,t_n)}{\partial t_n} + \nu_r \frac{\partial}{\partial t_n}\int_0^{t_n} \rho(t_n - t_n')\, w(\xi\,,t_n')\, dt_n' + v_{ph}\tau_g \left\{ \frac{\partial \Phi_z(\xi\,,t_n)}{\tau_g \partial t_n} - E_x\left(\xi\,,\frac{L}{v_{ph}\tau_g}\,,t_n\right) + E_x(\xi\,,0\,,t_n)\right\} , \tag{A.12}$$

$$-\frac{\partial w(\xi\,,t_n)}{\partial \xi} = q \cdot \frac{\partial v(\xi\,,t_n)}{\partial t_n} + \nu_g v(\xi\,,t_n) - q \cdot \frac{\partial}{\partial t_n} + \nu_g \int_0^h E_y(\xi\,,\xi'\,,t_n)\, d\xi' \quad . \tag{A.13}$$

By using the finite-difference formulas for the voltage v, and the current w, the discretized telegrapher's equations are obtained and represented as follows:

$$-\frac{1}{\Delta\xi}\left(v_{k,l+1} - v_{k-1,l+1}\right) = \frac{p}{\Delta t_n}\left(w_{k-\frac{1}{2},l+1} - w_{k-\frac{1}{2},l}\right) + \nu_r \left[\frac{1}{2}\rho_o w_{k-\frac{1}{2},l+1} - \frac{1}{2}\left(\rho_o - 2\rho_1\right) w_{k-\frac{1}{2},l} + v_{ph}\tau_g \frac{\partial \Phi_z(\xi\,,t_n)}{\tau_g \partial t_n} - v_{ph}\tau_g E_x\left(\xi\,,\frac{L}{v_{ph}\tau_g}\,,t_n\right) + v_{ph}\tau_g E_x(\xi\,,0\,,t_n) - \sum_{m=0}^{l-1}\left(\rho_{l-m+1} - \rho_{l-m}\right) w_{k-\frac{1}{2},m}\right] , \tag{A.14}$$

$$-\frac{1}{\Delta\xi}\left(w_{k+\frac{1}{2},l}-w_{k-\frac{1}{2},l}\right) = \frac{q}{\Delta t_n}\left(v_{k,l+1}-v_{k,l}\right)+\nu_g\cdot\frac{1}{2}\left(v_{k,l+1}+v_{k,l}\right)+ \frac{\Delta t_n}{q}\cdot\left[q\tau_g\frac{\partial}{\partial t_n}+\nu_g\right]\int_0^h E_y\left(\xi\,,\xi'\,,t_n\right)d\xi' \quad . \tag{A.15}$$

The two above equations are then reduced to the following expressions by re-arranging the terms on both sides:

$$v_{k,l+1} = \left(\frac{1-\frac{1}{q}\frac{\Delta t_n}{2}}{1+\frac{1}{q}\nu_g\frac{\Delta t_n}{2}}\right)-\left(\frac{\frac{1}{q}\cdot\frac{\Delta t_n}{\Delta\xi}}{1+\frac{1}{q}\nu_g\frac{\Delta t_n}{2}}\right)\left(w_{k+\frac{1}{2},l}-w_{k-\frac{1}{2},l}-w_{k-\frac{1}{2},l}\right) + \left(\frac{1}{1+\frac{1}{q}\nu_g\frac{\Delta t_n}{2}}\right)\cdot\left(\Delta t_n\tau_g\frac{\partial}{\tau_g\Delta t_n}+\frac{1}{q}\Delta t_n\nu_g\right)\int_0^\infty E_y\left(\xi\,,\xi'\,,t_n\right)\,, \tag{A.16}$$

$$w_{k-\frac{1}{2},l+1} = \left(\frac{1-\frac{1}{p}\frac{\nu_r\Delta t_n}{2}}{1+\frac{1}{p}\nu_r\frac{\Delta t_n}{2}}\right)w_{k-\frac{1}{2},l}-\left(\frac{\frac{1}{p}\cdot\frac{\Delta t_n}{\Delta\xi}}{1+\frac{1}{p}\nu_r\frac{\Delta t_n}{2}}\right)\left(v_{k,l+1}-v_{k-1,l+1}\right) -\left[\frac{\partial}{\tau_g\Delta t_n}+E_x\left(\xi\,,\frac{L}{v_{ph}\tau_g}\,,t_n\right)+v_{ph}\tau_g E_x\left(\xi\,,0\,,t_n\right)\right] \cdot\left(\frac{\frac{1}{p}}{1+\frac{1}{p}\nu_r\frac{\Delta t_n}{2}}\right)\left(\Delta t_n v_{ph}\tau_g\right) \quad . \tag{A.17}$$

For a cylindrical conductor above a lossy ground, the velocity of propagation of the induced voltage is given by:

$$v_{ph}=\frac{1}{\sqrt{l_{ext}c_{st}}} \quad , \tag{A.18}$$

and the characteristic impedance of the line is defined by:

$$Z_o=\sqrt{\frac{l_{ext}}{c_{st}}} \quad . \tag{A.19}$$

From the two above equations, one can obtain the following relations:

$$Z_o = \frac{v_{ph}}{l_{eq}} \quad , \tag{A.20}$$

$$Z_o = v_{ph} c_{eq} \quad . \tag{A.21}$$

It follows from equations (A.8) and (A.9) that $p = 1$ and $q = 1$. Under this circumstance, the discretization transmission line equations become:

$$\begin{aligned} v_{k,l+1} = & \left(\frac{1 - \nu_g \frac{\Delta t_n}{2}}{1 + \nu_g \frac{\Delta t_n}{2}}\right) v_{k,l} - \left(\frac{\frac{\Delta t_n}{\Delta \xi}}{1 + \nu_g \frac{\Delta t_n}{2}}\right) \cdot \left(w_{k+\frac{1}{2},l} - w_{k-\frac{1}{2},l}\right) + \\ & \left(\frac{1}{1 + \nu_g \frac{\Delta t_n}{2}}\right) \cdot \left(\Delta t_n \cdot \tau_g \cdot \frac{\Delta v_e(\xi, t_n)}{\Delta t_n \cdot \tau_g} + \nu_g \cdot \Delta t_n \cdot v_e(\xi, t_n)\right) , \end{aligned} \tag{A.22}$$

$$\begin{aligned} w_{k-\frac{1}{2},l+1} = & \left(\frac{1 + \frac{1}{2}\nu_r \Delta t_n (\rho_o - 2\rho_1)}{1 + \frac{1}{2}\nu_r \rho_o \Delta t_n}\right) w_{k-\frac{1}{2},l} - \\ & \left(\frac{\Delta t_n}{1 + \frac{1}{2}\nu_r \rho_o \Delta t_n}\right) \cdot (v_{k,l+1} - v_{k-1,l+1}) + \\ & \left(\frac{\nu_r \Delta t_n}{1 + \frac{1}{2}\nu_r \rho_o \Delta t_n}\right) \cdot \left(\sum_{m=0}^{l-1} \rho_{l-m+1} - \rho_{l-m}\right) w_{k-\frac{1}{2},m} - \\ & \left(\frac{v_o \tau_g \Delta t_n}{1 + \frac{1}{2}\nu_r \rho_o \Delta t_n}\right) \cdot \left(\frac{\Delta \Phi_z}{\tau_g \Delta t_n} + E_x(\xi, \xi', t_n) - E_x(\xi, 0, t_n)\right) . \end{aligned} \tag{A.23}$$

where ρ_o is the normalized skin-effect resistance at the zero time step, $l = 0$, and ρ_1 is the normalized skin-effect resistance at the first time step, $l = 1$.

Appendix B

The finite-difference equations for the combined linear loads

For a series combination of a resistor R and an inductor L, the voltage equations are given by:

$$v_r = R \cdot i \quad , \tag{B.1}$$

$$v_l = L \cdot \frac{di}{dt} \quad . \tag{B.2}$$

The corresponding finite-difference expressions are represented by:

$$(v_{m,l+1})_r = \frac{R}{Z_o} \cdot w_{m+\frac{1}{2},l} \quad , \tag{B.3}$$

$$(v_{m,l+1})_l = \frac{L}{Z_o \tau_g t_n} \cdot \left(w_{m+\frac{1}{2},l} - w_{m+\frac{1}{2},l-1} \right) \quad . \tag{B.4}$$

The total voltage across the load is the sum of the voltage v_r and v_l and is written as:

$$v_{m,l+1} = \frac{R}{Z_o} w_{m+\frac{1}{2},l} + \frac{L}{Z_o \tau_g t_n} \left(w_{m+\frac{1}{2},l} - w_{m+\frac{1}{2},l-1} \right) \quad , \tag{B.5}$$

$$v_{m,l+1} = \left(\frac{R}{Z_o} + \frac{L}{Z_o \tau_g t_n} \right) w_{m+\frac{1}{2},l} - \left(\frac{L}{Z_o \tau_g t_n} \right) w_{m+\frac{1}{2},l-1} \quad .$$

By re-arranging the terms on both sides, the above equation is put as:

$$w_{m+\frac{1}{2},l} = \left(\frac{1}{R\tau_g t_n + L}\right) \cdot \left(L \cdot w_{m+\frac{1}{2},l-1} + Z_o \tau_g t_n \cdot v_{m,l+1}\right) \quad . \tag{B.6}$$

The above formula is simplified by defining the following coefficients:

$$K_1 = \frac{R\tau_g t_n + L}{L} \quad , \tag{B.7}$$

$$K_2 = \frac{Z_o \tau_g t_n}{L + R\tau_g t_n} \quad , \tag{B.8}$$

and the resulting formula is given by:

$$K_1 \cdot w_{m+\frac{1}{2},l} = w_{m+\frac{1}{2},l-1} + K_2 \cdot v_{m,l+1} \quad . \tag{B.9}$$

From the above formula, the following expressions is written:

$$\begin{aligned}
K_1 \cdot w_{m+\frac{1}{2},1} &= w_{m+\frac{1}{2},0} + K_2 v_{m,2} \ , \text{ where } l = 1 \ , \\
K_1^2 \cdot w_{m+\frac{1}{2},2} &= K_1 w_{m+\frac{1}{2},1} + K_1 K_2 v_{m,3} \ , \text{ where } l = 2 \ , \\
K_1^3 \cdot w_{m+\frac{1}{2},3} &= K_1^2 w_{m+\frac{1}{2},2} + K_1^2 K_2 v_{m,4} \ , \text{ where } l = 3 \ , \\
K_1^4 \cdot w_{m+\frac{1}{2},4} &= K_1^3 w_{m+\frac{1}{2},3} + K_1^3 K_2 v_{m,5} \ , \text{ where } l = 4 \ , \\
&\vdots \\
K_1^N \cdot w_{m+\frac{1}{2},N} &= K_1^{N-1} w_{m+\frac{1}{2},N-1} + K_1^{N-1} K_2 v_{m,N+1} \ , \text{ where } l = N \ .
\end{aligned}$$

By summing up the above expressions, a general formula is obtained and written as:

$$w_{m+\frac{1}{2},N} = \left(\frac{K_2}{K_1}\right) v_{m,N+1} + K_2 \sum_{n=2}^{NN} \frac{K_1^{n-2}}{K_1^N} v_{m,n} \quad \text{, where } 2 \leq NN \leq N \quad . \tag{B.10}$$

By substitution of the above formula into the discretized telegrapher's equations, the finite-difference equation governing the voltage at the load is derived and represented by:

$$\begin{aligned} v_{m,N+1} \quad = \quad & \left(\frac{g_{11}}{1+g_{12}\frac{K_2}{K_1}}\right) v_{m,N} - \left(\frac{g_{12}K_2}{1+g_{12}\frac{K_2}{K_1}}\right) \sum_{n=2}^{NN} \frac{K_1^{n-2}}{K_1^N} v_{m,n} \\ + \quad & \left(\frac{g_{12}}{1+g_{12}\frac{K_2}{K_1}}\right) w_{m-\frac{1}{2},N} + e_1 \quad , \end{aligned} \tag{B.11}$$

where e_1 is the equivalent sources due to the external electromagnetic field and the coefficients g_{11} and g_{12} represent:

$$g_{11} = \frac{1-\frac{1}{2}\nu_g t_n}{1+\frac{1}{2}\nu_g t_n} \quad , \tag{B.12}$$

$$g_{12} = \frac{\frac{t_n}{\Delta\xi}}{1+\frac{1}{2}\nu_g t_n} \quad . \tag{B.13}$$

The final expression used in the finite-difference algorithm to represent the voltage at the load is derived from the above equation and given as follows:

$$\begin{aligned} v_{m,N+1} \quad = \quad & \left[\frac{1}{\left(1+\frac{1}{2}\nu_g t_n\right)\left(L+R\tau_g t_n\right)^2 + Z_o L \tau_g t_n}\right] \\ \cdot \quad & \left[\left(1-\frac{1}{2}\nu_g t_n\right)\left(L+R\tau_g t_n\right)^2 v_{m,N}\right. \\ - \quad & \left(L+R\tau_g t_n\right)\left(Z_o\tau_g t_n\right) \sum_{n=2}^{NN} \left(\frac{R\tau_g t_n + L}{L}\right)^{n-2-NN} v_{m,N} \\ + \quad & \left.\left(L+R\tau_g t_n\right) w_{m-\frac{1}{2},N}\right] + e_2 \quad , \end{aligned} \tag{B.14}$$

(B.15)

where e_2 is due to the external electromagnetic field excitation.

In the case of a parallel combination of a resistor R and a capacitor C, the current in the load is the sum of the currents in the resistor and the capacitor. The corresponding finite-difference equation for the current in the load is given by:

$$w_{m+\frac{1}{2},l} = Z_o \left(\frac{1}{R} + \frac{C}{\tau_g t_n} \right) v_{m,l+1} - \frac{Z_o C}{\tau_g t_n} v_{m,l} \quad . \tag{B.16}$$

By substitution of the above expression into the discretized telegrapher's eqautions, the finite-difference equation of the voltage at the load is derived and written as:

$$\begin{aligned} v_{m,l+1} \quad = \quad & \frac{R\tau_g t_n}{R\tau_g t_n + g_{12} Z_o \left(\tau_g t_n + RC\right)} \\ & \cdot \left[\left(g_{11} + g_{12} \frac{Z_o C}{\tau_g t_n} \right) v_{m,l} + g_{12} w_{m-\frac{1}{2},l} + e_3 \right] \quad . \end{aligned} \tag{B.17}$$

where the coefficients g_{11} and g_{12} have been defined in equations (B.12) and (B.13), and e_3 represents the equivalent sources due to the external time-varying electromagnetic field.

Appendix C

Computer program for the finite-difference algorithm

```
c*************************************************************************
c                                                                        *
c    This program is to predict the induced voltages and currents of     *
c    a lossy transmission line excited by an electromagnetic pulse       *
c    by taking into account the transient skin-effect in the line.       *
c                                                                        *
c                  ( All parameters are in SI units. )                   *
c                                                                        *
c*************************************************************************
c.....
c.....
      PROGRAM TDFD
c.....
c.....
      PARAMETER(NX=101,NT=602,FAC2=5.D-2)
c.....NX is the total number of space steps between the beginning
c.....and the end of the line.
c.....NT is the total number of time steps.
c.....FAC2 is the total number of space steps between the line
c.....and the ground.
c.....
c.....
      DOUBLE PRECISION V(NX,NT),A(NX+1,NT),SR(NT),TOTL(NT)
      DOUBLE PRECISION WHR,WDTH,P,Q,DX,DT
      DOUBLE PRECISION C(5),G(5),PK(4),RL(4),CP,LS
      DOUBLE PRECISION ESUM(4),NUM(4),EX(8),EFAC(6),ETKL(3),ELKL(4)
      DOUBLE PRECISION L0,C0,V0,VC0,TAOC,TAOG,Z0,RC0,RG0,DE,TYME
      DOUBLE PRECISION RD,G0,LLEN,E0,T1,T2,TT,PI,ZLR,ZLI,ADJ
      DOUBLE PRECISION SIGC,SIGG,MUE,MUER,MUE0,MM,SUM1,SUM2,SUM3
      DOUBLE PRECISION CAP1,CAP2,L1,L2,Z1R,Z1I,DIST,FAC,TRM1
      DOUBLE PRECISION HITE,INHITE,EPSI,PHI,PHI1,PHI2,PHI3,PHI4,PHI5
      DOUBLE PRECISION CASE,HN,M0,RT,CT,COEF1,COEF2
      DOUBLE PRECISION DELAYC,DELAY1,DELAY2,ELKL0,DEYDX,DEXDY,M1
      DOUBLE PRECISION NUM3,XT,M2,SUMM1,SUMM2,PRO,ARB,EPLN,ER,EP
      COMPLEX*16 Z1,ZL
      INTEGER*4 M,N,I,J,II,JJ,STP,VAR,KP,PWR,IH,IK,TK,IJ,JI
      INTEGER*4 ME1,ME2,MX1,MX2
c.....
c.....
      OPEN(1,FILE='SKIN.OUT',STATUS='OLD')
      OPEN(2,FILE='VOLT.OUT',STATUS='OLD')
      OPEN(3,FILE='CURRENT.OUT',STATUS='OLD')
c.....output files
c.....
c.....
      PI=4.D0*DATAN(1.D0)
c.....
c.....
c--------------------------------------
c
c   Data input
c
c--------------------------------------
c.....
```

```
c.....
      EPLN=8.8542D-12
      ER=1.D0
      EP=ER*EPLN
c.....EPLN is the permittivity of the free space.
c.....ER is the dielectric constant.
c.....EP is the permittivity of the propagation medium.
c.....
c.....
      MUE0=4.D-7*PI
      MUER=1.D0
      MUE=MUE0*MUER
c.....MUE0 is the permeability of the free space.
c.....MUER is the relative permeability.
c.....MUE is the permeability of the propagation medium.
c.....
c.....
      SIGC=5.8D7
      SIGG=1.D-2
c.....SIGC is the conductivity of the conductor line.
c.....SIGG is the conductivity of the lossy ground.
c.....
c.....
      RAD=1.D-3
c.....radius of the transmission line
c.....
c.....
c     WHR=1.941445146
c     WDTH=1.1094D-3
c.....dimensions of a flat conductor
c.....WHR is the effective w to h ratio.
c.....WDTH is the effective width of the ribbon.
c.....
c.....
      HITE=10.D-2
c.....HITE is the distance between the line and the ground.
c.....
c.....
      LLEN=1.D0
c.....total length of the transmission line
c.....
c.....
c     L0=1.9685D-7*LOG(2.D0*PI/WHR)
c.....inductance of a flat conductor above ground
c.....
c.....
      L0=2.D-7*LOG(2.D0*HITE/RAD)
c.....inductance of a cylindrical conductor above ground
c.....
c.....
c     L0=0.1504D-8
c.....equivalent inductance of a transmission line
c.....This parameter is used for a system of multi-conductors.
c.....
```

```
c.....
      C0=ER/(VC0**2*L0)
c     C0=2.D0*PI*EPLN/LOG(2.D0*HITE/RAD)
c.....capacitance of the transmission line
c.....
c.....
c     C0=0.1605D-11
c.....equivalent capacitance of the line
c.....This parameter is used for a system of multi-conductors.
c.....
c.....
      RC0=1.D0/(SIGC*PI*(RAD**2))
c     RC0=4.9651D0
c.....the d.c. resistance of the lossy line
c.....
c.....
      G0=0.01D0*C0
c.....conductance of the transmission line
c.....
c.....
      VC0=1.D0/DSQRT(MUE0*EPLN)
      V0=1.D0/DSQRT(MUE*EP)
c     V0=1.D0/DSQRT(L0*C0)
c.....VC0 is the speed of light.
c.....V0 is the velocity of propagation of the induced voltage
c.....on the lossy transmission line.
c.....
c.....
      TAOC=MUE*SIGC*(RAD**2)
      TAOG=MUE*SIGG*(HITE**2)
c.....TAOC is the intrinsic time constant of the round conductor
c.....TAOG is the intrinsic time constant of the lossy ground
c.....
c.....
      VI=TAOG/TAOC
c.....the ratio of the time constant of the ground
c.....to the time constant of the cylindrical conductor
c.....
c.....
c     Z0=48.3D0
c.....characteristic impedance of a flat conductor above ground
c.....
c.....
      Z0=DSQRT(L0/C0)
c.....characteristic impedance of a cylindrical conductor above ground
c.....
c.....
      ZLR=Z0
      ZLI=0.D0
      ZL=DCMPLX(ZLR,ZLI)
      CAP2=0.D0
      L2=0.D0
c.....load at the receiving end of the line
c.....ZLR is the real part of the load
```

```
c.....ZLI is the imaginary part of the load:
c.....ZLI is  0 for matched load;
c.....ZLI is +1 for purely inductive load;
c.....ZLI is -1 for purely capacitive load.
c.....CAP2 is the capacitance.
c.....L2 is the inductance.
c.....
c.....
      Z1R=Z0
      Z1I=0.D0
      Z1=DCMPLX(Z1R,Z1I)
      CAP1=0.D0
      L1=0.D0
c.....load at the beginning of the line
c.....Z1R is the real part of the load
c.....Z1I is the imaginary part of the load:
c.....Z1I is  0 for matched load;
c.....Z1I is +1 for purely inductive load;
c.....Z1I is -1 for purely capacitive load.
c.....CAP1 is the capacitance.
c.....L1 is the inductance.
c.....
c.....
c     CP=95.D-12*WDTH
c     LS=.48D0*L0*HITE/2.D0
c.....parameters to represent a right-angled bent flat conductor
c.....CP is the stray capacitance
c.....LS is the leakage inductance
c.....
c.....
      E0=10.D3
c.....peak of the applied electric field
c.....
c.....
      T1=1.2D6
      T2=1.D9
c.....T1 and T2 are the coefficients in per second
c.....of the double exponential form representing
c.....the applied electric field
c.....
c.....
      RD=10.D0*HITE
c.....radial distance between the excitation source and
c.....the beginning of the transmission line
c.....
c.....
      ADJ=RD/V0
c.....time taken for the applied field to reach the
c.....beginning of the transmission line.
c.....
c.....
      CASE=1.D0
c.....type of polarization of the electric field
c.....CASE is 1 for parallel polarization
```

```
c.....CASE is 2 for perpendicular polarization
c.....
c.....
      EPS'=45.D0*PI/180.D0
      PHI1=45.D0*PI/180.
      PHI=PHI1
c.....direction of the applied electromagnetic field
c.....EPSI is the anlge of incidence
c.....PHI is the azimuth angle
c.....
c.....
c     PHI1=PHI
c     PHI2=PHI1-90.D0*PI/180.D0
c     PHI3=PHI2+90.D0*PI/180.D0
c     PHI4=PHI3-90.D0*PI/180.D0
c     PHI5=PHI4+90.D0*PI/180.D0
c.....Azimuth angle changes in case of a bent line.
c.....
c.....
      HN=0.D0
c.....to initialize the magnetic flux normal to the plane
c.....passing through the line and perpendicular to the ground
c.....
c.....
      M=NX-1
      MM=DFLOAT(M)
      N=NT-1
c.....
c.....
      FAC=1.D0
c.....FAC is a constant ratio of the time step to the space step
c.....
c.....
      P=1.D0
      Q=1.D0
c.....parameters used to vary the ratio of the
c.....discretization time step to the space step
c.....
c.....
      DT=LLEN/V0/TAOG/MM
c.....DT is the discretization time step
c.....
c.....
      DE=HITE/V0/TAOG*FAC2
c.....DE is the space step counting from the line to the ground
c.....
c.....
      DO 5 J=1,N+1
       DO 5 I=1,M+1
        V(I,J)=0.D0
5     CONTINUE
      DO 7 J=1,N+1
       DO 7 I=1,M+2
        A(I,J)=0.D0
```

```
7     CONTINUE
c.....to initialize the voltage and the current
c.....
c.....
c-----------------------------------------------
c.....
c.....
      DO 16 J=1,N+1
       SR(J)=0.D0
       TOTL(J)=0.D0
16    CONTINUE
c.....to initialize the normalized transient skin-effect resistance
c.....
c.....
      KON=1.D0/(PI*(HITE**2)*SIGG*RC0)
c.....a parameter used in the formulation of
c.....the transient skin-effect resistance
c.....
c.....
      IF (((N+1)*DT).LT.(1.D-1)) THEN
c.....
c.....
c-----------------------------------------------------
c
c   Calculate the transient skin-effect resistance
c   by using an asymptotic expression
c
c-----------------------------------------------------
c......
c......
       C(1)=(KON+1.D0/DSQRT(VI))/2.D0/DSQRT(PI)
       C(2)=-(KON-1.D0)/4.D0
       C(3)=(KON/8.D0+3.D0*DSQRT(VI)/10.D0)*2.D0/DSQRT(PI)
       C(4)=3.D0*VI/16.D0
       C(5)=(-3.D0*KON/32.D0+63.D0*DSQRT(VI)/256.D0)*4.D0
     1 /3.D0/DSQRT(PI)
       DO 17 J=2,N+1
        ETA=(J-1)*DT
        SR(J)=C(1)/DSQRT(ETA)+C(2)+C(3)*DSQRT(ETA)
     1  +C(4)*ETA+C(5)*ETA*DSQRT(ETA)
17     CONTINUE
       M2=(SR(3)-SR(4))/DT
       M1=(SR(2)-SR(3))/DT
       M0=2.D0*M1-M2
       SR(1)=M0*DT+SR(2)
       DO 622 J=1,N+1
        TYME=DFLOAT(J-1)*DT*TAOG+ADJ
        WRITE(1,*) TYME,SR(J)
622    CONTINUE
      ENDIF
c.....
c.....
      IF (((N+1)*DT).GE.(1.D-1)) THEN
c.....
```

```
c.....
c-----------------------------------------------
c
c   Calculate the roots of the bessel function
c   of the first kind
c
c-----------------------------------------------
c......
c......
        DO 88 I=1,1000
         B=4.D0*I+1.D0
         DO 881 JK=2,10,2
          CHEK=(PI*B)**JK
          CHK(JK)=1.D0/CHEK
          IF (CHEK.GE.1.D30) THEN
           IF (JK.EQ.2) THEN
            DO 882 JL=4,10,2
             CHK(JL)=0.D0
882          CONTINUE
           ELSEIF (JK.EQ.4) THEN
            DO 883 JL=6,10,2
             CHK(JL)=0.D0
883          CONTINUE
           ELSEIF (JK.EQ.6) THEN
            DO 884 JL=8,10,2
              CHK(JL)=0.D0
884          CONTINUE
           ELSE
            CHK(10)=0.D0
           ENDIF
           GO TO 885
          ENDIF
881      CONTINUE
885      TM(1)=1.D0
         TM(2)=6.D0*CHK(2)
         TM(3)=6.D0*CHK(4)
         TM(4)=4.716D3/5.D0*CHK(6)
         TM(5)=3.902418D6/35.D0*CHK(8)
         TM(6)=8.95167324D8/35.D0*CHK(10)
         RT(I)=(TM(1)-TM(2)+TM(3)-TM(4)+TM(5)-TM(6))*PI*B/4.D0
88      CONTINUE
c.....
c.....
c--------------------------------------
c
c   Continue the computations of the
c   transient skin-effect resistance
c
c--------------------------------------
c......
c......
        DO 496 J=2,N+1
c......
c......
```

```
c-----------------------------------------
c
c    The transient skin-effect resistance
c    of the cylindrical conductor
c
c-----------------------------------------
c.......
c.......
         DO 89 II=1,1000
          NUM3=(RT(II)**2)*((J-1)*DT*TAOG+ADJ)/TAOG
          IF (NUM3.GT.87.D0) THEN
           TOTL(J)=0.D0
          ELSE
           TOTL(J)=TOTL(J)+DEXP(-NUM3)
          ENDIF
89       CONTINUE
         SR(J)=1.D0+TOTL(J)
c.......
c.......
c-----------------------------------------
c
c     The transient skin-effect resistance
c     of the lossy ground
c
c-----------------------------------------
c.......
c.......
         TT=DFLOAT(J-1)
         XT=DSQRT(TAOG/(TT*DT*TAOG+ADJ))
         ERFC=1-2.D0/DSQRT(PI)*(XT-XT**3/3.D0+XT**5/10.D0-XT**7/42.D0
      1  +XT**9/2.16D2-XT**11/1.32D3+XT**13/9.36D3-XT**15/7.56D4
      2  +XT**17/6.8544D5-XT**19/6.89472D6)
         IF (XT.GE.9.23D0) THEN
          XT=9.23
          RSUP=1.D37
          GO TO 1357
         ENDIF
         IF (((1.D37)/DEXP(XT**2)).LE.(DABS(ERFC))) THEN
          RSUP=1.D37
          GO TO 1357
         ENDIF
         RSUP=MUE0/PI/TAOG*(1.D0/2.D0/DSQRT(PI)*XT+(DEXP(XT**2)*ERFC
      1  -1.D0)/4.D0)
c.......
c.......
c-----------------------------------
c
c     Calculate the total transient
c     skin-effect resistance
c
c-----------------------------------
c.......
c.......
1357     SR(J)=SR(J)+RSUP/RC0
```

```
496     CONTINUE
        M2=(SR(3)-SR(4))/DT
        M1=(SR(2)-SR(3))/DT
        M0=2.D0*M1-M2
        SR(1)=M0*DT+SR(2)
        DO 694 J=1,N+1
         TYME=DFLOAT(J-1)*DT*TAOG+ADJ
         WRITE(1,*) TYME,SR(J)
694     CONTINUE
       ENDIF
c.....
c.....
c-----------------------------------------
c.....
c.....
c      DO 991 J=10,500
c       V(1,J)=5.D0*(1.D0-DEXP(-(J-1)*DT*TAOG*LOG(9.D0)/10.D-9))
c991   CONTINUE
c      IJ=1
c      DO 992 J=500,10,-1
c       JI=J+2*IJ-1
c       V(1,JI)=5.D0*(1.D0-DEXP(-(J-1)*DT*TAOG*LOG(9.D0)/10.D-9))
c       IJ=IJ+1
c992   CONTINUE
c.....a trapezoidal pulse excitation at the beginning of the line
c.....with a rise time of 10 ns, and
c.....with a pulse width of 499 times the time step.
c.....
c.....
       RL(1)=(Z1R*TAOG*DT+L1)/L1
       RL(2)=(Z0*TAOG*DT)/(L1+Z1R*TAOG*DT)
       RL(3)=(ZLR*TAOG*DT+L2)/L2
       RL(4)=(Z0*TAOG*DT)/(L2+ZLR*TAOG*DT)
c.....parameters for a resistor in series with an inductor
c.....
c.....
c      RT=Z0
c      CT=50.D-12
c.....a parallel combination of a resistance RT and a capacitance CT
c.....
c.....
       G(1)=5.D-1*G0*V0*TAOG*Z0*DT
       PK(2)=G(1)
       G(2)=FAC/(1.D0+G(1))
       G(1)=(1.D0-G(1))/(1.D0+G(1))
       G(3)=5.D-1*RC0*V0*TAOG/Z0*DT
c      G(4)=FAC/(1.D0+G(3))
       G(4)=FAC/(1.D0+SR(1)*G(3))
c      PK(1)=V0*TAOG*DT/(1.D0+G(3))
       PK(1)=V0*TAOG*DT/(1.D0+SR(1)*G(3))
       PK(3)=1.D0/(1.D0+PK(2))
       PK(4)=2.D0*PK(2)/(1.D0+PK(2))
       G(5)=2.D0*G(3)/(1.D0+SR(1)*G(3))
c      G(3)=(1.D0-G(3))/(1.D0+G(3))
```

```
      G(3)=(1.D0-(2.D0*SR(2)-SR(1))*G(3))/(1.D0+SR(1)*G(3))
c.....coefficients of the discretization telegrapher's equations
c.....
c.....
c-----------------------------------
c.....
c.....
      DO 70 J=1,N
       WRITE(*,*) J
c......calculations in time steps
c......
c......
       DO 60 I=1,M+1
c.......calculations in space steps
c.......
c.......
c        IF (I.LE.21) THEN
c         PHI=PHI1
c        ENDIF
c        IF ((I.GT.21).AND.(I.LE.41)) THEN
c         PHI=PHI2
c        ENDIF
c        IF ((I.GT.41).AND.(I.LE.61)) THEN
c         PHI=PHI3
c        ENDIF
c        IF ((I.GT.61).AND.(I.LE.81)) THEN
c         PHI=PHI4
c        ENDIF
c        IF (I.GT.81) THEN
c         PHI=PHI5
c        ENDIF
c.......to change the azimuth angle accordingly
c.......in the case of a bent line
c.......
c.......
        CALL FIELD(RD,I,J,DX,DT,DE,TAOG,V0,PHI,EPSI,CASE,HITE,
     1  ADJ,T1,T2,E0,HN,ELKL0,ETKL,ELKL,Q,FAC2)
c.......jump and calculate the applied electric field
c.......
c.......
c        IF ((I.EQ.21).OR.(I.EQ.41).OR.(I.EQ.61).OR.(I.EQ.81)) THEN
c         V(I,J+1)=(1.D0/(1.D0+CP/(DT*TAOG)))*(G(1)*V(I,J)-G(2)
c    1    *(CP/(DT*TAOG)*(V(I-1,J)-LS/(2.D0*Z0*DT*TAOG)*(A(I-1,J+1)
c    2    -A(I-1,J))))+PK(3)*(ETKL(1)-ETKL(2))+PK(4)*ETKL(3))
c        ENDIF
c.......to calculate the voltage at the discontinuity of a bent line
c.......
c.......
c-----------------------------------------
c.......
c.......
        IF (I.EQ.(M+1)) THEN
c.......
c.......
```

```
c.......include boundary conditions at
c.......the receiving end of the line
c.......
c........
          IF ((DREAL(ZL).GT.0.D0).AND.(DREAL(ZL).NE.Z0).AND.
     1    (DIMAG(ZL).EQ.0.D0)) THEN
           V(I,J+1)=DREAL(ZL)/(DREAL(ZL)+G(2)*Z0)*(G(1)*V(I,J)
     1     +G(2)*A(I,J)+PK(3)*(ETKL(1)-ETKL(2))+PK(4)*ETKL(3))
          ENDIF
c........purely resistive load or open circuit
c........
c........
          IF (CDABS(ZL).EQ.0.D0) THEN
           V(I,J+1)=0.D0
          ENDIF
c........short circuit
c........
c........
         IF (ZL.EQ.DCMPLX(Z0,0.D0)) THEN
          V(I,J+1)=1.D0/(1.D0+G(2))*(G(1)*V(I,J)+G(2)*A(I,J)+
     1    PK(3)*(ETKL(1)-ETKL(2))+PK(4)*ETKL(3))
         ENDIF
c.......matched load
c.......
c.......
         IF ((DREAL(ZL).EQ.0.D0).AND.(DIMAG(ZL).NE.0.D0)) THEN
c.......purely reactive load
c.......
c........
          IF (DIMAG(ZL).GT.0.D0) THEN
c........purely inductive load
           IF (J.LT.3) THEN
            V(I,J+1)=L/(L+G(2)*Z0*TAOG*DT)*(G(2)*A(I,J)+ETKL(1)
     1      -G(1)*ETKL(2))
            GO TO 222
           ENDIF
           SUM1=0.D0
           DO 40 JJ=3,J
            SUM1=SUM1+V(I,JJ)
40         CONTINUE
           V(I,J+1)=L2/(L2+G(2)*Z0*DT*TAOG)*(G(1)*V(I,J)+G(2)*A(I,J)
     1     +ETKL(1)-G(1)*ETKL(2))-G(2)*Z0*DT*TAOG/(L2+G(2)*Z0*TAOG
     2     *DT)*SUM1
          ELSE
c........purely capacitive load
           V(I,J+1)=(G(1)*TAOG*DT+G(2)*Z0*CAP2)/(TAOG*DT+G(2)*Z0*CAP2)
     1     *V(I,J)+G(2)*TAOG*DT/(TAOG*DT+G(2)*Z0*CAP2)*A(I,J)+TAOG*DT
     2     /(TAOG*DT+G(2)*Z0*CAP2)*(ETKL(1)-G(1)*ETKL(2))
          ENDIF
         ENDIF
c.......
c.......
         IF ((DREAL(ZL).NE.0.D0).AND.(DIMAG(ZL).NE.0.D0)) THEN
c.......combination of linear loads
```

```
c.......
c.........
          IF (DIMAG(ZL).GT.0.D0) THEN
c.........series combination of resistance and inductance
           IF (J.LT.2) THEN
            V(I,J+1)=(G(1)*V(I,J)+G(2)*A(I-1,J)+ETKL(1)-G(1)
     1      *ETKL(2))/(1.D0+G(2)*RL(4)/RL(3))
            GO TO 222
           ENDIF
           SUMM1=0.D0
           DO 440 JJ=2,J
            IF ((RL(3)**(JJ-2-J)).LE.(1.E-35)) THEN
             PRO=0.
            ELSE
             PRO=RL(3)**(JJ-2-J)
            ENDIF
            SUMM1=SUMM1+PRO*V(I,JJ)
440        CONTINUE
           V(I,J+1)=(G(1)*V(I,J)+G(2)*A(I-1,J)+ETKL(1)-G(1)
     1     *ETKL(2)-G(2)*RL(4)*SUMM1)/(1.+G(2)*RL(4)/RL(3))
          ELSE
c.........parallel combination of resistance and capacitance
           COEF1=1.D0/(1.D0+G(2)*Z0*(TAOG*DT+RT*CT)/(RT*TAOG*DT))
           COEF2=G(1)+G(2)*Z0*CT/(TAOG*DT)
           V(I,J+1)=COEF1*(COEF2*V(I,J)+G(2)*A(I,J))
          ENDIF
         ENDIF
c.......
c.......
c-----------------------------------------
c.......
c.......
         IF (I.NE.(M+1)) THEN
c.......
c.......
c.......calculate the propagation of the
c.......induced voltages and currents
c.......
c.........
          IF (I.EQ.1) THEN
c.........
c.........
c.........include boundary conditions
c.........at the beginning of the line
c.........
c..........
           IF ((DREAL(Z1).GT.0.D0).AND.(DREAL(Z1).NE.Z0).AND.
     1     (DIMAG(Z1).EQ.0.D0)) THEN
            V(I,J+1)=DREAL(Z1)/(DREAL(Z1)+G(2)*Z0)*(G(1)*V(I,J)
     1      -G(2)*A(I+1,J)+PK(3)*(ETKL(1)-ETKL(2))+PK(4)*ETKL(3))
           ENDIF
c.........purely resistive load or open cirucit
c..........
c..........
```

```
            IF (CDABS(Z1).EQ.0.D0) THEN
             V(I,J+1)=0.D0
            ENDIF
c.........short circuit
c.........
c.........
            IF (Z1.EQ.DCMPLX(Z0,0.D0)) THEN
             V(I,J+1)=(G(1)*V(I,J)-G(2)*A(I+1,J)+PK(3)*(ETKL(1)-ETKL(2))
     1        +PK(4)*ETKL(3))/(1.D0+G(2))
            ENDIF
c.........matched load
c.........
c.........
            IF ((DREAL(Z1).EQ.0.D0).AND.(DIMAG(Z1).NE.0.D0)) THEN
c.........purely reactive loads
c.........
c..........
             IF (DIMAG(Z1).GT.0.D0) THEN
c..........purely inductive load
              IF (J.LT.3) THEN
               V(I,J+1)=L1/(L1+G(2)*Z0*TAOG*DT)*(-G(2)*A(I+1,J)
     1          +ETKL(1)-G(1)*ETKL(2))
               GO TO 222
              ENDIF
              SUM3=0.D0
              DO 47 JJ=3,J
               SUM3=SUM3+V(I,JJ)
47            CONTINUE
              V(I,J+1)=(L1*(G(1)*V(I,J)-G(2)*A(I+1,J)+ETKL(1)-G(1)
     1         *ETKL(2))-G(2)*Z0*TAOG*DT*SUM3)/(L1+G(2)*Z0*TAOG*DT)
             ELSE
c..........purely capacitive load
              V(I,J+1)=((G(1)*TAOG*DT+G(2)*Z0*CAP1)*V(I,J)-G(2)*TAOG
     1         *DT*A(I+1,J)+TAOG*DT*(ETKL(1)-G(1)*ETKL(2)))/(TAOG*DT
     2         +G(2)*Z0*CAP1)
             ENDIF
            ENDIF
c.........
c.........
            IF ((DREAL(ZL).NE.0.D0).AND.(DIMAG(ZL).NE.0.D0)) THEN
c.........combination of linear loads
c.........
c..........
             IF (DIMAG(ZL).GT.0.D0) THEN
c..........series combination of resistance and inductance
              IF (J.LT.2) THEN
               V(I,J+1)=(G(1)*V(I,J)-G(2)*A(I+1,J)+ETKL(1)-G(1)
     1          *ETKL(2))/(1.D0+G(2)*RL(2)/RL(1))
               GO TO 222
              ENDIF
              SUMM2=0.D0
              DO 488 JJ=2,J
               IF ((RL(1)**(JJ-2-J)).LE.(1.E-35)) THEN
                PRO=0.D0
```

```
               ELSE
                PRO=RL(1)**(JJ-2-J)
               ENDIF
               SUMM2=SUMM2+PRO*V(I,JJ)
488           CONTINUE
              V(I,J+1)=(G(1)*V(I,J)-G(2)*A(I+1,J)-G(2)*RL(2)*SUMM2
     1        +ETKL(1)-G(1)*ETKL(2))/(1.D0+G(2)*RL(2)/RL(1))
             ENDIF
            ENDIF
           ELSE
            V(I,J+1)=G(1)*V(I,J)-G(2)*(A(I+1,J)-A(I,J))+PK(3)*(ETKL(1)
     1      -ETKL(2))+PK(4)*ETKL(3)
           ENDIF
          ENDIF
c.......
c.......
          SUM2=0.D0
          DO 550 STP=1,J
           SUM2=SUM2+(SR(J-(STP-1)+1)-SR(J-(STP-1)))*A(I,STP)
550       CONTINUE
222       IF (I.EQ.1) GO TO 60
          A(I,J+1)=G(3)*A(I,J)-G(4)*(V(I,J+1)-V(I-1,J+1))+G(5)*SUM2
     1    -PK(1)*(HN-ELKL0)
          A(I-1,J)=A(I,J+1)
c.......calculate the induced current
c.......
c.......
60       CONTINUE
70      CONTINUE
c.....
c.....
c-------------------------------------
c
c    write output files
c
c-------------------------------------
        DO 1000 J=1,N+1
         TYME=DFLOAT(J-1)*DT*TAOG+ADJ
         WRITE(2,80) TYME,V(1,J),V(NX,J)
         WRITE(3,80) TYME,A(1,J)/Z0,A(NX,J)/Z0
80       FORMAT(3(2X,D17.7))
1000    CONTINUE
9999    STOP
        END
c.....
c.....
c-----------------------------------------------------------
c
c     subroutine to calculate the applied electric field
c
c-----------------------------------------------------------
c.....
c.....
        SUBROUTINE FIELD(RD,I,J,DX,DT,DE,TAOG,V0,PHI,EPSI,CASE,HITE,
```

```
     1                   ADJ,T1,T2,E0,HN,ELKL0,ETKL,ELKL,Q,FAC2)
      DOUBLE PRECISION RD,DX,DT,DE,TAOG,V0,PHI,EPSI,CASE,HITE,FAC2,
      DOUBLE PRECISION T1,T2,E0,HN,ELKL0,DELAYC,ESUM(4),DELAY1,DELAY2
      DOUBLE PRECISION NUM(4),EX(8),ETKL(3),ELKL(4),EFAC(6),DEYDX
      DOUBLE PRECISION DEXDY,ADJ,Q
      INTEGER*4 KK,KP
      DELAYC=RD+(I-1)*DT*TAOG*V0*DSIN(PHI)*DCOS(EPSI)
      ESUM(1)=0.D0
      ESUM(2)=0.D0
      ESUM(3)=0.D0
      ESUM(4)=0.D0
      DO 117 KK=1,DINT(1.D0/FAC2)
       INHITE=DFLOAT(KK-1)*DE*V0*TAOG
       CALL XPO(NUM,EX,DELAY1,DELAY2,DELAYC,INHITE,PHI,V0,J,
     1           DT,TAOG,ADJ,T1,T2)
c.....
c.....
c-------------------------------------------------
c
c       In the case of non-uniform field excitation
c
c
c       ME1=DINT(27.5D0/LLEN*MM)
c       ME2=DINT(42.5D0/LLEN*MM)
c       IF (((I.GE.ME1).AND.(I.LE.ME2)).AND.(KK.LE.17)) THEN
c        DO 1903 IH=1,8
c         EX(IH)=1.D-1*EX(IH)
c1903    CONTINUE
c       ENDIF
c
c-------------------------------------------------
c.....
c.....
        IF (CASE.EQ.1.D0) THEN
         EFAC(1)=E0*(EX(1)-EX(2)+EX(3)-EX(4))
         EFAC(2)=E0*(EX(5)-EX(6)+EX(7)-EX(8))
         ESUM(1)=ESUM(1)+DSIN(EPSI)*EFAC(1)*DE
         ESUM(2)=ESUM(2)+DSIN(EPSI)*EFAC(2)*DE
         EFAC(3)=(EX(5)*T1-EX(6)*T2)*DSIN(PHI)*DCOS(EPSI)/V0
         EFAC(4)=(EX(7)*T1-EX(8)*T2)*DSIN(PHI)*DCOS(EPSI)/V0
         DEYDX=E0*DSIN(EPSI)*(EFAC(3)+EFAC(4))
        ELSE
         DEYDX=0.D0
        ENDIF
        EFAC(5)=(-EX(5)*T1+EX(6)*T2)*DCOS(PHI)/V0
        EFAC(6)=(EX(7)*T1-EX(8)*T2)*DCOS(PHI)/V0
        IF (CASE.EQ.1.D0) THEN
         DEXDY=DCOS(PHI)*DCOS(EPSI)*(EFAC(5)-EFAC(6))
        ELSE
         DEXDY=DSIN(PHI)*(EFAC(5)-EFAC(6))
        ENDIF
        ESUM(3)=ESUM(3)+(DEYDX-DEXDY)*DE
117    CONTINUE
       IF (CASE.EQ.1.D0) THEN
```

```
        ETKL(1)=V0*TAOG*ESUM(1)
        ETKL(2)=V0*TAOG*ESUM(2)
        ETKL(3)=5.D-1*(ETKL(1)-ETKL(2))
       ELSE
        ETKL(1)=0.D0
        ETKL(2)=0.D0
        ETKL(3)=0.D0
       ENDIF
       HN=-V0*TAOG*ESUM(3)
       IF (CASE.EQ.2.D0) THEN
        INHITE=HITE
        CALL XPO(NUM,EX,DELAY1,DELAY2,DELAYC,INHITE,PHI,V0,J,
      1           DT,TAOG,ADJ,T1,T2)
       ENDIF
       EFAC(1)=E0*(EX(1)-EX(2)-EX(3)+EX(4))
       EFAC(2)=E0*(EX(5)-EX(6)-EX(7)+EX(8))
       IF (CASE.EQ.1.D0) THEN
         ELKL0=5.D-1*DCOS(PHI)*DCOS(EPSI)*(EFAC(1)+EFAC(2))
       ELSE
         ELKL0=5.D-1*DSIN(PHI)*(EFAC(1)+EFAC(2))
       ENDIF
       RETURN
       END
c.....
c.....
c-----------------------------------------
c
c     subroutine to evaluate the
c     double exponential function
c
c-----------------------------------------
c.....
c.....
       SUBROUTINE XPO(NUM,EX,DELAY1,DELAY2,DELAYC,INHITE,PHI,V0,J,
      1                DT,TAOG,ADJ,T1,T2)
       DOUBLE PRECISION DELAY1,DELAY2,DELAYC,INHITE,PHI,V0,DT,TAOG
       DOUBLE PRECISION NUM(4),EX(8),ADJ,T1,T2
       INTEGER*4 J,KP
       DELAY1=(DELAYC-INHITE*DCOS(PHI))/V0
       DELAY2=(DELAYC+INHITE*DCOS(PHI))/V0
       NUM(1)=(J*DT*TAOG+ADJ)-DELAY1
       NUM(2)=(J*DT*TAOG+ADJ)-DELAY2
       NUM(3)=((J-1)*DT*TAOG+ADJ)-DELAY1
       NUM(4)=((J-1)*DT*TAOG+ADJ)-DELAY2
       DO 383 KP=1,4
        IF (NUM(KP).GE.0.D0) THEN
         IF ((T1*NUM(KP)).LT.87.D0) THEN
          EX(2*KP-1)=DEXP(-T1*NUM(KP))
         ENDIF
         IF ((T2*NUM(KP)).LT.87.D0) THEN
          EX(2*KP)=DEXP(-T2*NUM(KP))
         ENDIF
        ELSE
         EX(2*KP-1)=0.D0
```

```
          EX(2*KP)=0.D0
         ENDIF
383     CONTINUE
        RETURN
        END
```

```
c*********************************************************************
c                                                                     *
c  This program generates the equivalent inductance and              *
c  capacitance of a transmission line above ground and               *
c  parallely-coupled to the other conductor lines.                    *
c                                                                     *
c*********************************************************************
c.....
c.....
      program EQLC
c.....
c.....
      parameter(n=3)
c.....n is the total number of conductors
c.....
c.....
      double precision u,f(n),ds(n),d(n),a(n,n),pi
      double precision ind(n,n),cap(n,n),b(n,n)
      double precision fac1,fac2,sum,eq,l0,c0
      integer t,t1,t2,lnum
c.....ind(n,n) is the inductance matrix
c.....cap(n,n) is the capacitance matrix
c.....l0 is the equivalent inductance of the line
c.....c0 is the equivalent capacitance of the line
c.....
c.....
      open(1,file='eqlc.out',status='old')
      open(2,file='eqlc.input',status='old')
c.....eqlc.input is the input file that consists the
c.....inductance and capacitance matrices;
c.....eqlc.out is the output file
c.....
c.....
      pi=4.d0*datan(1.d0)
c.....
c.....
      do 2 i=1,n
        read(2,*) (ind(i,j),j=1,n)
2     continue
      do 4 i=1,n
        read(2,*) (cap(i,j),j=1,n)
4     continue
c.....
c.....
      do 10 i=1,n
        do 20 j=1,n
          u=-2.d0*dcos(j*pi/dfloat(n+1))
c.........u is the variable of the characteristic polynomial f(u)
          do 40 l=1,n
            f(1)=1.d0
            f(2)=u
            if (l.gt.2.) then
              f(l)=u*f(l-1)-f(l-2)
            endif
```

```
40          continue
            ds(j)=0.d0
c.........ds(j) is the normalization factor
            do 30 k=1,n
              ds(j)=ds(j)+(f(k))**2
30          continue
            d(j)=dsqrt(ds(j))
            a(i,j)=f(i)/d(j)
c.........a(i,j) is the eigenvalue of the transformation matrix [M]
            write(1,100) i,j,a(i,j)
100         format(i4,i4,f10.4)
20        continue
10      continue
c.....
c.....
        do 60 t=1,2
          if (t.eq.1) then
            do 70 t1=1,n
              do 70 t2=1,n
                b(t1,t2)=ind(t1,t2)
70          continue
          else
            do 80 t1=1,n
              do 80 t2=1,n
                b(t1,t2)=cap(t1,t2)
80          continue
          endif
c.......assign b(i,j) as the matrix of inductance or capacitance
c.......
c.......
          do 999 lnum=1,n
            fac1=a(1,lnum)*(a(1,lnum)*b(1,1)+a(2,lnum)*b(1,2))
            fac2=a(n,lnum)*(a(n-1,lnum)*b(n-1,n)+a(n,lnum)
     1           *b(n,n))
            sum=0.d0
            if (n.eq.2) then
              sum=0.d0
            else
              do 50 i=2,n-1
                sum=sum+a(i,lnum)*(a(i-1,lnum)*b(i-1,i)+a(i,lnum)*b(i,i)
     1              +a(i+1,lnum)*b(i+1,i))
50            continue
            endif
            eq=fac1+fac2+sum
c.........'eq' is the calculated equivalent inductance or capacitance
c.........
c.........
            if (t.eq.1) then
              l0=eq
              write(1,300) lnum,l0
300           format(1x,'line #',i1,' L0 =',e10.4)
            else
              c0=eq
              write(1,400) lnum,c0
```

```
400          format(1x,'line #',i1,' C0 =',e10.4)
           endif
c.........output data
c.........
c.........
999      continue
60     continue
       stop
       end
```

Bibliography

[1] Al. Timotin, "Longitudinal Transient Parameters of A Unifilar Line with Ground Return", *Revue Roumaine des Sciences Techniques - Electrotechnique et Energetique*, 12, 4, p.523-535, Bucarest, 1967.

[2] G. I. Costache, "Transient Proximity Effect and Longitudinal Transient Parameters of A Bifilar Transmission Line", *Revue Roumaine des Sciences Techniques - Electrotechnique et Energetique*, 16, 1, p.111-124, Bucarest, 1971.

[3] Al. Timotin, "Wave Propagation on Unifilar Line with Ground Return", *Revue Roumaine des Sciences Techniques - Electrotechnique et Energetique*, 15, 2, p.175-194, Bucarest, 1970.

[4] Y. Kami and R. Sato, "Equivalent Circuit for the Transmission Line under the Electromagnetic Environment", *IEEE International Symposium on EMC*, p.139-146, Boulder, Colorado, 1981.

[5] Diethard Hansen, Hans Schaer, Dietrich Koeigstein, Henk Hoitink, Heyno Garbe, and D. V. Giri, "Response of an Overhead Wire near a NEMP Simulator", *IEEE Transactions on Electromagnetic Compatibility*, Vol.32, No.1, February 1990.

[6] Y.Kami and R. Sato, "Circuit-concept Approach to Externally Excited Transmission Lines", *IEEE Transactions on Electromagnetic Compatibility*, Vol. 27, No.4, pp.177-183, November 1985.

[7] Al. Timotin and A Nica, "A Method of Numerical Integration of the Telegrapher's Equation for Transmission Lines with Losses", *Revue Roumaine des Sciences Techniques - Electrotechnique et Energetique*, 23, 1, p.71-84, Bucarest, 1978.

[8] R. Radulet, Al. Timotin, A. Tugulea, and A. Nica, "The Transient Response of the Electric Lines Based on The Equations with Transient Line-parameter", *Revue Roumain des Sciences Techniques - Electrotechnique et Energetique*, 23, 1, p.3-19, Bucarest, 1978.

[9] Brain M. Neale and A. Gopinath, "Microstrip Discontinuity Inductances", *IEEE Transactions on Microwave Theory and Techniques*, Vol.26, No.10, October 1978.

[10] Peter Silvester and Peter Benedek, "Microstrip Discontinuity Capacitances for Right-angled Bends, T-junctions, and Crossings", *IEEE Transactions on Microwave Theory and Techniques*, Vol.21, No.5, May 1973.

[11] G. Bridges and L. Shafai, "Plane Wave Coupling to Multiple Conductor Transmission Lines above a Losssy Earth", *IEEE Transactions on Electromagnetic Compatibility*, Vol.31, No.1, February 1989.

[12] Y. Kami and R. Sato, "Transient Response of a Transmission Line Excited by an Electromagnetic Pulse", *IEEE Transactions on Electromagnetic Compatibility*, Vol.30, No.4, November 1988.

[13] F. Schlagenhaufer and H. Singer, "Investigations of Field-Excited Multiconductor Lines with Nonlinear Loads", *IEEE International Symposium on Electromagnetic Compatibility*, pp.95-99, Washington D.C., 1990.

[14] Niyazi Ari and Walter Blumer, "Analytic Formulation of the Response of a Two-Wire Transmission Line Excited by a Plane Wave", *IEEE Transactions on Electromagnetic Compatibility*, Vol.30, No.4, November 1988.

[15] David S. Gao, Andrew T. Yang, and Sung Mo Kang, "Modeling and Simulation of Interconnection Delays and Crosstalks in High-Speed Integrated Circuits", *IEEE Transactions on Circuits and Systems*, Vol.37, No.1, January 1990.

[16] Fabio Romeo and Mauro Santomauro, "Time-domain Simulation of n Coupled Transmission Lines", *IEEE Transactions on Microwave Theory and Technqiues*, Vol. MTT-35, No.2, February 1987.

[17] Clayton R. Paul, "A Simple Spice Model for Coupled Transmission Lines", *IEEE International Symposium on Electromagnetic Compatibility*, pp.327-333, 1988.

[18] Ashok K. Agrawal, Harold J. Price, and Shyam H. Gurbaxani, "Transient Response of Multiconductor Transmission Lines Excited by a Nonuniform Electromganetic Field", *IEEE Transactions on Electromagnetic Compatibility*, Vol.22, No.2, May 1980.

[19] Fung Yuel Chang, "Transient Analysis of Lossless Coupled Transmission Lines in a Nonhomogeneous Dielectric Medium", *IEEE Transactions on Microwave Theory and Techniques*, Vol. 18, No.9, September 1978.

[20] Clayborned D. Taylor and J. Philip Castillo, "On Electromagnetic-Field Excitation of Unshielded Multiconductor Cables", *IEEE Transactions on Electromagnetic Compatibility*, Vol.20, No.4, November 1978.

[21] Wolfgang J. R. Hoefer, "Equivalent Series Inductivity of a Narrow Transverse Slit in Microstrip", *IEEE Transactions on Microwave Theory and Techniques*, Vol.25, No.10, October 1977.

[22] A. Gopinath and Chandra Gupta, "Capacitance Parameters of Discontinuties in Microstriplines", *IEEE Transactions on Microwave Theory and Techniques*, Vol.26, No.10, October 1978.

[23] Chandra Gupta and Ananid Gopinath, "Equivalent Circuit Capacitance of Microstrip Step Change in Width", *IEEE Transactions on Microwave and Techniques*, Vol.25, No.10, October 1977.

[24] Peter Benedek and P. Silvester, "Equivalent Capacitances for Microstrip Gaps and Steps", *IEEE Transactions on Microwave Theory and Techngiues*, Vol.20, No.11, November 1972.

[25] Rene J. P. Douville and David S. James, "Experimental Study of Symmetric Microstrip Bends and Their Compensation", *IEEE Transactions on Microwave Theory and Techniques*, Vol.26, No.3, March 1978.

[26] Richard F. Hess, "EMP Coupling Analysis Using the Frequency (Transfer Function) Method with the SCEPTRE Computer Program", *IEEE Transactions on Electromganetic Compatibility*, pp.181-185, August 1975.

[27] Raymond Luebbers, Forrest P. Hunsberger, Karl S. Kunz, Ronald B. Standler, and Michael Schneider, "A Frequency-Dependent Finite-Difference Time-Domain Formulation for Dispersive Materials", *IEEE Transactions on Electromagnetic Compatibility*, Vol.32, No.3, August 1990.

[28] Larry K. Warne and Kenneth C. Chen, "A Bound on EMP Coupling", *IEEE Transactions on Electromagnetic Compatibility*, Vol.32, No.3, August 1990.

[29] Raouf Lawrence Khan and George I. Costache, "Finite Element Method Applied to Modeling Crosstalk Problems on Printed Circuit Boards", *IEEE Transactions on Electromgnetic Compatibility*, Vol.31, No.1, February 1989.

[30] G. I. Costache, "Calculation of Eddy Currents and Skin Effect in Nonmagnetic Conductors by the Finite Element Method", *Revue Roumaine des Sciences Techniques - Electrotechniques et Energetique*, 21, 3, pp.357-363, Bucarest, 1976.

[31] H. Garbe and D. Hansen, "EMI Response of Cable Systems to Transients Considering Complex Transfer Impedance", *IEEE International Symposium on Electromagnetic Compatibility*, pp.24-29, 1988.

[32] M. D.'Amore and M. Feliziani, "EMP Coupling to Coaxial Shielded Cables", *IEEE International Symposium on Electromagnetic Compatibility*, pp.37-43, 1988.

[33] M. K. "Andy" Anderson, "Field-To-Wire Coupling 1 to 18 GHz", *IEEE International Symposium on Electromagnetic Compatibility*, pp.45-49, 1988.

[34] Patrick Griffin, Gerard Capraro, Andrew McMahon, Arlon Adams, Jose Perini, and Anthony Pesta, "SHF/EHF Field-To-Wire Coupling Model", *IEEE International Symposium on Electromagnetic Compatibility*, pp.50-53, 1988.

[35] Roger A. Dalke, "A Numerical Method for The Analysis of Coupling to Thin Wire Structures", *IEEE International Symposium on Electromagnetic Compatibility*, pp.55-61, 1988.

[36] Richard S. Fellion, "Rapid Wire-To-Wire Matrix Multiplication", *IEEE International Symposium on Electromagnetic Compatibility*, pp.62-65, 1988.

[37] H. D. Bruns, H. Singer, and J. Nitsch, "Numerical Investigations on Pulse Coupling to Single and Multiple Conductor Systems", *IEEE International Symposium on Electromagnetic Compatibility*, pp.112-117, 1988.

[38] J. Beilfuss, A. Bell, B. Gray, and R. Hamrick, "Multiconductor Cable Response Dependency on Propagation Modes", *IEEE International Symposium on Electromagnetic Compatibility*, pp. 118-123, 1988.

[39] Yu Chang, Michael Rudko, Chang Yu Wu, and William F. McCarthy, "On System Modeling of ESD Penetration of a General Two-Layer Plate", *IEEE Intenational Symposium on Electromagnetic Compatibility*, pp.200-203, 1988.

[40] S. Caniggia, L.Catello, and V. Costa, "Models for Circuit Simulators to Analyze Crosstalk and Radiation into Wires", *IEEE International Symposium on Electromagnetic Compatibility*, pp.304-311, 1988.

[41] Fred Gardiol, "Comments about Time Domain Techniques in Electromagnetics", *IEEE MTT-S Newsletter*, pp.43-44, Summer/Fall 1989.

[42] Jose E. Schutt-Aine, "Scattering Parameter Transient Analysis of Transmission Lines Loaded with Nonlinear Terminations", *IEEE Transactions on Microwave Theory and Techniques*, Vol.36, No.3, March 1988.

[43] F. Schlagenhaufer and H. Singer, "Investigations of Field-Excited Multiconductor Lines with Nonlinear Loads", *IEEE International Symposium on Electromagnetic Compatibility*, pp.95-99, Washington D.C., 1990.

[44] Alireza H. Mohammadian and Chen-To Lai, "Transients on Lossy Transmission Lines with Arbitrary Boundary Conditions", *IEEE Transactions on Antennas and Propagation*, Vol.32, No.4, April 1984.

[45] Frederick M. Tesche, "On the Inclusion of Loss in time-domain Solutions of Electromagnetic Interaction Problems", *IEEE Transactions on Electromagnetic Compatibility*, Vol.32, No.1, February 1990.

[46] Paolo Bernardi and Renato Cicchetti, "Response of a Planar Microstrip Line Excited by an External Electromagnetic Field", *IEEE Transactions on Electromagnetic Compatibility*, Vol.32, No.2, May 1990.

[47] S. Celozzi and M. Feliziani, "EMP-Coupling To Twisted-Wire Cables", *IEEE International Symposium on Electromagnetic Compatibility*, pp.85-89, Washington D.C., 1990.

[48] Kenneth K.. Mei, Andreas Cangellaris, and Diogenes J. Angelakos, "Conformal Time Domain Finite Difference Method", *Radio Science*, Vol.19, No.5, pp.1145-1147, September-October, 1984.

[49] R. E. Collin, "Foundations of Microwave Engineering", *McGraw Hill, Incorporated*, 1966.

[50] David K. Cheng, "Field and Wave Electromagnetics", *Addison-Wesley Publishing Company*, 2nd edition, 1989.

[51] Samuel Y. Liao, "Microwave Circuit Analysis and Amplifier Design", *Prentice-Hall, Incorporated*, 1987.

[52] William H. Beyer, "Standard Mathematical Tables", *CRC Press, Incorporated*, 28th edition, 1987.

[53] Erwin Kreyszig, "Advanced Engineering Mathematics", *John Wiley and sons*, 5th edition, 1983.

[54] Henry W. Ott, "Noise Reduction Techniques in Electronic systems", *John Wiley and Sons*, 1988.